CHAPTER – 7

Formulation and Characterization of Ezetimibe Drug Nanocrystals

ABSTRACT

Drug nanocrystals (NCs) have been widely accepted as potent formulations to overcome poor solubility, dissolution and bioavailability problems of hydrophobic drugs. The present study was aimed to develop NCs of ezetimibe (Eze), a model BCS class II and hypocholesterolemic drug using bottom up precipitation methods. D-α-tocopheryl polyethylene glycol 1000 succinate (TPGS), and L-ascorbic acid-2-glucoside (AA2G), were the two stabilizers whose potential in developing Eze NCs was investigated. Particle size and zeta potential portrayed the potential of both the stabilizers in producing Eze NCs. The optimized NC formulations were evaluated for *in-vitro* solubility, dissolution, solid state characters and *in-vivo* pharmacokinetic and pharmacodynamic performance. The NC formulations significantly ($p < 0.05$) increased the solubility and dissolution properties of the drug compared to pure drug. The PXRD and DSC studies confirmed the retention of crystallinity and the SEM images indicated lack of aggregation in dried NCs. The TPGS NCs presented significantly superior pharmacokinetic and pharmacodynamic profiles upon oral administration. The present study thus corroborated TPGS NCs to be a promising choice of formulation for the oral delivery of Eze.

7.1 INTRODUCTION

Generation of active pharmaceutical ingredients (APIs) by novel drug discovery technologies like high throughput screening and combinatorial chemistry has been producing clinically proven therapeutically active APIs [Lipinski et al., 1976]. However, 70-90% of these clinically proven APIs were identified with low aqueous solubility which is a major hindrance to their oral bioavailability [Thayer, 2010]. Oral route is the most preferred route of administration and poor solubility is one of the main challenges to develop oral dosage forms with acceptable bioavailability.

The potential benefit of drug nanocrystals (NCs) in improving the solubility, dissolution and oral bioavailability of poorly soluble drugs has been well established over the last two decades [Ige et al., 2013; Liu et al., 2013]. NCs are encapsulating-carrier free nanoparticles and are known for their manufacturing simplicity. NCs are produced either by top down fragmentation or bottom up amalgamation [Srivalli and Mishra, 2015a]. The USFDA considers an NC product as "new drug" because, its markedly superior and unique pharmacokinetic profile is not bioequivalent or comparable to any other solubilized form of the same drug, not even to the drug's own micronized form, administered at the same dosage [Singare et al., 2010]. In this study, an attempt was made to prepare NCs of a poorly water soluble drug, ezetimibe (Eze), by bottom up precipitation methods and to study the effect of optimized NC formulations on the pharmacodynamic performance of Eze.

Eze is a model BCS class II drug and a hypocholesterolemic agent. The oral absorption of Eze shows inter-subject variability and its bioavailability could be as low as 35% due to its poor solubility and P-gp efflux. Eze acts by inhibiting the small intestinal absorption of cholesterol [Bandyopadhyay et al., 2012]. The P-gp molecules at the

intestinal brush border cause P-gp efflux of Eze and thus interfere with the absorption of Eze. So far, though few cyclodextrin complexes [Patel et al., 2008] and cocrystal formulations [Snehal et al., 2012] were attempted, it was only the colloidal drug delivery systems (CDDS) that reported improvement in *in-vitro* dissolution as well as *in-vivo* bioavailability of Eze which signified the effect of nanosize on the improved performance of Eze. Among the different CDDS, Eze was formulated as self nanoemulsifying systems reported in liquid [Bandyopadhyay et al., 2012] and solid forms [Dixit and Nagarsenker, 2008] and as nanoemulsion formulations [Bali et al., 2010 and 2011]. All these formulations contained several components which made the optimization of their preparation laborious and time taking. Furthermore, their preparation involved use of large amounts of surfactants and cosurfactants, which, from the toxicological stand point, is a legitimate concern. NCs are one of the CDDS that reached the market fastest as their formulation involves simple dispersion of drug in either aqueous or nonaqueous media containing one or more GRAS stabilizers (drug:stabilizer ratio considered between 2:1 and 20:1 on a weight basis). NCs exist at the epicenter of the CDDS because of their formulation simplicity, lack of drug loading problems, upscalability and ability to reduce bioavailability variations [Gao et al., 2013]. Currently, there are six licensed and regulatory approved NC products in the market, five of them are oral dosage forms, of which, for four of the products, the rationale for the development of NC based dosage form was specifically, enhanced bioavailability with reduced variations or food effects [Srivalli and Mishra, 2015a]. Therefore, we aimed to improve the oral absorption of Eze by formulating NCs. Till date, only Gulsun et al. [2011] prepared and conducted *in-vitro* characterization of Eze NCs, but, failed to reduce the particle size (PS) effectively. Eze NCs were prepared

using Pluronic F 127 as stabilizer and employing ball milling (PS result was 1259±62 nm) and ultrasonic probe (1736±88 nm) methods [Gulsun et al., 2011]. In the present study, we investigated the effect of two stabilizers, L-ascorbic acid-2-glucoside (AA2G) and D-α-tocopheryl polyethylene glycol 1000 succinate (TPGS) on the NC formation of Eze.

AA2G is a novel hydrophilic (non-surfactant) excipient that has been approved as a food additive and is expected to be used as a principle solubilizer in fat-soluble vitamin formulations and in other cosmetic products [Inoue et al., 2007]. Inoue et al. [2007] reported formation of nanoparticles and improvement in aqueous solubility and dissolution properties of clarithromycin on co-grinding with AA2G [Inoue et al., 2007]. AA2G has not been studied as an NC stabilizer so far. TPGS is a non-ionic surfactant that has been approved as a safe excipient by USFDA and is being widely explored as stabilizer for NCs. It lacks pharmacokinetic interactions with drugs and has a safety record in biomedical applications with no reports on its unrelated pharmacological effects [Guo et al., 2013]. It has P-gp inhibitory activity, has been widely in use to evade the P-gp efflux of substrate drugs [Srivalli and Lakshmi, 2012; Liu et al., 2010] and so, we hypothesized that it may aid in improving the absorption of Eze. The objective of the current part of investigation was to prepare AA2G NCs (ANCs) and TPGS NCs (TNCs) of Eze. The TNCs were further classified as plain TNCs (PTNCs) and electrostatically stabilized TNCs (ESTNCs). The ANCs were prepared by solvent-antisolvent precipitation followed by high speed homogenization and sonication. TNCs and ESTNCs were prepared by evaporative precipitation into aqueous solution (EPAS) method with subsequent sonication. Dried NCs obtained by freeze drying were

evaluated for solubility, solid state characteristics, dissolution, pharmacokinetics and pharmacodynamic performance.

7.2 MATERIALS

Eze was a kind gift from Lupin Ltd. (Pune, India). TPGS and AA2G were obtained as generous gift samples from Antares Health Products, Inc. (Illinois, USA) and Nagase Pvt. Ltd. (Mumbai, India), respectively. Acetone, mannitol and sodium lauryl sulphate (SLS) were purchased from Merck specialities Pvt. Ltd.

7.3 METHODS

7.3.1 Optimization of preparation of L-ascorbic acid-2-glucoside drug nanocrystals (ANCs) and D-α-tocopheryl polyethylene glycol 1000 succinate drug nanocrystals (TNCs) for confirmatory trials – application of experimental designs

7.3.1.1 Experimental designs

When conducting an experiment, a set of input factors may be assumed to influence the response output. For each factor, a predefined number of levels may be defined. In the early stages of experimentation, the experiment may be often simplified by only including two levels, where one level is defined as high and the other as low. The different combinations of high and low level for the factors are presented in a design matrix. The experiments are conducted for different combinations of levels for the given factors, and the response is measured after each run. The analysis can then be performed

based on the measured variation in the response. Proper planning should be conducted prior to performing the experiment. The planning should ensure a time efficient and economic analysis, without compromising the information being searched for. As an initial step, the goal of the analysis should be clearly defined. The goal may for example, in the case of this chapter, be to optimize the NCs in terms of particle size (PS), polydispersity index (PDI) and zeta potential (ZP). With this goal in mind, the experimental designs were chosen carefully in order to achieve a proper balance between the need for accurate information and limitations in terms of time, cost and complexity in the analysis. The choice of an experimental design depends on the objectives of the experiment and the number of factors to be investigated. According to the experimental objective they meet, the design types may be classified as follows:

Comparative objective: If one has one or several factors under investigation, but the primary goal of one's experiment is to make a conclusion about one a-priori important factor, (in the presence of, and/or in spite of the existence of the other factors), and the question of interest is whether or not that factor is "significant", (i.e., whether or not there is a significant change in the response for different levels of that factor), then one has a *comparative problem* and one needs a *comparative design* solution.

Screening objective: The primary purpose of the experiment is to select or *screen out* the few important main effects from the many less important ones. These *screening designs* are also termed main effects designs.

Response Surface (method) objective: The experiment is designed to allow us to estimate interaction and even quadratic effects, and therefore give us an idea of the (local) shape of the response surface we are investigating. For this reason, they are termed *response surface method (RSM) designs*. RSM designs are used to: find

improved or optimal process settings; troubleshoot process problems and weak points; and make a product or process more *robust* against external and non-controllable influences. "Robust" means relatively insensitive to the influences, a desirable property in the development of pharmaceutical formulations.

Optimizing responses when factors are proportions of a mixture objective: If one has factors that are proportions of a mixture and one wants to know what the "best" proportions of the factors are so as to maximize (or minimize) a response, then one needs a *mixture design.*

Optimal fitting of a regression model objective: If one wants to model a response as a mathematical function (either known or empirical) of a few continuous factors and one desires "good" model parameter estimates (i.e., unbiased and minimum variance), then one needs a *regression design.*

In context of pharmaceutical formulation development, the widely applicable experimental objectives are screening and response surface determination. For the purpose of screening, a full or fractional factorial designs for less number of factors like 2 to 4; and for 5 or more factor analysis, fractional factorial or Plackett-Burman designs (PBDs) are used. Similarly, to derive the response surface, Central composite designs (CCDs) or Box-Behnken designs (BBDs) are available for 2 to 4 factor analysis. In order to generate the response surface for higher number of factors, the factors may be initially screened to extract important factors and then a CCD or BBD may be applied [http://www.itl.nist.gov/div898/handbook/pri/section3/pri33.htm].

PBD is used to identify the most important factors early in the experimentation phase when complete knowledge about the system is usually unavailable. This design is an efficient screening method to identify the active factors using as few experimental runs

as possible. PBDs are very efficient screening designs when only main effects are of interest and should be used to study main effects when it can be assumed that two-way interactions are negligible. These are very economical designs with the run number a multiple of four. A PBD of 12 runs may be used for an experiment containing up to 11 factors. In practical use, two-level full or fractional factorial designs, and PBDs are often used to screen for the important factors that influence process output measures or product quality. These designs are useful for fitting first-order models (which detect linear effects) and can provide information on the existence of second-order effects (curvature) when the design includes center points. PBDs are applicable in screening; when neglecting higher order interactions is possible; in two-level multi-factor experiments; when there are more than four factors (if there are between two to four variables, a full factorial can be performed); to economically detect large main effects; designs the number of experiments, N = 4, 8, 12, 20, 24, 28 and 36 (as multiples of 4) [http://legacy.statease.com/dex8files/manual/dx/DX8-03A-TwoLevel-P1.pdf].

The RSM models may involve main effects alone or in combination with interactions and they may have quadratic and rarely cubic terms to account for the response surface curvature. Quadratic models are almost always sufficient for industrial applications. RSMs estimate interaction and even quadratic effects, and therefore give an idea of the (local) shape of the response surface being investigated. The desirable properties of a response surface design are; satisfactory distribution of information across the experimental region - *rotatability*; fitted values are as close as possible to observed values - *minimize residuals or error of prediction*; good lack of fit detection; internal estimate of error; constant variance check; transformations can be estimated; suitability for blocking; sequential construction of higher order designs from simpler designs;

minimum number of treatment combinations; good graphical analysis through simple data patterns; and good behavior when errors in settings of input variables occur [http://www.itl.nist.gov/div898/handbook/pri/section3/pri3363.htm].

BBD is an independent quadratic RSM based design as it does not contain an embedded factorial or fractional factorial design. In this design, the treatment combinations are at the midpoints of edges of the process space and at the center. These designs are rotatable or near rotatable and require 3 levels for each factor chosen to study [http://www.itl.nist.gov/div898/handbook/pri/section3/pri3362.htm].

A Box-Wilson CCD (or simply CCD) is an RSM that contains an embedded factorial or fractional factorial design. So, a CCD serves a dual purpose of screening as well as generation of response space. This design comes with center points that are augmented with a group of 'star points' that allow estimation of curvature. If the distance from the center of the design space to a factorial point is unit for each factor, the distance from the center of the design space to a star point is 'α' > ±1. The precise value of α depends on certain properties desired for the design and on the number of factors involved. Similarly, the number of center point runs the design is to contain also depends on the number of factors involved. CCDs have greater capability for orthogonal blocking and higher prediction quality over the entire design space, compared to BBDs. These designs are rotatable and require 5 levels for each factor, require factor setting outside the range of the factors in the factorial part [http://www.itl.nist.gov/div898/handbook/pri/section3/pri3361.htm].

7.3.1.2 Screening studies and optimization of preparation of ANCs

AA2G is a hydrophilic polyol that has not been employed as an NC stabilizer so far and therefore, PBD is the best first choice option as a complete knowledge about NC formulation development employing this stabilizer was unavailable and also, there was a need to screen with a higher number of factors. Once the significant factors were extracted, there will be a need to understand interactions between the factors. So, a subsequent BBD was applied based on RSM principle as it takes the combinations of all the levels between the factors and provides the interaction details. BBD requires fewer treatment combinations than a CCD involving the same number of factors. Since the vital or main effects have already been extracted using PBD, further optimization of ANCs was performed employing a BBD.

7.3.1.2.1 Planned preparation method of ANCs

ANCs were prepared by using Eze and AA2G in varying % w/v concentrations. Eze and AA2G were dissolved in organic solvent and distilled water, respectively. Eze containing organic solution was added drop wise to AA2G dissolved aqueous phase under continuous magnetic stirring. The suspension was further homogenized, centrifuged and the supernatant was replaced by aqueous AA2G solution (% w/v AA2G corresponding to the formulation batch under study). The suspension may be finally sonicated until the drug particles were completely dispersed in AA2G solution. This conceived method of preparation of ANCs was optimized by applying a PBD and a subsequent BBD.

7.3.1.2.2 PBD for screening the main effects for the preparation of ANCs

PBDs are used while beginning a new pharmaceutical experiment in order to identify the most important main effects of input formulation and processing variables on the

output parameters. A factorial method, 2-level, 11-factor, PBD with statistical model incorporating main effects and linear terms was utilized in order to optimize and to quantify the influence of various independent variables on the physicochemical properties of ANCs.

Since AA2G was not reported previously as an NC stabilizer, several factors were assumed to have had their effects on the PS, PDI and ZP of ANCs. Drug concentration (% w/v), AA2G concentration (% w/v), S/AS (Solvent:Antisolvent ratio), magnetic stirring rate (RPM), temperature (˚C), solvent type, homogenization time (min), batch size (mL), stirring time (min), homogenization speed (RPM) and sonication (5 min intermittent) were opted as eleven independent variables. Each critically selected variable was varied at two different levels, which were coded as -1 and +1 analogous to high and low levels, respectively as summarized in Table 7.1. The medium or 0 level of each of the factor has been shown separately in Table 7.2 as this level of each factor was considered at constant level for the 'one factor at a time analysis'.

The PS (Y_1), PDI (Y_2) and ZP (Y_3) of ANCs were the dependent variables studied. The design matrix along with one factor plots and first order linear models were generated by using Design-Expert software (Version 7.0; Stat-Ease, Minneapolis, MN). All the experiments were performed in triplicate and in a randomized manner to minimize any possible source of experimental errors and thereby, variability of the response. The purpose of replication was to account for the experimental error and to increase the precision of the experiments. The mean values were reported under the run results. The correlation between any one independent variable and a response variable was ascertained by 2D 'one factor at a time' plot.

Table 7.1. Coded levels of the applied independent variables and constraints of the studied dependent variables of PBD.

Independent variables	**Coded levels of variables**	
	Low	**High**
	-1	**1**
X_1 = A = Drug concentration (% w/v)	100	200
X_2 = B = AA2G concentration (% w/v)	50	200
X_3 = C = S/AS (Solvent:Antisolvent ratio)	0.02	0.1
X_4 = D = Magnetic stirring rate (RPM)	400	1000
X_5 = E = Temperature (˚C)	25	40
X_6 = F = Solvent type	Ethanol	Acetone
X_7 = G = Homogenization time (min)	20	40
X_8 = H = Batch size (mL)	5	10
X_9 = J = Stirring time (min)	15	30
X_{10} = K = Homogenization speed (RPM)	5000	1500
X_{11} = L = Sonication (5 min intermittent)	No	Yes
Dependent variables (Responses)	**Constraints**	
Y_1 = Particle Size (nm)	Minimize	
Y_2 = Polydispersity Index	Minimize	
Y_3 = Zeta potential (mV)	Maximize	

The effect of independent variables was modeled using the following first order linear equation generated by the applied 11 factor 12 run PBD.

$$Y = K_o + K_1X_1 + K_2X_2 + K_3X_3 + K_4X_4 + K_5X_5 + K_6X_6 + K_7X_7 + K_8X_8 + K_9X_9 + K_{10}X_{10} + K_{11}X_{11} + E$$

Or

$$Y = K_o + K_1A + K_2B + K_3C + K_4D + K_5E + K_6F + K_7G + K_8H + K_9J + K_{10}K + K_{11}L + E$$

- where Y represents the measured response associated with each factor level combinations; X_1, X_2, X_3, X_4, X_5, X_6, X_7, X_8, X_9, X_{10} and X_{11} are the coded values of independent variables, A, B, C, D, E, F, G, H, J, K and L, respectively. K_o is the intercept; K_i (for i = 1, 2, and so on till 11) are the linear main effects associated with each of the studied independent factors; K_i is the regression coefficient of the main factors effects and E is the random error.

Table 7.2. Coded levels of PBD when the independent variables were considered constant for one factor at a time analysis.

Independent variable	**Coded level (Medium)**
	0
X_1 = A = Drug concentration (% w/v)	150
X_2 = B = AA2G concentration (% w/v)	125
X_3 = C = S/AS (Solvent:Antisolvent ratio)	0.06
X_4 = D = Magnetic stirring rate (RPM)	700
X_5 = E = Temperature (˚C)	32.5
X_6 = F = Solvent type	Acetone
X_7 = G = Homogenization time (min)	30
X_8 = H = Batch size (mL)	7.5
X_9 = J = Stirring time (min)	22.5
X_{10} = K = Homogenization speed (RPM)	1000
X_{11} = L = Sonication (5 min intermittent)	Yes
Dependent variables (Responses)	**Constraints**
Y_1 = Particle Size (nm)	Minimize
Y_2 = Polydispersity Index	Minimize
Y_3 = Zeta potential (mV)	Maximize

Linear regression analysis by employing ANOVA was applied in order to ascertain the influence and significance of each of the factors along with their main effects on the response variables. The adequacies of the developed regression factorial model and the liner equations were evaluated by the correlation co-efficient (R^2). Numerical output of ANOVA was represented in terms of *p*-value. Further, optimization was performed by employing desirability function to find out the levels of independent variables that would yield ANCs with desired quality traits.

Pareto analysis

Visualizing the magnitude of the chosen effects may be accomplished by displaying them on an ordered bar chart, the Pareto chart. The vertical axis shows the t-value of the absolute effects. This dimensionless statistic scales the effects in terms of standard deviations. The appearance of the chart remains normal until the design encounters botched factor levels, missing data and the like. In other words, the t-value scale provides a more accurate measure of relative effects. The quantitative detail on the chosen model effects and those remaining for estimation of error may be derived from the effects list which also provides the % contribution of each factor to the variations in response variable.

Statistical analysis of PBD model

The statistics in detail may be drawn from the ANOVA table. Linear regression models and the first-order linear equations showing all the main effects of the various independent variables on dependent variables and also the one factor at a time analysis plots were generated by the results of the experimental design with the help of Design-Expert software.

7.3.1.2.3 BBD for optimization of the preparation of ANCs

RSM is a powerful statistical technique for designing pharmaceutical experiments, in modeling and analyzing the influence of input formulation and processing variables on the output parameters. A 3-level, 3-factor, BBD RSM with statistical modeling incorporating interactive and polynomial terms was utilized in order to optimize and to quantify the influence of independent variables on physicochemical properties of ANCs. Based on initial screening in the preliminary studies by PBD, AA2G:Eze ratio (X_1 or A), homogenization speed (RPM) (X_2 or B) and organic phase/aqueous phase ratio or otherwise, the Solvent:Antisolvent ratio, S/AS (X_3 or C) were opted as three independent variables. Each critically selected variable was varied at three different levels, which were coded as -1, 0 and +1 analogous to high, medium and low levels, respectively as summarized in Table 7.3. The PS (Y_1), PDI (Y_2) and ZP (Y_3) of ANCs were the dependent variables studied.

Table 7.3. Coded levels of the applied independent variables and constraints of the studied dependent variables of BBD.

Independent variable	**Coded levels of variables**		
	Low	**Medium**	**High**
	-1	**0**	**1**
X_1 = A = AA2G:Eze ratio	0.5	1	1.5
X_2 = B = Homogenization speed (RPM)	10,000	15,000	20,000
X_3 = C = S/AS (Solvent:Antisolvent ratio)	0.05	0.1	0.15
Dependent variables (Responses)	**Constraints**		
Y_1 = Particle Size (nm)	Minimize		
Y_2 = Polydispersity Index	Minimize		
Y_3 = Zeta potential (mV)	Maximize		

The design matrix along with quadratic response surface and second order polynomial model were generated by using Design-Expert software. All the experiments were performed in triplicate and in a randomized manner to minimize any possible source of experimental errors and thereby, variability of the response. The purpose of replication was to account for the experimental error and to increase the precision of the experiments. The mean values were reported under the run results.

The correlation between any two independent variables and a response variable was ascertained by 3D response surface plots. The effect of independent variables was modeled using the following non-linear polynomial equation generated by the BBD:

$$Y = K_o + K_1X_1 + K_2X_2 + K_3X_3 + K_{12}X_1X_2 + K_{13}X_1X_3 + K_{23}X_2X_3 + K_{11}X_1^2 + K_{22}X_2^2 + K_{33}X_3^2 + E$$

or

$$Y = K_o + K_1A + K_2B + K_3C + K_{12}AB + K_{13}AC + K_{23}BC + K_{11}A^2 + K_{22}B^2 + K_{33}C^2 + E$$

- where Y represents the measured response associated with each factor level combinations; X_1, X_2 and X_3 are the coded values of independent variables, A, B and C, respectively. K_o is the intercept; K_i (for i = 1, 2, and 3) are the linear effects, the K_{ii} are the quadratic effects, the K_{ij} (for i, j = 1, 2, and 3, i < j) are the interaction between the i^{th} and j^{th} variables, and E is the random error. K_i, K_{ii}, and K_{ij} are all the regression coefficients where K_i represents the main effects, the K_{ii} represents the quadratic effects of the main factors, and K_{ij} represents the interaction between any two of the main factors.

Multiple linear regression analysis by employing ANOVA was applied in order to ascertain the influence and significance of factors along with their interactive effects on the response variables. The adequacies of the developed regression model and the

polynomial equations were evaluated by the correlation co-efficient (R^2) and determining the lack of fit value. Numerical output of ANOVA was represented in terms of *p*-value. Further, optimization was performed by employing desirability function to find out the levels of independent variables that would yield ANCs with desired quality traits.

7.3.1.3 Optimization of preparation of TNCs

TPGS is a well known NC stabilizer and has an established record of nanonizing several drugs. Therefore, the number of factors to be studied to optimize the TNCs was reduced by conducting an extensive literature review of several published TPGS based NCs. Hence, a separate and elaborate screening stage may be cut down in the optimization of TNCs. Instead, in order to maintain the quality of optimization process by experimental design approach, a more efficient RSM that facilitated a study of higher levels of each factor, when compared to a BBD, a CCD was applied.

7.3.1.3.1 Planned preparation method of TNCs

During preliminary trials, TNCs were prepared by EPAS technique using a constant % w/v Eze and varying % w/v TPGS concentration. Eze and TPGS were dissolved in acetone and distilled water, respectively. 1 mL organic phase containing 100 mg drug was added drop wise to aqueous phase at 25 ˚C under continuous magnetic stirring. The suspension was stirred further to allow complete evaporation of the organic solvent. Thus obtained suspension was finally subjected to intermittent probe sonication for 5 min. This is the conceived preparation method of plain TNCs (PTNCs) where drug and TPGS were the only ingredients of formulation. Preliminary studies suggested that addition of small amount of SLS for electrostatic stabilization improved all the

physicochemical properties of TNCs, the PS, PDI and ZP. So, electrostatically stabilized TNCs (ESTNCs) were prepared in the same way as PTNCs after including SLS as an ionic surfactant in the aqueous phase. This conceived preparation method of ESTNCs was optimized by applying a CCD.

7.3.1.3.2 CCD for optimization of the preparation of ESTNCs

RSM by CCD is one of the most useful experimental designs in the optimization process and has been extensively used to develop quadratic response surface models. CCD is an economic experimental design strategy that offers the possibility of investigating a high number of independent variables at different levels with only a limited number of experiment runs. Its rotatable nature enables identification of optimum responses around its centre point without changing the predicting variance. The preparation of ESTNCs was optimized by investigating the effect of two different formulation variables namely, TPGS:Eze ratio and SLS:TPGS ratio; and one process variable, the stirring rate (RPM). The effect of these three independent variables on the PS, PDI and ZP of ESTNCs was studied. A full-factorial rotatable CCD was applied and the applied factors and their corresponding levels were selected based on our extensive literature review and preliminary experiments, as given in Table 7.4.

For the purpose of statistical analysis, the variables were coded as ±1 for the factorial points, 0 for the centre points and ±α for the axial points. The three-factor CCD design generated a total of 20 runs (8 factorial points, 6 axial points and 6 replicates at the center points) and the same was used to fit a second-order response surface in order to optimize the formulation and process factors affecting the responses (PS, PDI and ZP) of the ESTNC formulations. All experiments runs were performed in triplicate and in a randomized manner to minimize the effects of variability of the responses observed due

to systematic errors. The purpose of replication was to account for the experimental error and to increase the precision of the experiments. The mean values were reported under the run results.

Table 7.4. Coded levels of the applied independent variables and constraints of the studied dependent variables of CCD.

Independent variables	**Coded levels of variables**				
	- 1.682 (-α)	**-1**	**0**	**1**	**1.682 (+α)**
X_1 = A = TPGS:Eze ratio	0.16	0.5	1	1.5	1.84
X_2 = B = SLS:TPGS ratio	0.02	0.05	0.1	0.15	0.18
X_3 = C = Stirring rate (RPM)	159.1	500	1000	1500	1840.9
Dependent variables (Responses)	**Constraints**				
Y_1 = Particle Size (nm)	Minimize				
Y_2 = Polydispersity Index	Minimize				
Y_3 = Zeta potential (mV)	Maximize				

The star points represent extreme low or high values for each factor in the design and allow for the estimation of second-order effects. The star points are at distance, α, from the centre based on the properties desired for the design and the number of factors in the design. Alpha (α) is the axial distance from the centre points which makes the design rotatable. Rotatability is a very desirable property in RSM, which provides good predictions at points equally distant from the centre. The responses could be related to the selected variables by a second-order polynomial equation as follows:

$$Y = K_o + K_1X_1 + K_2X_2 + K_3X_3 + K_{12}X_1X_2 + K_{13}X_1X_3 + K_{23}X_2X_3 + K_{11}X_1^2 + K_{22}X_2^2 + K_{33}X_3^2 + E$$

or

$Y = K_o + K_1A + K_2B + K_3C + K_{12}AB + K_{13}AC + K_{23}BC + K_{11}A^2 + K_{22}B^2 + K_{33}C^2 + E$

- where Y represents the measured response associated with each factor level combinations; X_1, X_2 and X_3 are the coded values of independent variables, A, B and C, respectively. K_o is the intercept; K_i (for i = 1, 2, and 3) are the linear effects, the K_{ii} are the quadratic effects, the K_{ij} (for i, j = 1, 2, and 3, i < j) are the interaction between the i^{th} and j^{th} variables, and E is the random error.

A positive coefficient of the independent factor indicates that the dependent response value increases directly with the increasing value of the independent variables whereas if the response value decreases with the increasing input of variables, then the coefficient of the independent factor is negative. Data was analyzed using Design-Expert software to yield the correlation coefficient (R^2) and determine the optimum parameter combinations. Statistical significance of the model and the factor coefficients were estimated by ANOVA. Probability-value, $p < 0.05$ was considered as statistically significant. The accuracy of the model was checked by the coefficient of determination, R^2 which measures the 'goodness of fit' of the model. When R^2 approaches unity, the empirical model fits the actual experimental data. The relationships between the responses and the variables were visualized by the aid of two-dimensional contour and three-dimensional response surface plots to evaluate the relative influence of the parameters and to also predict the experimental results for other combinations. The optimal values of the independent variables were obtained by solving the quadratic equation and analyzing the response surfaces and contour plots. Subsequently, the experimentally optimized formulations were prepared to verify the responses predicted by the equation, therefore evaluating the validity of the model.

7.3.2 Preparation and characterization of ANCs and TNCs

7.3.2.1 Preparation of ANCs (confirmatory trials)

ANCs were prepared by using 1% w/v Eze and varying AA2G as 0.25%, 0.5% and 1% w/v. Eze and AA2G were dissolved in acetone and distilled water, respectively. 1 mL of 100 mg drug containing acetone solution was added drop wise to AA2G dissolved aqueous phase at 25 ˚C under continuous magnetic stirring at 1000 rpm. The suspension was stirred for 30 min and homogenized at 15000 rpm for 20 min. Following homogenization, the suspension was centrifuged and the supernatant was replaced by aqueous AA2G solution (% w/v AA2G corresponding to the formulation batch under study). The suspension was immediately subjected to 5 min intermittent sonication until the drug particles were completely dispersed in AA2G solution. The obtained nanosuspension was freeze-dried to obtain ANCs. The freeze-drying procedure was as follows: 1% w/v mannitol was added as cryoprotectant and the suspension was rapidly frozen at -20 ˚C for 12 h. Primary freeze drying of the pre-frozen samples was carried out for 24 h at -60 ˚C and below 15 Pascal followed by secondary drying cycle at 20 ˚C for 8 h.

7.3.2.2 Preparation of PTNCs (confirmatory trials)

TNCs were prepared by EPAS technique using 1% w/v Eze and varying TPGS concentration as 0.25%, 0.5% and 1% w/v. Eze and TPGS were dissolved in acetone and distilled water, respectively. 1 mL organic phase containing 100 mg drug was added drop wise to aqueous phase at 25 ˚C under continuous magnetic stirring at 1000 rpm. The suspension was stirred for 30 min at 1000 rpm and then stirred for 3 h at 200 rpm to

allow complete evaporation of the organic solvent. Thus obtained suspension was finally subjected to intermittent probe sonication for 5 min and freeze-dried to collect TNCs. The freeze-drying procedure was the same as described for ANCs.

7.3.2.3 Preparation of ESTNCs (confirmatory trials)

ESTNCs were prepared in the same way as TNCs with 1% w/v TPGS concentration after including SLS as an ionic surfactant in the aqueous phase. The effect of SLS was studied at concentrations, 0.05%, 0.1% and 0.15% w/v.

7.3.2.4 Particle size (PS), polydispersity index (PDI) and zeta potential (ZP) measurements

Fixed angle (165˚) dynamic light scattering (Delsa Nano C, Beckman coulter) was employed to measure the PS and PDI. The ZP measurements were made by estimating the electrophoretic mobility of particles under applied electric field. Samples were appropriately diluted with distilled water and the measurements were made in triplicate.

7.3.2.5 Solid state characterization

Fourier transform infra-red (FTIR) spectra were recorded using FTIR spectrophotometer (FTIR-8400S, Shimadzu Co., Kyoto, Japan) over the range of 4000-400 cm^{-1}. All the samples were co-ground with anhydrous KBr, pelletized and scanned at 20 ˚C with the number of reference scans set as 20 and a resolution of 4 cm^{-1}. Differential scanning calorimetry (DSC) analyses were carried out using DSC-822^e (Mettler Toledo, AG, Analytical, Switzerland) by heating the samples between 10 ˚C and 300 ˚C. DSC of TPGS was obtained by heating from 10 ˚C to 160 ˚C. 4-7 mg samples were accurately

weighed in aluminium pans and heated at the rate of 10 ºC/min under constant nitrogen purging at 10 ml/min to obtain the thermograms. Powder X-Ray diffraction (PXRD) patterns were recorded by employing X-ray diffractometer (PW3050/60 X'pert PRO, PANalytical, Netherlands) with Cu anode at 40 kV and 30 mA. Sample holders were filled at 20 ˚C and PXRD data were collected in the range $10^{\circ}<2\theta<80^{\circ}$. The surface morphological properties were investigated by SEM (FEI, QUANTA-200, Netherlands). The dry samples were sprinkled gently at 20 ˚C lab conditions using spatula on to a carbon tape adhered to the sample holder and microphotographs were taken at an accelerating voltage of 20 kV at varying magnifications. Atomic force microscopy (AFM) (NT-MDT Solver Next, Limerick, Ireland) was used to study the surface morphology and size distribution. A drop of freshly prepared nanosuspension was placed on a borosilicate glass cover slip and air-dried to obtain a fine film for AFM observation. Images were captured in noncontact mode at a scanning rate of 0.5 Hz.

7.3.2.6 Drug content

Known amounts of NC systems equivalent to 10 mg of drug were dissolved in 5 mL methanol, sonicated for 1 min and filtered. After appropriate dilutions, the solutions were assayed for Eze content at 232 nm using UV-Vis spectrophotometer. The readings were taken in triplicate and the average was noted.

7.3.2.7 Saturation aqueous solubility studies

Excess amounts of drug and NC systems were added to 10 mL distilled water. After shaking continuously on rotary shaker for one week at room temperature, the suspensions were filtered and the drug amount was measured at 232 nm.

7.3.2.8 Dissolution

The procedure followed was the same as described under the section 5.3.2.8. Dissolution was studied for 60 min and the dissolution efficiency (DE) representing the area under the dissolution curve up to 60 min was calculated for each of the systems. Additionally, $t_{80\%}$ and $t_{90\%}$ values were noted for the NC systems.

7.3.2.9 Stability

The optimized formulations, ANC-F3 and ESTNC-F8, were subjected to stability studies at 30±2 ˚C/70±5% RH for 6 months. Six batches of freshly prepared and freeze-dried powder NCs, each of ANC-F3 and ESTNC-F8, were filled in air-tight glass vials, sealed and stored in stability chamber (Narang Industries, New Delhi, India) at 30±2 ˚C/70±5% RH. The freshly prepared batches were redispersed and characterized for mean PS, PDI and ZP and were further tested for drug content, aqueous solubility and dissolution tests. After 6 months, the samples were withdrawn and characterized for all the above test results. The results obtained were analysed by comparing the values noted before and after 6 months.

7.3.2.10 *In-vivo* preclinical pharmacokinetic study

7.3.2.10.1 Animals

The study protocol was approved and guided by the Central Animal Ethical Committee, Institute of Medical Sciences, Banaras Hindu University, Varanasi, India. Male Albino Wister rats (200 – 250 g) were used and the animals were divided into three groups of six animals each. The standard - group I, test - group II, and test – group III, received

pure drug suspension, F8 (ESTNC), and F3 (ANC), respectively. The animals were housed in polypropylene cages and kept at standard laboratory conditions (25±2 ˚C and 55±5% RH). Six animals per cage were accommodated with free access to standard laboratory diet (Lipton feed, Mumbai, India) and water *ad libitum*.

7.3.2.10.2 Dosing and sampling

All the animals used were fasted overnight for the study and dosed orally using 18-gauge oral feeding needle. A single dose pharmacokinetic study was conducted and all the treatment group animals received 2 mL of 50 mg/kg body weight equivalent dose of Eze, via oral administration. The animal groups, I, II, and III, received pure drug, F3 (ANC), and F8 (ESTNC), respectively, dispersed in 0.25% w/v NaCMC. After anaesthetizing the rats with diethyl ether, 500 µL blood samples were collected by retro-orbital puncture at 0 (pre-dose), 0.5, 1, 1.5, 2, 2.5, 4, 12, and 24 h, into heparinized microcentrifuge tubes. After blood sampling at each time point, the blood loss was compensated by immediately injecting same volume of normal saline. Plasma was immediately separated by centrifugation at 5000 rpm for 20 min, spiked with IS and stored at -20 °C until bioanalysis.

7.3.2.10.3 Drug extraction – same as described under the section 5.3.2.10.3.

7.3.2.10.4 Plasma drug analysis – same as described under the section 5.3.2.10.4.

7.3.2.10.5 Pharmacokinetic parameters – same as described under the section 5.3.2.10.5.

7.3.2.11 Antihypercholesterolemic activity

Approval to perform the activity study was obtained from the Central Animal Ethical Committee, Institute of Medical Sciences, Banaras Hindu University, Varanasi, India

and their guidelines were followed throughout the study. Male Albino Wister rats (200 – 250 g) were used and the animals were divided into five groups of six animals each. The control - group I, standard - group II, test – group III, test – group IV and test – group V received cholesterol, pure drug suspension along with cholesterol, Eze-TPGS PM along with cholesterol, formulation F3 along with cholesterol, and formulation F8 along with cholesterol, respectively. Six animals per one polypropylene cage were accommodated at 25±2 ˚C and 55±5% RH with free access to standard laboratory diet (Lipton feed, Mumbai, India) and water *ad libitum*.

The study was carried out for a total period of 8 weeks wherein the first four weeks, all the animals were fed with 200 mg cholesterol in 2 mL coconut oil as high fat diet for inducing hypercholesterolemia [Dixit and Nagarsenker, 2008; Bandyopadhyay et al., 2012; Srivalli and Mishra, 2015b]. At the end of fourth week, the plasma cholesterol levels were measured for all the groups and the values were considered as baseline values for the following four week study, the actual antihypercholesterolemic activity study. The first four weeks is a stage 1, hypercholesterolemic induction study and the next four weeks is the stage 2, antihypercholesterolemic activity (pharmacodynamic) study.

The pharmacodynamic study was carried out for 28 days and the animals were fed and dosed orally using 18-gauge oral feeding needle. For the purpose of the study, all the groups were induced with hypercholesterolemia by administering high fat diet (200 mg cholesterol in 2 mL coconut oil). Two hours following the administration of high fat diet, the treatment groups, II, III IV and V were respectively dosed with pure drug, Eze-TPGS PM, freeze-dried F3 and freeze-dried F8, dispersed in 0.25% w/v NaCMC. The daily dose for rats was calculated by considering the rat to human being surface area

ratio [Bandyopadhyay et al., 2012; Dixit and Nagarsenker, 2008]. Volume of vehicle (200 µl) and dose levels of 1 mg Eze or equivalent formulation/kg body weight/day were kept constant in each case. Blood samples were collected by retro-orbital puncture into anticoagulated microcentrifuge tubes (heparin treated), at weekly intervals, on day 0 (pre-dose), 7, 14, 21 and 28 after anaesthetizing the rats with diethyl ether. Plasma was separated by centrifugation at 5000 rpm for 20 min and stored at 2 ˚C until further use. Percent changes in the plasma levels of total cholesterol (TC) for antihypercholesterolemic activity, and percent changes in the plasma levels of triglycerides (TG), high-density lipoprotein cholesterol (HDL) and low-density lipoprotein cholesterol (LDL) for lipid profile analysis, were analysed using *in-vitro* Cogent diagnostic kits (Span Diagnostics Ltd., Surat, India).

7.3.2.12 Statistical analysis

The results were shown as Mean±SD. The data pertaining to the PS, solubility, dissolution and pharmacokinetic studies were analyzed by one-way ANOVA and post hoc Tukey multiple comparison test ($p < 0.05$). The results of pharmacodynamic study were analyzed by two-way ANOVA and Bonferroni's multiple comparison post hoc test. The statistical terms used in PBD, BBD and CCD were: df = degrees of freedom; Adj. R-Squared = Adjusted R-Squared; Pred. R-Squared = Predicted R-Squared; Adeq. Prec. = Adequate Precision; C.V. = Coefficient of Variation; Prob > F is the significance level; and PRESS = Predicted Residual Sum of Squares.

7.4 RESULTS AND DISCUSSION

7.4.1 Optimization of preparation of ANCs and TNCs for confirmatory trials – application of experimental designs

7.4.1.1 Screening studies and optimization of preparation of ANCs

7.4.1.1.1 PBD for screening the main effects in the preparation of ANCs

A total of 12 batches were run by varying the eleven independent variables, drug concentration (% w/v), AA2G concentration (% w/v), S/AS (Solvent:Antisolvent ratio), magnetic stirring rate (RPM), temperature (˚C), solvent type, homogenization time (min), batch size (mL), stirring time (min), homogenization speed (RPM) and sonication (5 min intermittent) at two different levels, for different possible combinations as per the design matrix generated by PBD and as presented in Table 7.1, in coded terms. The results obtained for the dependent variables such as PS (Y_1), PDI (Y_2) and ZP (Y_3) of ANCs, from the so performed experiments were summarized in Table 7.5.

The positive sign in the linear first degree equation suggests a synergistic effect whereas the negative sign indicates an inverse effect. When the constraint for a desired response is high, then all the positive signed factors should be considered at an optimal high level and all the negative signed factors should be considered at an optimal low level. The considerations turn vice-versa when the constraint for a desired response is low. Two-dimensional 'one factor at a time' plots were constructed using respective linear first degree equations for each of the dependent variable, graphically, keeping all the remaining factors at a constant level, as described in Table 7.2.

Table 7.5. PBD experimental runs.

Run No.	Independent variables											Dependent variables		
	X_1	X_2	X_3	X_4	X_5	X_6	X_7	X_8	X_9	X_{10}	X_{11}	Y_1	Y_2	Y_3
1	1	1	- 1	1	1	1	- 1	- 1	- 1	1	- 1	780.9	0.17	21.3
2	- 1	1	1	- 1	1	1	1	- 1	- 1	- 1	1	1321.4	0.33	22.97
3	1	- 1	1	1	- 1	1	1	1	- 1	- 1	- 1	1310.9	0.42	14.92
4	- 1	1	- 1	1	1	- 1	1	1	1	- 1	- 1	987	0.3	22.24
5	- 1	- 1	1	- 1	1	1	- 1	1	1	1	- 1	1168.9	0.36	16.9
6	- 1	- 1	- 1	1	- 1	1	1	- 1	1	1	1	1098.2	0.32	17.6
7	1	- 1	- 1	- 1	1	- 1	1	1	- 1	1	1	1168.7	0.38	15.2
8	1	1	- 1	- 1	- 1	1	- 1	1	1	- 1	1	1186.5	0.36	21
9	1	1	1	- 1	- 1	- 1	1	- 1	1	1	- 1	980.9	0.22	21.76
10	- 1	1	1	1	- 1	- 1	- 1	1	- 1	1	1	640.3	0.14	22.54
11	1	- 1	1	1	1	- 1	- 1	- 1	1	- 1	1	1448.1	0.41	15.24
12	- 1	- 1	- 1	- 1	- 1	- 1	- 1	- 1	- 1	- 1	- 1	1649.8	0.53	17.4

7.4.1.1.1.1 Influence of PBD independent variables on PS (Y_1)

Based on pareto analysis, the effects of the terms, B, D, H and K were selected to check the probability ("*p*-value") for the PBD model and to determine the coefficients for the selected effects. Clicking or selecting the next biggest bar, L, on the pareto chart and application of ANOVA to evaluate the significance of the effect of factor, L ($p < 0.05$ is significant) indicated that the term, L did not pass the 0.05 test (for L, $p = 0.0765 >$

0.05). Therefore, the ANOVA table was built by clicking off or deslecting the term, L. The PBD pareto chart for the response, PS, was given in Figure 7.1.

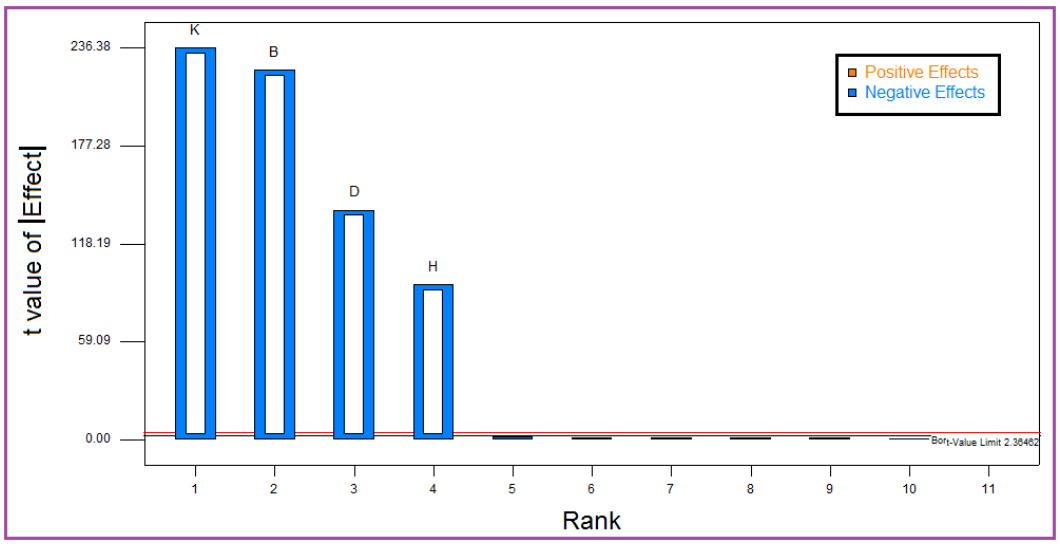

Figure 7.1. Pareto analysis of effect of independent variables applied using PBD on the response, PS.

The percent contribution of each of the investigated independent factors, the PBD ANOVA details and the summary statistics of PBD, to study the variations in the response, PS of ANCs, were given in Table 7.6, 7.7 and 7.8, respectively.

The model F-value of 33367.97 implies the PBD model is significant. There is only a 0.01% chance that a "Model F-Value" this large could occur due to noise. The factors with the values of "Prob > F" less than 0.05 indicate model terms are significant. In this case B, D, H, K are significant model terms. All the remaining model terms are not significant. Model reduction by not counting the insignificant model terms may improve the predictability of the model. The "Pred R-Squared" of 0.9998 is in reasonable agreement with the "Adj R-Squared" of 0.9999. "Adeq Precision" measures the signal to

noise ratio. A ratio greater than 4 is desirable. The obtained ratio of 618.282 indicates an adequate signal. So, the model was used to navigate the design space.

Table 7.6. Percent contribution of each of the applied factors of the two level PBD factorial model to the variations in the response, PS of ANCs.

Factor	% Contribution	Remark
A-Drug Conc	0.00106094	Trivial
B-AA2G Conc	37.2069	Vital
C-S/AS	3.53123E-006	Trivial
D-Magnetic stirring rate	14.3803	Vital
E-Temp	0.000692122	Trivial
F-Solvent type	0.000627775	Trivial
G-Homogenization time	0.00053714	Trivial
H-Batch size	6.54739	Vital
J-Stirring time	5.64997E-005	Trivial
K-Homogenization speed	41.8601	Vital
L-Sonication (5 min intermitent)	0.00226627	Trivial

Table 7.7. ANOVA for the PBD factorial model for analysing the response, PS of ANCs.

Source	Coefficient Estimate	F Value	p-value (Prob > F)	Remark
Constant	1145.13			
B	-162.30	49663.36	< 0.0001	Significant
D	-100.90	19194.70	< 0.0001	Significant
H	-68.08	8739.38	< 0.0001	Significant
K	-172.15	55874.43	< 0.0001	Significant

Table 7.8. Statistics summary of the PBD factorial model for analysing the response, PS of ANCs.

Statistic	**F Value**	***p*-value (Prob > F)**	**Remark**
Model	33367.97	< 0.0001	Significant
R-Squared			0.9999
Adj R-Squared			0.9999
Pred R-Squared			0.9998
Adeq Precision			618.282
C.V. %			0.22
PRESS			130.93

By varying the levels of independent variables in their limits, the PS of ANCs was obtained in the range of 640.3 to 1649.8 nm. The factors whose effect had F values with $p < 0.05$ were considered significant. In case of the response, PS, factors, B, D, H, K were the significant model terms. The reduced first-order linear equation describing an empirical relationship between particle size (Y_1) and independent variables, generated by linear regression analysis can be given as follows in terms of actual factors:

PS = + 2199.61667 - 2.16400 * AA2G Conc - 0.33633 * Magnetic stirring rate - 27.23333 * Batch size - 0.034430 * Homogenization speed

The equation suggests that the PS of ANCs was influenced negatively by AA2G concentration, magnetic stirring rate, batch size and homogenization speed. Accordingly, all the factors were considered at an optimal high levels, in order that a desired minimum optimal PS was achieved. The high R^2 value (0.9999) indicates reasonable agreement between predicted and experimental values (99.99% of variation in PS may be best explained by the applied independent variables). The 'one factor at a time' analysis plots to study the PS of ANCs were given in Figure 7.2.

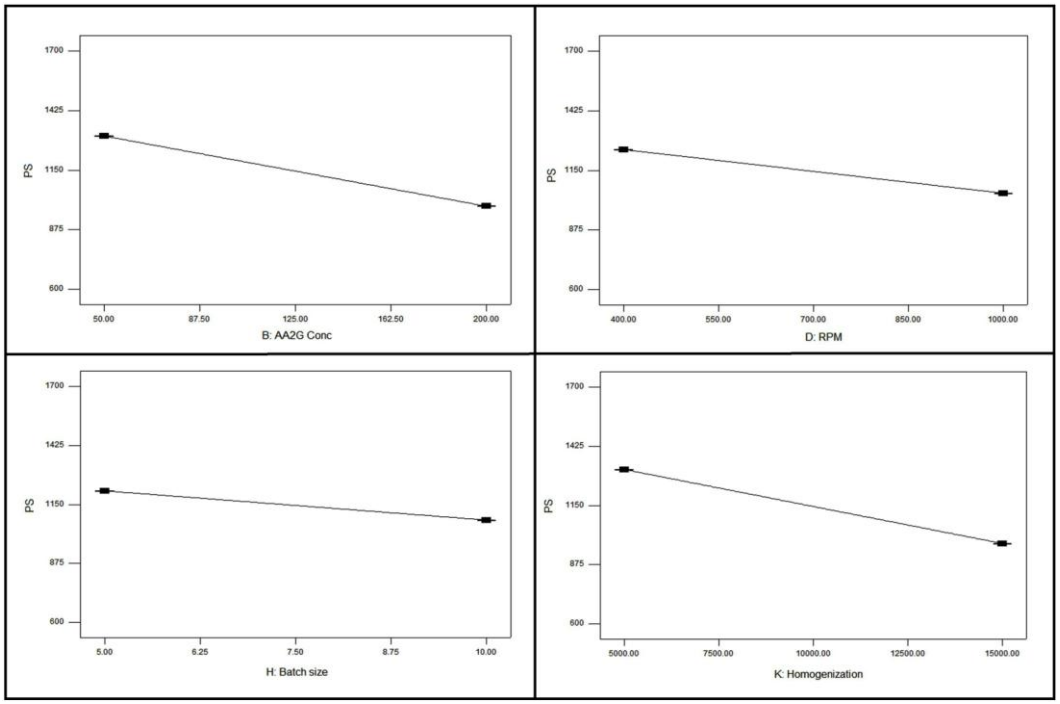

Figure 7.2. 'One factor at a time' analysis of effect of independent variables on the response, PS.

7.4.1.1.1.2 Influence of PBD independent variables on PDI (Y_2)

Based on pareto analysis, the effects of the terms, B, C, D, K and L were selected to check the probability ("*p*-value") for the PBD model and to determine the coefficients for the selected effects. Clicking or selecting the next biggest bar, E, on the Pareto Chart and application of ANOVA to evaluate the significance of the effect of factor, E ($p < 0.05$ is significant) indicated that the term, E did not pass the 0.05 test with any room to spare (for E, $p = 0.0493 \approx 0.05$). Therefore, the ANOVA table was built by clicking off or deslecting the term, E. The PBD pareto chart for the response, PDI, was given in Figure 7.3.

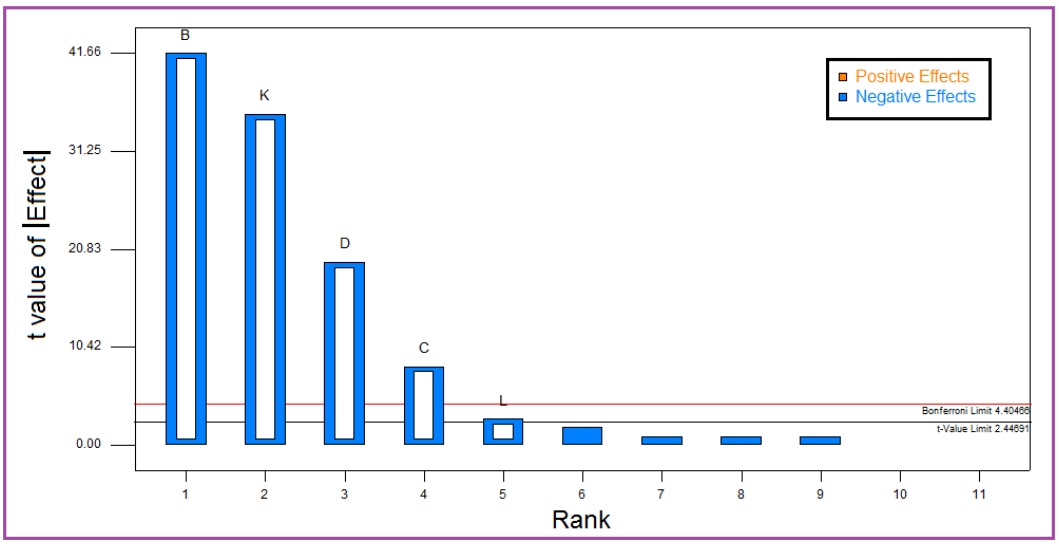

Figure 7.3. Pareto analysis of effect of independent variables applied using PBD on the response, PDI.

The model F-value of 685.71 implies the model is significant. There is only a 0.01% chance that a "Model F-Value" this large could occur due to noise. The factors with the values of "Prob > F" less than 0.05 indicate model terms are significant. In this case B, C, D, K, L are significant model terms. All the remaining model terms are not significant. Model reduction by not counting the insignificant model terms may improve the predictability of the model. The "Pred R-Squared" of 0.9930 is in reasonable agreement with the "Adj R-Squared" of 0.9968. "Adeq Precision" measures the signal to noise ratio. A ratio greater than 4 is desirable. The obtained ratio of 87.688 indicates an adequate signal. So, the model was used to navigate the design space. The percent contribution of each of the investigated independent factors, the PBD ANOVA details and the summary statistics of PBD, to study the variations in the response, PDI of ANCs, were given in Table 7.9, 7.10 and 7.11, respectively.

Table 7.9. Percent contribution of each of the applied factors of the two level PBD factorial model to the variations in the response, PDI of ANCs.

Factor	% Contribution	Remark
A-Drug Conc	0.0249563	Trivial
B-AA2G Conc	50.5366	Vital
C-S/AS	2.02146	Vital
D-Magnetic stirring rate	11.0057	Vital
E-Temp	0.0998253	Trivial
F-Solvent type	0.0249563	Trivial
G-Homogenization time	0	Trivial
H-Batch size	0.0249563	Trivial
J-Stirring time	0	Trivial
K-Homogenization	36.0369	Vital
L-Sonication (5 min intermitent)	0.224607	Vital

The PS distribution of ANCs was obtained in the range of 0.14 to 0.53 for selected levels and combinations of different variables. The factors whose effect had F value with $p < 0.05$ were considered significant. In case of the response, PDI, factors, B, C, D, K, L were the significant model terms.

Table 7.10. ANOVA for the PBD factorial model for analysing the response, PDI of ANCs.

Source	Coefficient Estimate	F Value	p-value (Prob > F)	Remark
Constant	0.33			
B	-0.075	1735.71	< 0.0001	Significant
C	-0.015	69.43	0.0002	Significant
D	-0.035	378.00	< 0.0001	Significant
K	-0.063	1237.71	< 0.0001	Significant
L	-5.000E-003	7.71	0.0321	Significant

Table 7.11. Statistics summary of the PBD factorial model for analysing the response, PDI of ANCs.

Statistics	**F Value**	**p-value (Prob > F)**	**Remark**
Model	685.71	< 0.0001	Significant
R-Squared			0.9983
Adj R-Squared			0.9968
Pred R-Squared			0.9930
Adeq Precision			87.688
C.V. %			1.90
PRESS			9.333E-004

The reduced first-order linear equation for PDI in terms of actual independent variables was obtained as follows.

For Sonication (5 min intermitent) level, 'No'

PDI = + 0.68917 - 1.00000E-003 * AA2G Conc - 0.37500 * S/AS - 1.16667E-004 * Magnetic stirring rate - 1.26667E-005 * Homogenization speed

For Sonication (5 min intermitent) level, 'Yes'

PDI = + 0.67917 - 1.00000E-003 * AA2G Conc - 0.37500 * S/AS - 1.16667E-004 * Magnetic stirring rate - 1.26667E-005 * Homogenization speed

The equation suggests that the PDI of ANCs was influenced negatively by AA2G concentration, S/AS, magnetic stirring rate and homogenization speed either in the presence or absence of 5 min intermittent sonication. Accordingly, all the factors were considered at optimal high levels, in order that a desired minimum optimal PDI was achieved. The R^2 value of 0.9983 suggests that 99.83% of variation in PDI was best

explained by the applied formulation and process variables. The 'one factor at a time' analysis plots to study the PDI of ANCs were given in Figure 7.4.

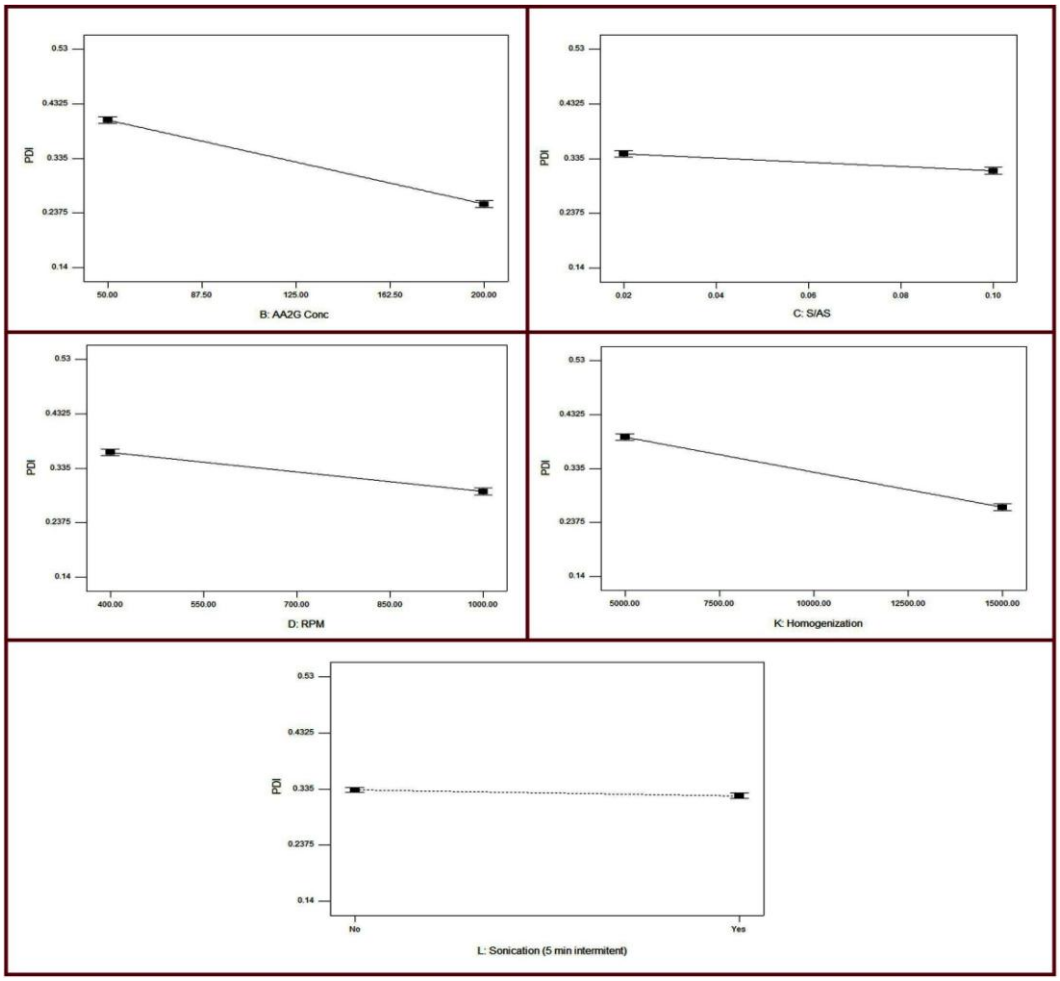

Figure 7.4. 'One factor at a time' analysis of effect of independent variables on the response, PDI.

7.4.1.1.1.3 Influence of PBD independent variables on ZP (Y_3)

Based on pareto analysis, the effects of the terms, A, B and H were selected to check the probability ("*p*-value") for the PBD model and to determine the coefficients for the selected effects. Clicking or selecting the next biggest bar, K, on the pareto chart and application of ANOVA to evaluate the significance of the effect of factor, K ($p < 0.05$ is

significant) indicated that the term, K did not pass the 0.05 test (for K, p = 0.0931 > 0.05). Therefore, the ANOVA table was built by clicking off or deslecting the term, K. The PBD pareto chart for the response, ZP, was given in Figure 7.5.

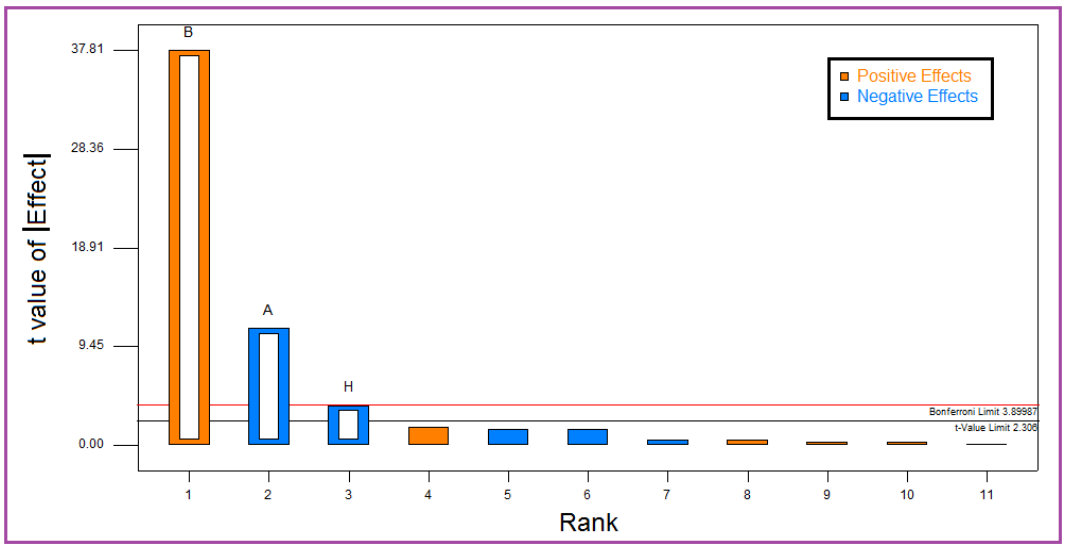

Figure 7.5. Pareto analysis of effect of independent variables applied using PBD on the response, ZP.

The model F-value of 523.17 implies the model is significant. There is only a 0.01% chance that a "Model F-Value" this large could occur due to noise. The factors with the values of "Prob > F" less than 0.05 indicate model terms are significant. In this case A, B, H are significant model terms. All the remaining model terms are not significant. Model reduction by not counting the insignificant model terms may improve the predictability of the model. The "Pred R-Squared" of 0.9886 is in reasonable agreement with the "Adj R-Squared" of 0.9930. "Adeq Precision" measures the signal to noise ratio. A ratio greater than 4 is desirable. The obtained ratio of 52.806 indicates an adequate signal. So, the model was used to navigate the design space. The percent contribution of each of the investigated independent factors, the PBD ANOVA details

and the summary statistics of PBD, to study the variations in the response, ZP of ANCs, were given in Table 7.12, 7.13 and 7.14, respectively.

Table 7.12. Percent contribution of each of the applied factors of the two level PBD factorial model to the variations in the response, ZP of ANCs.

Factor	% Contribution	Remark
A-Drug Conc	7.94585	Vital
B-AA2G Conc	90.6328	Vital
C-S/AS	0.0127631	Trivial
D-Magnetic stirring rate	0.146696	Trivial
E-Temp	0.142505	Trivial
F-Solvent type	0.00729647	Trivial
G-Homogenization time	0.00729647	Trivial
H-Batch size	0.914215	Vital
J-Stirring time	0.0127631	Trivial
K-Homogenization	0.177735	Trivial
L-Sonication (5 min intermitent)	6.83332E-005	trivial

The ZP of ANCs was obtained in the range of 14.92 to 22.97 for selected levels and combinations of different variables. The factors whose effect had F values with $p < 0.05$ were considered significant. In case of the response, ZP, factors, A, B, H were the significant model terms. All the factors with F values with $p < 0.05$ significantly affected the ZP. The significant model terms were as follows as per the reduced first-order linear equation.

ZP = + 17.71556 - 0.017050 * Drug Conc + 0.038389 * AA2G Conc - 0.11567 * Batch size

Table 7.13. ANOVA for the PBD factorial model for analysing the response, ZP of ANCs.

Source	**Coefficient Estimate**	**F Value**	***p*-value (Prob > F)**	**Remark**
Constant	19.09			
A	-0.85	125.35	< 0.0001	Significant
B	2.88	1429.76	< 0.0001	Significant
H	-0.29	14.42	0.0053	Significant

Table 7.14. Statistics summary of the PBD factorial model for analysing the response, ZP of ANCs.

Statistics	**F Value**	***p*-value (Prob > F)**	**Remark**
Model	523.17	< 0.0001	Significant
R-Squared			0.9949
Adj R-Squared			0.9930
Pred R-Squared			0.9886
Adeq Precision			52.806
C.V. %			1.38
PRESS			1.25

The equation suggests that the ZP of ANCs was influenced negatively by drug concentration and batch size whereas the AA2G concentration had a positive effect on ZP. All the directly related factors were considered at optimal high levels, and all those factors that inversly affected ZP were considered at optimal low levels in order that a desired maximum optimal ZP was achieved. The high R^2 value (0.9949) indicated that 99.49% of variation in ZP could be explained by the variations in formulation and process factors. The 'one factor at a time' analysis plots to study the ZP of ANCs were given in Figure 7.6.

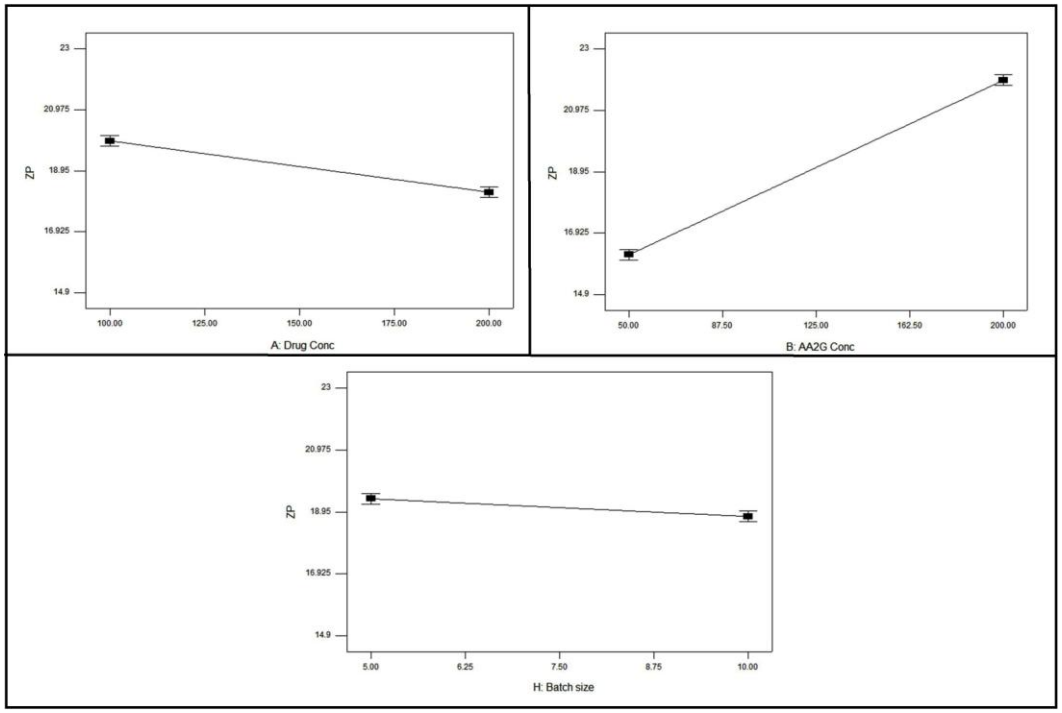

Figure 7.6. 'One factor at a time' analysis of effect of independent variables on the response, ZP.

7.4.1.1.1.4 Optimization of screening process for preparation of ANCs

The optimal desirability value for the output variables was constrained, to determine the optimum required value of independent variables. The composite desirability value after weighing the optimal desirability was predicted by the software, closer the value to 1, better is the experimental design. The optimization validation was performed based on the numerical optimization technique using the desirability approach. The optimization was performed by applying constraints during the factorial study with an objective of achieving maximum ZP of formulation while keeping the PS and PDI at minimum for the optimized formulation. The desirability value was 0.974 for the predicted input and output responses generated and suggested by the PBD design. Three replicate batches of

the optimized formulation with desired response, as suggested by the design, were finally prepared and the mean values of the results were presented in the Table 7.15. Low bias values validated the reliability of the applied PBD model for the screening purpose.

Table 7.15. Optimization validation of PBD.

Independent variables	**Predicted input levels**		
X_1 = A = Drug concentration (%w/v)	100.05		
X_2 = B = AA2G concentration (%w/v)	199.85		
X_3 = C = S/AS (Solvent:Antisolvent ratio)	0.07		
X_4 = D = RPM (magnetic stirring)	1000		
X_5 = E = Temperature (˚C)	28.04		
X_6 = F = Solvent type	Acetone		
X_7 = G = Homogenization time (min)	36.19		
X_8 = H = Batch size (mL)	10		
X_9 = J = Stirring time (min)	29.74		
X_{10} = K = Homogenization speed (rpm)	14997.2		
X_{11} = L = Sonication (5 min intermittent)	Yes		
Dependent variables (Responses)	**Predicted output**	**Experimental output**	**% Bias**
Y_1 = Particle Size (nm)	642.14	636.72	0.844053
Y_2 = Polydispersity Index	0.15	0.16	-6.66667
Y_3 = Zeta potential (mV)	22.53	21.44	4.837994

7.4.1.1.2 BBD for optimizing the preparation of ANCs

A total of 17 batches of ANCs were prepared by varying the three independent variables, i.e. AA2G:Eze ratio (X_1 or A), homogenization speed (X_2 or B) and organic phase/aqueous phase ratio or otherwise, the Solvent:Antisolvent ratio, S/AS (X_3 or C)

for all possible combinations as per design matrix generated by BBD. The results obtained for the dependent variables such as PS (Y_1), PDI (Y_2) and ZP (Y_3) of ANCs, from the so performed experiments were summarized in Table 7.16.

Table 7.16. BBD experimental runs.

Run No.	Independent variables (coded levels)			Dependent variables		
	X_1	X_2	X_3	Y_1	Y_2	Y_3
Factorial points						
1	- 1	- 1	0	1256.25	0.39	17
2	1	- 1	0	1189.25	0.35	22.4
3	- 1	1	0	1250.75	0.36	18
4	1	1	0	1109.75	0.29	22.7
5	- 1	0	- 1	1140	0.33	17.5
6	1	0	- 1	1033.13	0.28	22.8
7	- 1	0	1	1176.87	0.34	17.2
8	1	0	1	1064	0.29	22
9	0	- 1	- 1	804.5	0.25	20.98
10	0	1	- 1	752	0.21	21.54
11	0	- 1	1	828	0.27	20.94
12	0	1	1	795.5	0.22	22
Centre points						
13	0	0	0	620	0.12	21.24
14	0	0	0	614	0.11	21
15	0	0	0	624	0.11	20.86
16	0	0	0	626	0.13	22
17	0	0	0	618	0.12	20.56

Regression models and polynomial equations showing the main as well as the interactive effects of the various independent variables on dependent variables were

generated by the results of the experimental design with the help of Design-Expert software. The positive sign in polynomial equation suggests a synergistic effect whereas the negative sign indicates an inverse effect. Three-dimensional response surface plots were constructed using respective polynomial equations to reveal the interactive effect of any two independent variables on a given dependent variable, graphically, keeping the third one at a constant level.

7.4.1.1.2.1 Influence of BBD independent variables on PS (Y_1)

The *sequential model sum of squares test* selects the highest order polynomial where the additional terms are significant and the model is not aliased. The *sequential sum of squares test* suggested the quadratic model as the best to explain the variations in the response, PS of ANCs. The *lack of fit test* selects that desirable model which has an insignificant lack-of-fit. Non-significant lack of fit is what is required as the model needs to fit.

The quadratic model best passed the test to explain the variations in the response, PS of ANCs. The ANOVA data of - sequential model sum of squares test, lack of fit test, response surface quadratic BBD model; and the statistics summary of the BBD model, for analysing the response, PS of ANCs, were given in Tables, 7.17, 7.18, 7.19 and 7.20, respectively. The model F-value of 7111.81 implies the model is significant. There is only a 0.01% chance that a "Model F-Value" this large could occur due to noise. The factors with the values of "Prob > F" less than 0.05 indicate model terms are significant. In this case A, B, C, AB, BC, A^2, B^2, C^2 are significant model terms. All the remaining model terms are not significant. Model reduction by not counting the insignificant model terms may improve the predictability of the model. The "Lack of Fit F-value" of 0.25 implies the lack-of-fit is not significant relative to the pure error. There is a 85.61%

chance that a "Lack of Fit F-value" this large could occur due to noise. Non-significant lack of fit is a desirable characteristic.

Table 7.17. ANOVA data of sequential model sum of squares test applied to select an appropriate BBD model for analysing the response, PS of ANCs.

Source	**Sum of Squares**	**df**	**Mean Square**	**F Value**	***p*-value (Prob > F)**
Mean vs Total	1.414E+007	1	1.414E+007		
Linear vs Mean	28752.05	3	9584.02	0.13	0.9410
2FI vs Linear	1478.00	3	492.67	5.122E-003	0.9995
Quadratic vs 2FI	**9.618E+005**	**3**	**3.206E+005**	**20685.29**	**< 0.0001**
Cubic vs Quadratic	17.30	3	5.77	0.25	0.8561
Residual	91.20	4	22.80		
Total	1.513E+007	17	8.899E+005		

Table 7.18. ANOVA data of lack of fit test applied to select an appropriate BBD model for analysing the response, PS of ANCs.

Source	**Sum of Squares**	**df**	**Mean Square**	**F Value**	***p*-value (Prob > F)**
Linear	9.633E+005	9	1.070E+005	4694.61	< 0.0001
2FI	9.619E+005	6	1.603E+005	7031.11	< 0.0001
Quadratic	**17.30**	**3**	**5.77**	**0.25**	**0.8561**
Cubic	0.000	0			
Pure Error	91.20	4	22.80		

Table 7.19. ANOVA for the selected response surface quadratic BBD model for analysing the response, PS of ANCs.

Source	**Coefficient Estimate**	**F Value**	***p*-value (Prob > F)**	**Remark**
Constant	620.40			
A	-53.47	1475.54	< 0.0001	Significant
B	-21.25	233.07	< 0.0001	Significant
C	16.84	146.41	< 0.0001	Significant
AB	-18.50	88.33	< 0.0001	Significant
AC	-1.50	0.58	0.4709	Not significant
BC	5.00	6.45	0.0387	Significant
A^2	444.80	53746.06	< 0.0001	Significant
B^2	136.30	5046.72	< 0.0001	Significant
C^2	38.30	398.49	< 0.0001	Significant

Table 7.20. Statistics summary of the quadratic response surface BBD model for analysing the response, PS of ANCs.

Statistic	**F Value**	***p*-value (Prob > F)**	**Remark**
Model	7111.81	< 0.0001	Significant
Lack of Fit	0.25	0.8561	Not significant
R-Squared			0.9999
Adj R-Squared			0.9998
Pred R-Squared			0.9996
Adeq Precision			211.067
C.V. %			0.43
PRESS			419.25

The aim of the experimental design approach is to focus on the model maximizing the "Adjusted R-Squared" and the "Predicted R-Squared". The "Pred R-Squared" of 0.9996 is in reasonable agreement with the "Adj R-Squared" of 0.9998. "Adeq Precision" measures the signal to noise ratio. A ratio greater than 4 is desirable. The obtained ratio of 211.067 indicates an adequate signal. So, the model was used to navigate the design space.

By varying the levels of independent variables in their limits, the PS of ANCs was obtained in the range of 614 to 1256.25 nm. The second-order polynomial equation describing an empirical relationship between particle size (Y_1) and independent variables, generated by multiple linear regressions can be given as follows in terms of actual factors:

PS = + 3829.50000 - 3548.33500 * AA2G:Eze - 0.16241 * Homogenization speed - 2967.15000 * S/AS - 7.40000E-003 * AA2G:Eze * Homogenization speed + 0.020000 * Homogenization speed * S/AS + 1779.20000 * AA2G:Eze^2 + 5.45200E-006 * Homogenization speed^2 + 15320.00000 * S/AS^2

The equation suggests that the PS values were negatively influenced by all the three factors, AA2G:Eze ratio, homogenization speed and S/AS. Accordingly, all the factors were considered at optimal high levels, in order that a desired minimum optimal PS was achieved. The high R^2 value (0.9999) indicates reasonable agreement between predicted and experimental values (99.99% of variation in PS may be best explained by the applied independent variables).

The contour plots and response surface plots to study the effect of any two independent variables applied using BBD on the response, PS of ANCs were given in Figure 7.7.

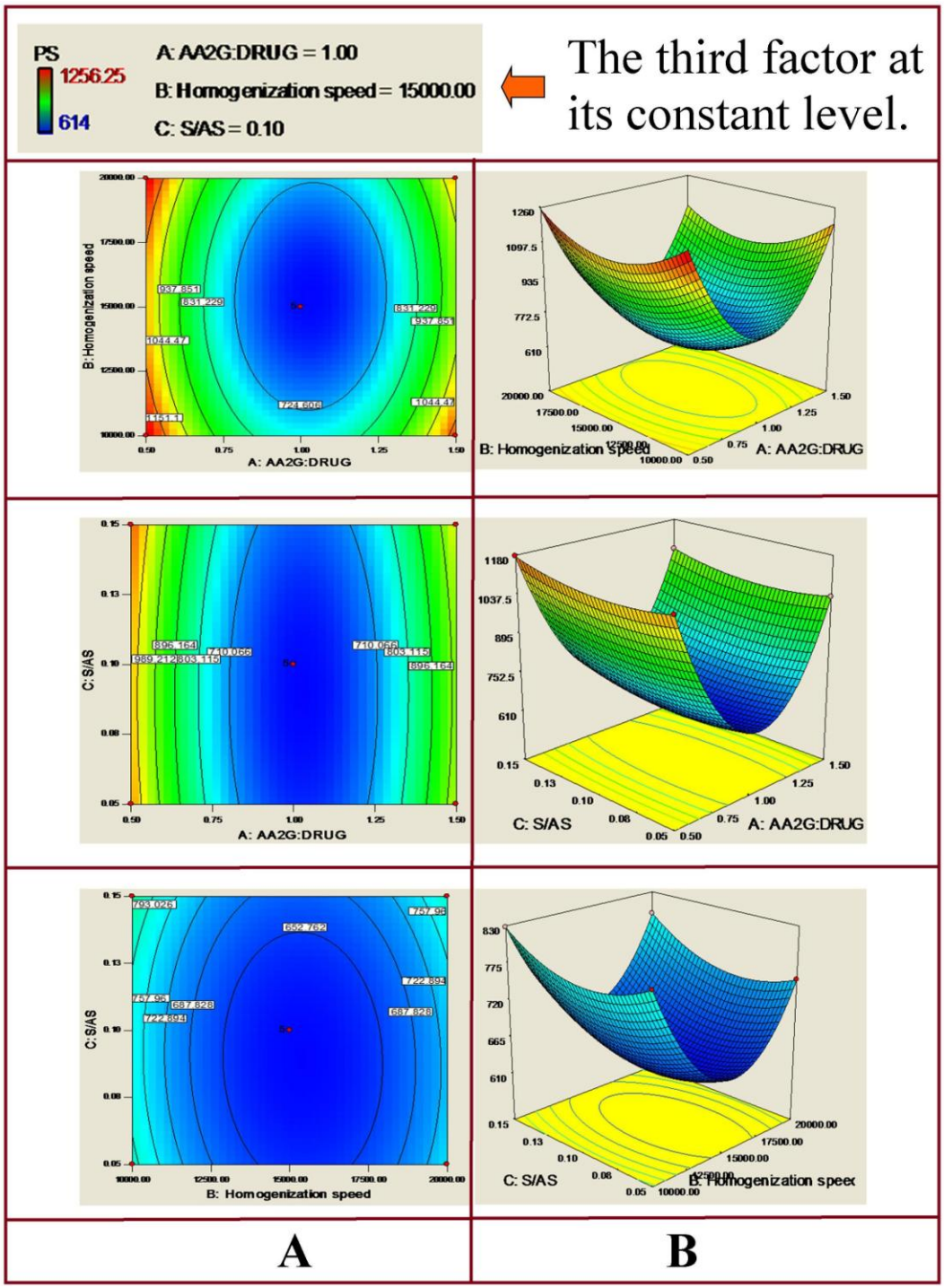

Figure 7.7. A. Contour plots and B. Response surface plots - showing effect of any two independent variables applied using BBD on the response, PS.

A monotonous decrement in PS was observed with an increase in stabilizer concentration (AA2G with respect to drug) which might be due to reduction of interfacial tension between aqueous and organic phase, which resulted in smaller size particles. Likewise, organic to aqueous phase ratio (S/AS) holds inverse proportionality with PS. Increase in organic to aqueous phase ratio lead to decrease in PS due to prevention of NC particles aggregation as a result of presence of the large amount of organic solvent to keep the drug in solubilized form, which imparted higher shear stress to break down the larger NC droplets. Very similarly, an increase in homogenization speed could have certainly achieved a smaller PS.

7.4.1.1.2.2 Influence of BBD independent variables on PDI (Y_2)

The *sequential model sum of squares test* selects the highest order polynomial where the additional terms are significant and the model is not aliased. The *sequential sum of squares test* suggested the quadratic model as the best to explain the variations in the response, PDI of ANCs. The *lack of fit test* selects that desirable model which has an insignificant lack-of-fit. Non-significant lack of fit is what is required as the model needs to fit. The quadratic model best passed the test to explain the variations in the response, PDI of ANCs. The model F-value of 382.31 implies the model is significant. There is only a 0.01% chance that a "Model F-Value" this large could occur due to noise.

The ANOVA data of - sequential model sum of squares test, lack of fit test, response surface quadratic BBD model; and the statistics summary of the BBD model, for analysing the response, PDI of ANCs, were given in Tables, 7.21, 7.22, 7.23 and 7.24, respectively.

Table 7.21. ANOVA data of sequential model sum of squares test applied to select an appropriate BBD model for analysing the response, PDI of ANCs.

Source	**Sum of Squares**	**df**	**Mean Square**	**F Value**	***p*-value (Prob > F)**
Mean vs Total	1.02	1	1.02		
Linear vs Mean	9.875E-003	3	3.292E-003	0.30	0.8214
2FI vs Linear	2.500E-004	3	8.333E-005	5.948E-003	0.9993
Quadratic vs 2FI	**0.14**	**3**	**0.047**	**1069.46**	**< 0.0001**
Cubic vs Quadratic	2.500E-005	3	8.333E-006	0.12	0.9442
Residual	2.800E-004	4	7.000E-005		
Total	1.17	17	0.069		

Table 7.22. ANOVA data of lack of fit test applied to select an appropriate BBD model for analysing the response, PDI of ANCs.

Source	**Sum of Squares**	**df**	**Mean Square**	**F Value**	***p*-value (Prob > F)**
Linear	0.14	9	0.016	222.33	< 0.0001
2FI	0.14	6	0.023	332.90	< 0.0001
Quadratic	**2.500E-005**	**3**	**8.333E-006**	**0.12**	**0.9442**
Cubic	0.000	0			
Pure Error	2.800E-004	4	7.000E-005		

Table 7.23. ANOVA for the selected response surface quadratic BBD model for analysing the response, PDI of ANCs.

Source	Coefficient Estimate	F Value	*p*-value (Prob > F)	Remark
Constant	0.12			
A	-0.026	126.52	< 0.0001	Significant
B	-0.023	92.95	< 0.0001	Significant
C	6.250E-003	7.17	0.0316	Significant
AB	-7.500E-003	5.16	0.0573	Not significant
AC	0.000	0.000	1.0000	Not significant
BC	-2.500E-003	0.57	0.4735	Not significant
A^2	0.15	2203.38	< 0.0001	Significant
B^2	0.078	595.49	< 0.0001	Significant
C^2	0.041	162.44	< 0.0001	Significant

Table 7.24. Statistics summary of the quadratic response surface BBD model for analysing the response, PDI of ANCs.

Statistic	F Value	*p*-value (Prob > F)	Remark
Model	382.31	< 0.0001	Significant
Lack of Fit	0.12	0.9442	Not significant
R-Squared			0.9980
Adj R-Squared			0.9954
Pred R-Squared			0.9944
Adeq Precision			53.480
C.V. %			2.69
PRESS			8.375E-004

The factors with the values of "Prob > F" less than 0.05 indicate model terms are significant. In this case A, B, C, A^2, B^2, C^2 are significant model terms. All the remaining model terms are not significant. Model reduction by not counting the insignificant model terms may improve the predictability of the model. The "Lack of Fit F-value" of 0.12 implies the lack-of-fit is not significant relative to the pure error. There is a 94.42% chance that a "Lack of Fit F-value" this large could occur due to noise. Non-significant lack of fit is a desirable characteristic. The "Pred R-Squared" of 0.9944 is in reasonable agreement with the "Adj R-Squared" of 0.9954. "Adeq Precision" measures the signal to noise ratio. A ratio greater than 4 is desirable. The obtained ratio of 53.480 indicates an adequate signal. So, the model was used to navigate the design space.

The PS distribution of ANCs was obtained in the range of 0.11 to 0.39 for selected levels and combinations of different variables. The polynomial equation for PDI in terms of actual independent variables was obtained as follows.

PDI = + 1.64000 - 1.21550 * AA2G:Eze - 9.47000E-005 * Homogenization speed - 3.00500 * S/AS + 0.60400 * $AA2G:Eze^2$ + 3.14000E-009 * Homogenization $speed^2$ + 16.40000 * S/AS^2

The equation suggests that the PDI values were negatively influenced by all the three factors, AA2G:Eze ratio, homogenization speed and S/AS. Accordingly, all the factors were considered at an optimal high levels, in order that a desired minimum optimal PDI was achieved. The R^2 value of 0.9980 suggests that 99.8% of variation in PDI was best explained by the applied formulation and process variables. The contour plots and response surface plots to study the effect of any two independent variables applied using BBD on the response, PDI of ANCs were given in Figure 7.8.

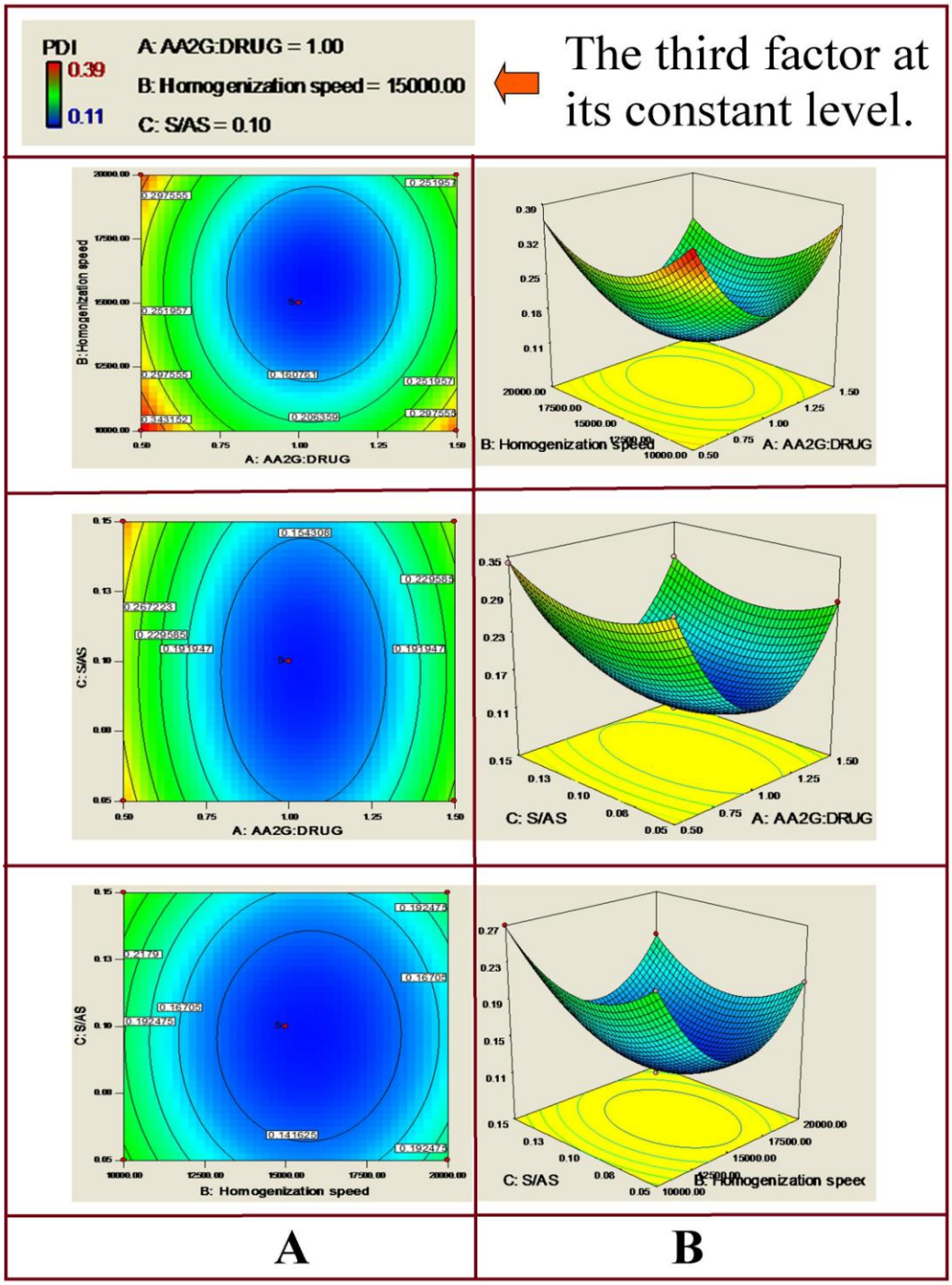

Figure 7.8. A. Contour plots and B. Response surface plots - showing effect of any two independent variables applied using BBD on the response, PDI.

More homogenous NCs were obtained with an increase in stabilizer concentration (AA2G with respect to drug) which might be due to the same reason that resulted in smaller size particles, the reduction of interfacial tension between aqueous and organic phase. Increase in organic to aqueous phase ratio (S/AS) lead to decrease in PDI with smaller PS due to prevention of aggregation of NC particles as a result of presence of the large amount of organic solvent to keep the drug in solubilized form, which imparts higher shear stress to break down the larger NC droplets. Also, high homogenization speed could have generated homogenously dispersed smaller particles. Lack of sufficient stabilizer concentration for stabilization of newly generated NC surfaces widens the PS distribution. Whereas high surfactant concentration and organic to aqueous phase ratio (S/AS) decreases PDI by reducing interfacial tension and enforcing monodispersity.

7.4.1.1.2.3 Influence of BBD independent variables on ZP (Y_3)

The *sequential model sum of squares test* selects the highest order polynomial where the additional terms are significant and the model is not aliased. The *sequential sum of squares test* suggested the quadratic model as a suitable model to explain the variations in the response, ZP of ANCs. The *lack of fit test* selects that desirable model which has an insignificant lack-of-fit. Non-significant lack of fit is what is required as the model needs to fit. The quadratic model best passed the test to explain the variations in the response, ZP of ANCs. Though the liner model also passed the *sequential sum of squares test*, the *sequential sum of squares test* and the *lack of fit test* together suggested the quadratic model as the best model to explain the variations in the response, ZP of ANCs. The ANOVA data of - sequential model sum of squares test, lack of fit test, response surface quadratic BBD model; and the statistics summary of the BBD model,

for analysing the response, ZP of ANCs, were given in Tables, 7.25, 7.26, 7.27 and 7.28, respectively.

Table 7.25. ANOVA data of sequential model sum of squares test applied to select an appropriate BBD model for analysing the response, ZP of ANCs.

Source	**Sum of Squares**	**df**	**Mean Square**	**F Value**	***p*-value (Prob > F)**
Mean vs Total	7235.56	1	7235.56		
Linear vs Mean	52.13	3	17.38	25.39	< 0.0001
2FI vs Linear	0.25	3	0.083	0.095	0.9609
Quadratic vs 2FI	**7.17**	**3**	**2.39**	**11.26**	**0.0045**
Cubic vs Quadratic	0.30	3	0.10	0.34	0.7991
Residual	1.18	4	0.30		
Total	7296.59	17	429.21		

Table 7.26. ANOVA data of lack of fit test applied to select an appropriate BBD model for analysing the response, ZP of ANCs.

Source	**Sum of Squares**	**df**	**Mean Square**	**F Value**	***p*-value (Prob > F)**
Linear	7.71	9	0.86	2.90	0.1591
2FI	7.47	6	1.24	4.21	0.0929
Quadratic	**0.30**	**3**	**0.10**	**0.34**	**0.7991**
Cubic	0.000	0			
Pure Error	1.18	4	0.30		

Table 7.27. ANOVA for the selected response surface quadratic BBD model for analysing the response, ZP of ANCs.

Source	**Coefficient Estimate**	**F Value**	***p*-value (Prob > F)**	**Remark**
Constant	21.13			
A	2.53	240.38	< 0.0001	Significant
B	0.37	5.02	0.0600	Not significant
C	-0.085	0.27	0.6178	Not significant
AB	-0.18	0.58	0.4722	Not significant
AC	-0.13	0.29	0.6042	Not significant
BC	0.12	0.29	0.6042	Not significant
A^2	-1.30	33.46	0.0007	Significant
B^2	0.19	0.73	0.4219	Not significant
C^2	0.042	0.034	0.8586	Not significant

Table 7.28. Statistics summary of the quadratic response surface BBD model for analysing the response, ZP of ANCs.

Statistic	**F Value**	***p*-value (Prob > F)**	**Remark**
Model	31.18	< 0.0001	Significant
Lack of Fit	0.34	0.7991	Not significant
R-Squared			0.9757
Adj R-Squared			0.9444
Pred R-Squared			0.8906
Adeq Precision			16.361
C.V. %			2.23
PRESS			6.68

The model F-value of 31.18 implies the model is significant. There is only a 0.01% chance that a "Model F-Value" this large could occur due to noise. The factors with the values of "Prob > F" less than 0.05 indicate model terms are significant. In this case A, A^2 are significant model terms. All the remaining model terms are not significant. Model reduction by not counting the insignificant model terms may improve the predictability of the model. The "Lack of Fit F-value" of 0.34 implies the lack-of-fit is not significant relative to the pure error. There is a 79.91% chance that a "Lack of Fit F-value" this large could occur due to noise. Non-significant lack of fit is a desirable characteristic. The "Pred R-Squared" of 0.8906 is in reasonable agreement with the "Adj R-Squared" of 0.9444. "Adeq Precision" measures the signal to noise ratio. A ratio greater than 4 is desirable. The obtained ratio of 16.361 indicates an adequate signal. So, the model was used used to navigate the design space.

All the factors with F values with $p < 0.05$ significantly affected the ZP. The significant model terms as per the reduced equation were as follows:

$ZP = + 11.05250 + 16.98800 * AA2G:Eze - 5.19400 * AA2G:Eze^2$

The equation suggests that the ZP values were positively influenced by AA2G:Eze ratio and not by any other factors. Accordingly, the factor, AA2G:Eze ratio was considered at an optimal high level in order that a desired maximum optimal ZP was achieved. The high R^2 value (0.9757) indicated that 97.57% of variation in ZP could be explained by the variations in formulation and process factors.

The 3D model graphs (response surface plots) for ZP as a function of formulation and process factors were constructed by holding one of the factors at a constant level. The contour plots and response surface plots to study the effect of any two independent variables applied using BBD on the response, ZP of ANCs were given in Figure 7.9.

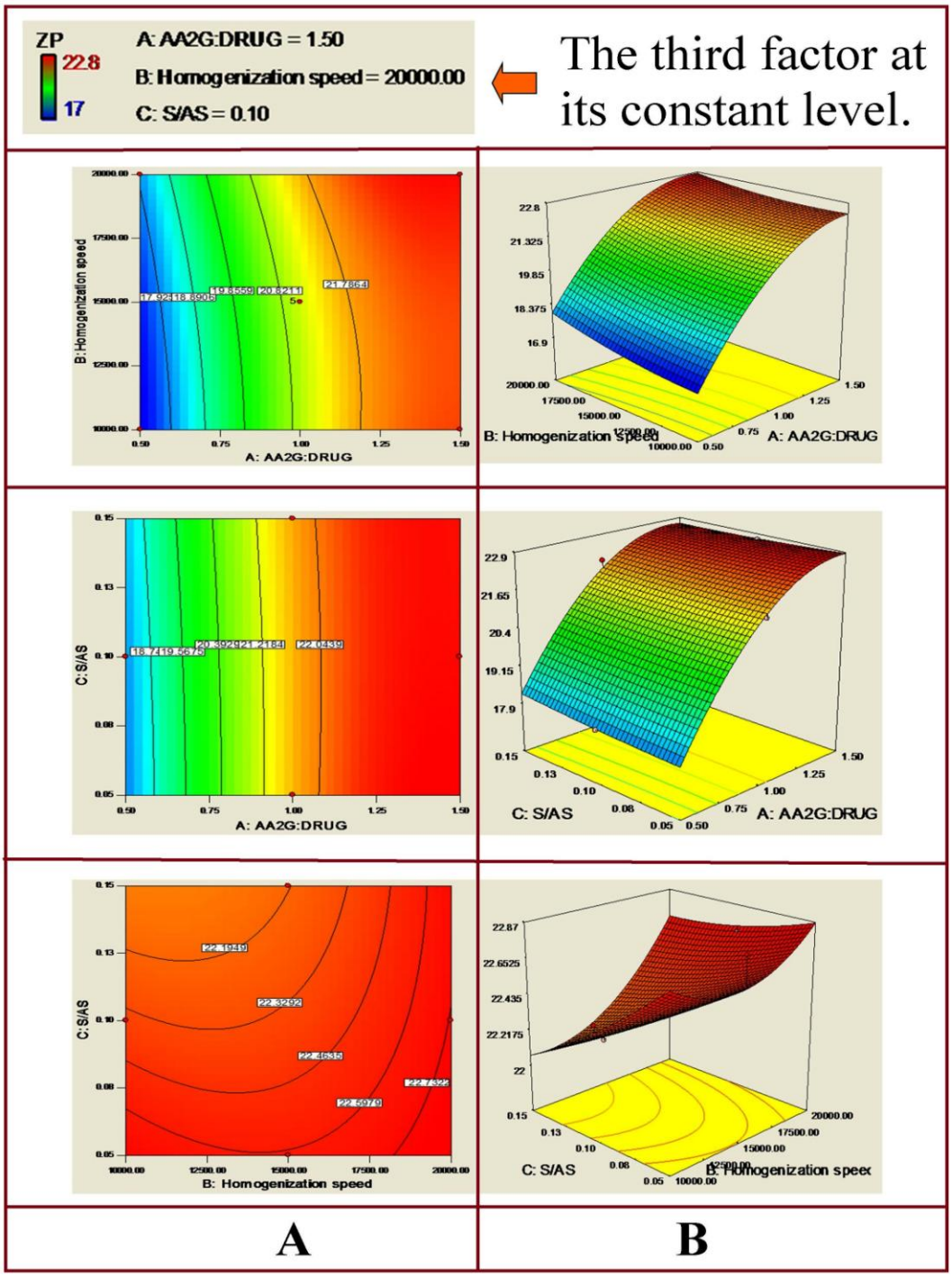

Figure 7.9. A. Contour plots and B. Response surface plots - showing effect of any two independent variables applied using BBD on the response, ZP.

The ZP values recorded for all the 17 batches ranged from a minimum of 17 to a maximum of 22.8 mV. The data clearly indicated that the mean ZP was dependent on the selected variables. However, the ZP values did not vary significantly with the changes in the homogenization speed or S/AS as ZP is a surface property which gets altered by variations in the stabilizer coating over the drug. ZP has nothing much to do with the homogenization speed or S/AS. Once the drug and stabilizer were stirred magnetically, the surface coating of stabilizer around the drug could have been already achieved to decide the electrical potential at the surface of the NCs with respect to the dispersion medium. The same was indicated by the generated regression equation where the ZP was determined soleley by the AA2G:Eze ratio factor. Single factor influence (non interactive main effect as per $p < 0.05$ test) on ZP response was further established by the relatively low R^2 value obtained for ZP response in comparison to PS and PDI. The low R^2 value suggested how the variation in ZP was influenced only up to 97.57% by the variations in the factors applied in this model (99% relation was suggested for PS and PDI as those responses were influenced by all the three applied factors).

7.4.1.1.2.4 Optimization of preparation of ANCs

On application of constraints to minimize the PS and PDI and to maximize the ZP by selecting the goals for the input independent variables as 'in range', the predicted optimum levels for the input variables were 1.12 of AA2G:Eze ratio; 16042.42 homogenization speed and 0.09 of S/AS (Solvent:Antisolvent ratio). According to the software, these predicted optimal input levels would generate responses as 630.975 nm PS, 0.119 PDI and 21.74 mV of ZP with a desirability of 0.917. These optimization values suggested by the software were matching with [indeed, relatively inferior, though not statistically significantly ($p > 0.05$), compared to] the design's own centre point

levels of the input variables. The mean PS, PDI and ZP achieved with the centre point levels of the input variables were 620.4 nm, 0.118 and 21.132 mV, respectively. So, instead of confirming the predicted values with experimental values, the ANC formulation was optimized based on the repeatability exhibited by the design's centre point levels of the input variables. Hence, the constraints were applied over again to minimize the PS and PDI and to maximize the ZP by selecting the goals for the input independent variables as 'equal to' and 'target' in order to match the centre point levels of the input variables as AA2G:Eze ratio = 1; homogenization speed = 15000 and S/AS (Solvent:Antisolvent ratio) = 0.1. Since the design facilitated replication of the formulation batch with the center point combination of independent variables, the desirability the center point combination of independent variables was examined. This time, the predicted responses were the replicates of the mean results of the all the trails performed with centre point levels of the input variables. The desirability was 0.91 with 0% bias. Therefore, the centre point levels of the input variables were considered optimum for confirmatory trials.

7.4.1.2 Optimization of the preparation of ESTNCs – application of CCD

A total of 20 batches of ESTNCs were prepared by varying the levels of the three independent variables, TPGS:Eze ratio, SLS:TPGS ratio and stirring rate (RPM) for all possible combinations as per the design matrix generated by CCD. The effect of these three independent variables on the PS, PDI and ZP of ESTNCs was studied. The range selected for each of the variables as shown in Table 7.4 was chosen based on our preliminary experiments. Table 7.29 shows the experimental results correlating the tested variables and the results, PS, PDI and ZP.

Table 7.29. CCD experimental runs.

Run No.	Independent variables (coded levels)			Dependent variables		
	X_1	X_2	X_3	Y_1	Y_2	Y_3
Factorial points						
1	- 1	- 1	- 1	735.13	0.32	28.64
2	1	- 1	- 1	790	0.42	21.24
3	- 1	1	- 1	830.16	0.4	55.7
4	1	1	- 1	566.48	0.27	32.21
5	- 1	- 1	1	673.36	0.3	29.29
6	1	- 1	1	585	0.26	20.18
7	- 1	1	1	778.4	0.32	58.5
8	1	1	1	370	0.051	32.1
Axial points						
9	- 1.682	0	0	1046.57	0.48	47.57
10	1.682	0	0	748.75	0.34	20.28
11	0	- 1.682	0	626.55	0.35	21.52
12	0	1.682	0	526	0.24	55.28
13	0	0	- 1.682	581.51	0.23	30.82
14	0	0	1.682	365	0.018	31.2
Centre points						
15	0	0	0	345	0.016	32.16
16	0	0	0	364	0.02	31.8
17	0	0	0	350	0.02	32.04
18	0	0	0	355	0.012	30.68
19	0	0	0	358	0.026	30.48
20	0	0	0	348	0.011	30.21

These three responses were individually fitted to a second order polynomial model. For each response (PS, PDI or ZP), the model which generated a higher F value was

identified as the best fitted model. Each model obtained was then validated by ANOVA. Three dimensional response surface plots were drawn for the optimization of ESTNCs. These plots are useful in studying the effects of any two factors on the response at one time, when the third factor is kept constant.

7.4.1.2.1 Influence of formulation variables and process conditions on PS (Y_1) of ESTNCs

The *sequential model sum of squares test* selects the highest order polynomial where the additional terms are significant and the model is not aliased. The *sequential sum of squares test* suggested the quadratic model as the best to explain the variations in the response, PS of ESTNCs. The *lack of fit test* selects that desirable model which has an insignificant lack-of-fit. Non-significant lack of fit is what is required as the model needs to fit. The quadratic model best passed the test to explain the variations in the response, PS of ESTNCs.

The ANOVA data of - sequential model sum of squares test, lack of fit test, response surface quadratic CCD model; and the statistics summary of the CCD model, for analysing the response, PS of ESTNCs, were given in Tables, 7.30, 7.31, 7.32 and 7.33, respectively.

The model F-value of 3657.00 implies the model is significant. There is only a 0.01% chance that a "Model F-Value" this large could occur due to noise. The factors with the values of "Prob > F" less than 0.05 indicate model terms are significant. In this case, X_1, X_2, X_3, X_{12}, X_{13}, X_1^2, X_2^2 and X_3^2 or A, B, C, AB, AC, A^2, B^2 and C^2 are significant model terms. All the remaining model terms are not significant. Model reduction by not counting the insignificant model terms may improve the predictability of the model.

Table 7.30. ANOVA data of sequential model sum of squares test applied to select an appropriate CCD model for analysing the response, PS of ESTNCs.

Source	Sum of Squares	df	Mean Square	F Value	*p*-value (Prob > F)
Mean vs Total	6.433E+006	1	6.433E+006		
Linear vs Mean	1.753E+005	3	58443.91	1.44	0.2689
2FI vs Linear	61381.97	3	20460.66	0.45	0.7206
Quadratic vs 2FI	**5.889E+005**	**3**	**1.963E+005**	**7825.30**	**< 0.0001**
Cubic vs Quadratic	0.70	4	0.18	4.198E-003	1.0000
Residual	250.13	6	41.69		
Total	7.259E+006	20	3.629E+005		

Table 7.31. ANOVA data of lack of fit test applied to select an appropriate CCD model for analysing the response, PS of ESTNCs.

Source	Sum of Squares	df	Mean Square	F Value	*p*-value (Prob > F)
Linear	6.502E+005	11	59112.39	1194.99	< 0.0001
2FI	5.889E+005	8	73606.79	1488.01	< 0.0001
Quadratic	**3.50**	**5**	**0.70**	**0.014**	**0.9999**
Cubic	2.80	1	2.80	0.057	0.8214
Pure Error	247.33	5	49.47		

Table 7.32. ANOVA for the selected response surface quadratic CCD model for analysing the response, PS of ESTNCs.

Source	Coefficient Estimate	F Value	*p*-value (Prob > F)	Remark
Constant	353.36			
A	-88.34	4248.92	< 0.0001	Significant
B	-29.84	484.88	< 0.0001	Significant
C	-64.37	2256.20	< 0.0001	Significant
AB	-79.82	2032.22	< 0.0001	Significant
AC	-35.99	413.20	< 0.0001	Significant
BC	2.32	1.71	0.2201	Not significant
A^2	192.25	21235.22	< 0.0001	Significant
B^2	78.62	3551.67	< 0.0001	Significant
C^2	42.20	1023.22	< 0.0001	Significant

Table 7.33. Statistics summary of the quadratic response surface CCD model for analysing the response, PS of ESTNCs.

Statistic	F Value	*p*-value (Prob > F)	Remark
Model	3657.00	< 0.0001	Significant
Lack of Fit	0.014	0.9999	Not significant
R-Squared			0.9997
Adj R-Squared			0.9994
Pred R-Squared			0.9995
Adeq Precision			195.497
C.V. %			0.88
PRESS			382.76

The "Lack of Fit F-value" of 0.014 implies the lack-of-fit is not significant relative to the pure error. There is a 99.99% chance that a "Lack of Fit F-value" this large could occur due to noise. Non-significant lack of fit is a desirable characteristic. The "Pred R-Squared" of 0.9995 is in reasonable agreement with the "Adj R-Squared" of 0.9994. "Adeq Precision" measures the signal to noise ratio. A ratio greater than 4 is desirable. The obtained ratio of 195.497 indicates an adequate signal. So, the model was used used to navigate the design space.

The following second order reduced quadratic model equation was derived by the best fit method to describe the relationship between the particle size (Y_1) and all the applied independent variables, TPGS:Eze ratio, SLS:TPGS ratio and stirring rate.

PS = + 1516.77472 - 1251.41724 * TPGS:Eze - 3786.48854 * SLS:TPGS - 0.33165 * Stirring rate - 3192.95000 * TPGS:Eze * SLS:TPGS - 0.14398 * TPGS:Eze * Stirring rate + 769.00398 * $TPGS:Eze^2$ + 31449.69567 * $SLS:TPGS^2$ + 1.68805E-004 * $Stirring\ rate^2$

A positive value (+) of coefficient in quadratic equation represents a synergistic effect or a direct relationship between the factors and the response, while a negative value (-) indicates an antagonistic effect or an inverse relationship between the factors and the response. The equation suggests that the PS values were negatively influenced by TPGS:Eze ratio, SLS:TPGS ratio and stirring rate. Accordingly, all the factors were considered at an optimal high levels, in order that a desired minimum optimal PS was achieved. The high R^2 value (0.9997) indicated that 99.97% of variation in PS was explained by the variations in formulation and process factors.

The contour plots and response surface plots to study the effect of any two independent variables applied using CCD on the response, PS of ESTNCs were given in Figure 7.10.

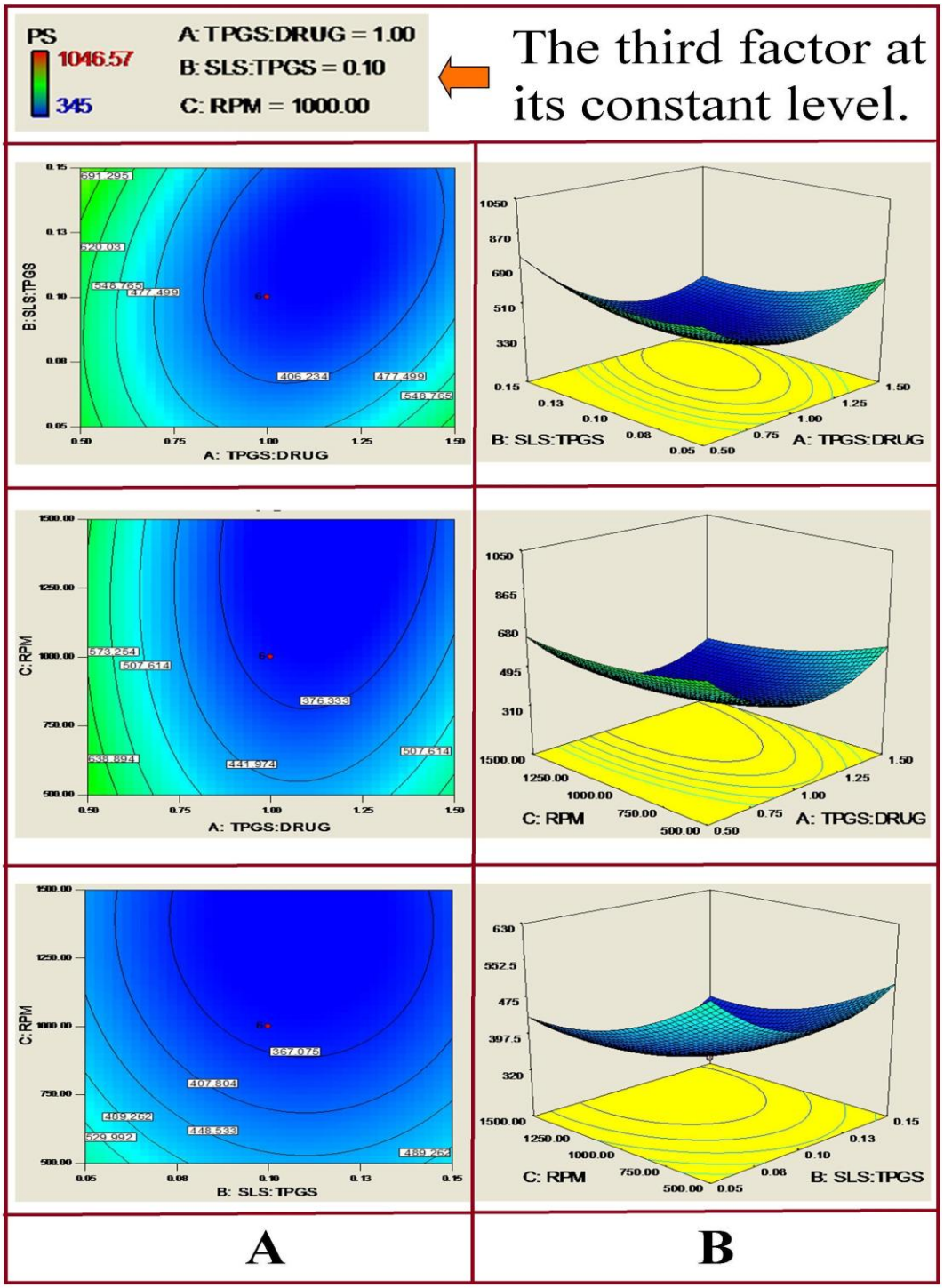

Figure 7.10. A. Contour plots and B. Response surface plots - showing effect of any two independent variables applied using CCD on the response, PS.

The PS values recorded for all the 20 batches showed a wide variation in response i.e., the response ranged from a minimum of 345 nm to a maximum of 1046.57 nm. The data clearly indicated that the mean PS was strongly dependent on the selected variables. The 3D model graphs (response surface plots) for PS as a function of formulation and process factors were constructed by holding one of the factors at a constant level.

PS is one of the critical factors for nanosized drug delivery systems. The drug release pattern, kinetics, and stability of nanoparticles are mainly determined by their diameter measured as PS. A monotonous decrease in PS was observed with an increase in stabilizer concentration (TPGS with respect to drug) which might be due to reduction of interfacial tension between aqueous and organic phase, which resulted in smaller particles. Additionally, higher surfactant concentration (SLS:TPGS) also could have offered sufficient interfacial stabilization against coalescence to retain smaller particles. Likewise, a high stirring rate could have certainly achieved a smaller PS.

7.4.1.2.2 Influence of formulation variables and process conditions on PDI (Y_2) of ESTNCs

The *sequential model sum of squares test* selects the highest order polynomial where the additional terms are significant and the model is not aliased. The *sequential sum of squares test* suggested the quadratic model as the best to explain the variations in the response, PDI of ESTNCs. The *lack of fit test* selects that desirable model which has an insignificant lack-of-fit. Non-significant lack of fit is what is required as the model needs to fit. The quadratic model best passed the test to explain the variations in the response, PDI of ESTNCs.

The ANOVA data of - sequential model sum of squares test, lack of fit test, response surface quadratic CCD model; and the statistics summary of the CCD model, for

analysing the response, PDI of ESTNCs, were given in Tables, 7.34, 7.35, 7.36 and 7.37, respectively.

Table 7.34. ANOVA data of sequential model sum of squares test applied to select an appropriate CCD model for analysing the response, PDI of ESTNCs.

Source	**Sum of Squares**	**df**	**Mean Square**	**F Value**	***p*-value (Prob > F)**
Mean vs Total	0.84	1	0.84		
Linear vs Mean	0.090	3	0.030	1.13	0.3669
2FI vs Linear	0.038	3	0.013	0.42	0.7385
Quadratic vs 2FI	**0.39**	**3**	**0.13**	**6562.87**	**< 0.0001**
Cubic vs Quadratic	3.530E-005	4	8.826E-006	0.33	0.8488
Residual	1.606E-004	6	2.677E-005		
Total	1.36	20	0.068		

Table 7.35. ANOVA data of lack of fit test applied to select an appropriate CCD model for analysing the response, PDI of ESTNCs.

Source	**Sum of Squares**	**df**	**Mean Square**	**F Value**	***p*-value (Prob > F)**
Linear	0.42	11	0.039	1207.19	< 0.0001
2FI	0.39	8	0.048	1511.63	< 0.0001
Quadratic	**3.642E-005**	**5**	**7.283E-006**	**0.23**	**0.9346**
Cubic	1.115E-006	1	1.115E-006	0.035	0.8591
Pure Error	1.595E-004	5	3.190E-005		

Table 7.36. ANOVA for the selected response surface quadratic CCD model for analysing the response, PDI of ESTNCs.

Source	Coefficient Estimate	F Value	*p*-value (Prob > F)	Remark
Constant	0.017			
A	-0.042	1233.34	< 0.0001	Significant
B	-0.033	736.78	< 0.0001	Significant
C	-0.061	2609.23	< 0.0001	Significant
AB	-0.057	1344.20	< 0.0001	Significant
AC	-0.035	496.65	< 0.0001	Significant
BC	-0.015	90.35	< 0.0001	Significant
A^2	0.14	14190.59	< 0.0001	Significant
B^2	0.098	7098.56	< 0.0001	Significant
C^2	0.038	1049.81	< 0.0001	Significant

Table 7.37. Statistics summary of the quadratic response surface CCD model for analysing the response, PDI of ESTNCs.

Statistic	F Value	*p*-value (Prob > F)	Remark
Model	2911.02	< 0.0001	Significant
Lack of Fit	0.23	0.9346	Not significant
R-Squared			0.9996
Adj R-Squared			0.9993
Pred R-Squared			0.9990
Adeq Precision			148.121
C.V. %			2.16
PRESS			5.063E-004

The model F-value of 2911.02 implies the model is significant. There is only a 0.01% chance that a "Model F-Value" this large could occur due to noise. The factors with the values of "Prob > F" less than 0.05 indicate model terms are significant. In this case, X_1, X_2, X_3, X_{12}, X_{13}, X_{23}, X_1^2, X_2^2 and X_3^2 or A, B, C, AB, AC, BC, A^2, B^2 and C^2 are all the significant model terms.

The "Lack of Fit F-value" of 0.23 implies the lack-of-fit is not significant relative to the pure error. There is a 93.46% chance that a "Lack of Fit F-value" this large could occur due to noise. Non-significant lack of fit is a desirable characteristic. The "Pred R-Squared" of 0.9990 is in reasonable agreement with the "Adj R-Squared" of 0.9993. "Adeq Precision" measures the signal to noise ratio. A ratio greater than 4 is desirable. The obtained ratio of 148.121 indicates an adequate signal. So, the model was used to navigate the design space.

The high R^2 value (0.9996) indicated that 99.96% of variation in PDI was explained by the variations in formulation and process factors. The PDI values recorded for all the 20 batches showed a wide variation in response i.e., the response ranged from a minimum of 0.011 to a maximum of 0.48. The data clearly indicated that the mean PDI was strongly dependent on the selected variables.

The 3D model graphs (response surface plots) for PDI as a function of formulation and process factors were constructed by holding one of the factors at a constant level. The contour plots and response surface plots to study the effect of any two independent variables applied using CCD on the response, PDI of ESTNCs were given in Figure 7.11.

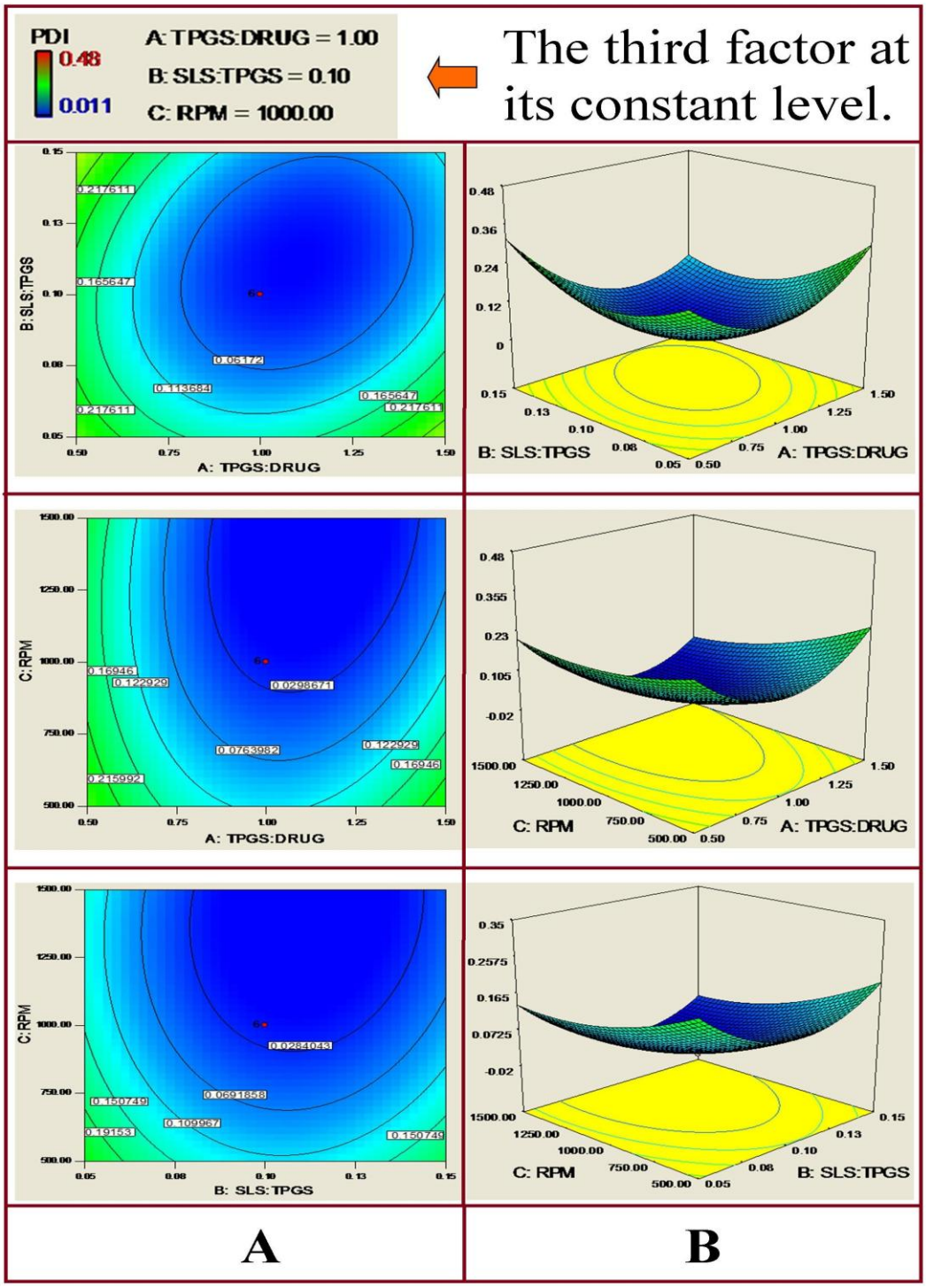

Figure 7.11. A. Contour plots and B. Response surface plots - showing effect of any two independent variables applied using CCD on the response, PDI.

The following second order reduced quadratic model equation was derived by the best fit method to describe the relationship between the PDI (Y_2) and all the applied independent variables, TPGS:Eze ratio, SLS:TPGS ratio and stirring rate.

PDI = + 0.96012 - 0.82628 * TPGS:Eze - 5.61908 * SLS:TPGS - 2.25587E-004 * Stirring rate - 2.29500 * TPGS:Eze * SLS:TPGS - 1.39500E-004 * TPGS:Eze * Stirring rate - 5.95000E-004 * SLS:TPGS * Stirring rate + 0.55558 * $TPGS:Eze^2$ + 39.29429 * $SLS:TPGS^2$ + 1.51112E-007 * $Stirring\ rate^2$

The equation suggests that the PDI values were negatively influenced by TPGS:Eze ratio, SLS:TPGS ratio and stirring rate. Accordingly, all the factors were considered at an optimal high levels, in order that a desired minimum optimal PDI was achieved.

NC fabrication results in nanosized particles whose size population often follows a multimodal distribution. The PDI is a very important dimensionless parameter that measures the width of the size distribution of particles in a nanosuspension sample. When this index is close to 1, the width of the size distribution becomes wide. A desired optimal value of PDI should be closer to 0 (0 being for monodispersed particles). Homogenously dispersed NCs were achieved with an increase in stabilizer concentration (TPGS with respect to drug) as high stabilizer amounts served to reduce the interfacial tension between aqueous and organic phase, which resulted in smaller evenly dispersed particles. Similarly, higher surfactant concentration (SLS:TPGS) also could have offered the interfacial stabilization against coalescence to retain well dispersed smaller particles. Besides, an increase in stirring rate could have also synergistically aided in achieving smaller homogenous NCs. An optimum amount of total stabilizer and surfactant concentration may reduce the surface tension of the system appropriately, leading to prolonged separation of particles. A high stirring rate

synergistically caused reduction in PS and uniform size distribution. Narrowly dispersed nanosized particles possess restricted Brownian movement making the nanoformulations kinetically stable.

7.4.1.2.3 Influence of formulation variables and process conditions on ZP (Y_3) of ESTNCs

The *sequential model sum of squares test* selects the highest order polynomial where the additional terms are significant and the model is not aliased. The *sequential sum of squares test* suggested the quadratic model as the best to explain the variations in the response, ZP of ESTNCs. The *lack of fit test* selects that desirable model which has an insignificant lack-of-fit. Non-significant lack of fit is what is required as the model needs to fit. The quadratic model best passed the test to explain the variations in the response, ZP of ESTNCs.

The ANOVA data of - sequential model sum of squares test, lack of fit test, response surface quadratic CCD model; and the statistics summary of the CCD model, for analysing the response, ZP of ESTNCs, were given in Tables, 7.38, 7.39, 7.40 and 7.41, respectively.

The model F-value of 661.60 implies the model is significant. There is only a 0.01% chance that a "Model F-Value" this large could occur due to noise. The factors with the values of "Prob > F" less than 0.05 indicate model terms are significant. In this case, X_1, X_2, X_{12}, X_{13}, X_1^2 and X_2^2 or A, B, AB, AC, A^2 and B^2 are significant model terms. All the remaining model terms are not significant. Model reduction by not counting the insignificant model terms may improve the predictability of the model. The "Lack of Fit F-value" of 0.13 implies the lack-of-fit is not significant relative to the pure error. There is a 97.86% chance that a "Lack of Fit F-value" this large could occur due to noise.

Non-significant lack of fit is a desirable characteristic. The "Pred R-Squared" of 0.9963 is in reasonable agreement with the "Adj R-Squared" of 0.9968. "Adeq Precision" measures the signal to noise ratio. A ratio greater than 4 is desirable. The obtained ratio of 83.157 indicates an adequate signal. So, the model was used to navigate the design space.

Table 7.38. ANOVA data of sequential model sum of squares test applied to select an appropriate CCD model for analysing the response, ZP of ESTNCs.

Source	**Sum of Squares**	**df**	**Mean Square**	**F Value**	***p*-value (Prob > F)**
Mean vs Total	22572.48	1	22572.48		
Linear vs Mean	2277.09	3	759.03	48.37	< 0.0001
2FI vs Linear	143.15	3	47.72	5.75	0.0100
Quadratic vs 2FI	**103.69**	**3**	**34.56**	**81.54**	**< 0.0001**
Cubic vs Quadratic	0.46	4	0.12	0.18	0.9391
Residual	3.78	6	0.63		
Total	25100.65	20	1255.03		

Table 7.39. ANOVA data of lack of fit test applied to select an appropriate CCD model for analysing the response, ZP of ESTNCs.

Source	**Sum of Squares**	**df**	**Mean Square**	**F Value**	***p*-value (Prob > F)**
Linear	247.32	11	22.48	29.97	0.0008
2FI	104.18	8	13.02	17.36	0.0030
Quadratic	**0.49**	**5**	**0.097**	**0.13**	**0.9786**
Cubic	0.027	1	0.027	0.036	0.8563
Pure Error	3.75	5	0.75		

Table 7.40. ANOVA for the selected response surface quadratic CCD model for analysing the response, ZP of ESTNCs.

Source	Coefficient Estimate	F Value	*p*-value (Prob > F)	Remark
Constant	31.23			
A	-8.22	2178.42	< 0.0001	Significant
B	9.95	3192.19	< 0.0001	Significant
C	0.21	1.47	0.2529	Not significant
AB	-4.17	328.58	< 0.0001	Significant
AC	-0.58	6.29	0.0310	Significant
BC	0.39	2.83	0.1232	Not significant
A^2	0.97	32.18	0.0002	Significant
B^2	2.56	221.96	< 0.0001	Significant
C^2	-0.058	0.11	0.7435	Not significant

Table 7.41. Statistics summary of the quadratic response surface CCD model for analysing the response, ZP of ESTNCs.

Statistic	F Value	*p*-value (Prob > F)	Remark
Model	661.60	< 0.0001	Significant
Lack of Fit	0.13	0.9786	Not significant
R-Squared			0.9983
Adj R-Squared			0.9968
Pred R-Squared			0.9963
Adeq Precision			83.157
C.V. %			1.94
PRESS			9.38

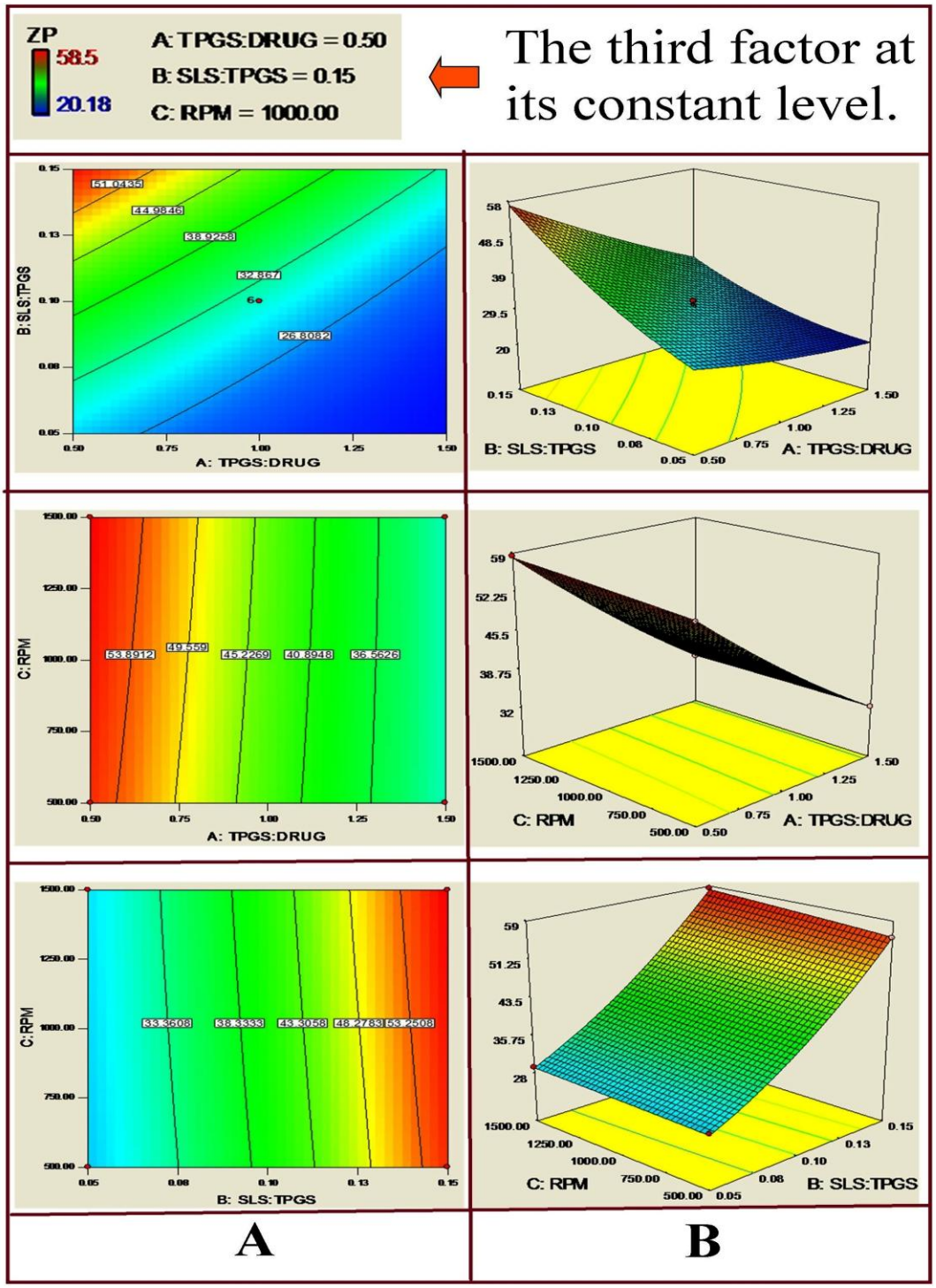

Figure 7.12. A. Contour plots and B. Response surface plots - showing effect of any two independent variables applied using CCD on the response, ZP.

The 3D model graphs (response surface plots) for ZP as a function of formulation and process factors were constructed by holding one of the factors at a constant level. The contour plots and response surface plots to study the effect of any two independent variables applied using CCD on the response, ZP of ESTNCs were given in Figure 7.12. The following second order reduced quadratic model equation was derived by the best fit method to describe the relationship between the ZP (Y_3) and all the applied independent variables, TPGS:Eze ratio, SLS:TPGS ratio and stirring rate.

ZP = + 23.76677 - 5.22866 * TPGS:Eze +146.07075 * SLS:TPGS - 166.90000 * TPGS:Eze * SLS:TPGS - 2.31000E-003 * TPGS:Eze * Stirring rate + 3.89164 * $TPGS:Eze^2$ + 1022.02429 * $SLS:TPGS^2$

The equation suggests that the ZP values were negatively influenced by TPGS:Eze ratio and positively affected by SLS:TPGS ratio. Accordingly, the factors TPGS:Eze ratio and SLS:TPGS ratio were considered at an optimal low and high levels, respectively, in order that a desired maximum optimal ZP was achieved.

The high R^2 value (0.9983) indicated that 99.83% of variation in ZP was explained by the variations in formulation and process factors. The ZP values recorded for all the 20 batches showed a wide variation in response i.e., the response ranges from a minimum of 20.18 to a maximum of 58.5 mV. The data clearly indicated that the mean ZP was strongly dependent on the selected variables.

Zeta potential is a scientific term for electrokinetic potential in colloidal dispersions and is a physical property which is exhibited by any particle in suspension. Zeta potential is a measure of the magnitude of the electrostatic or charge repulsion/attraction between particles, and is one of the fundamental parameters known to affect stability. It describes the nature of the electrostatic potential near the surface of a particle and it depends on

the properties of liquid as well as on properties of the dispersed particles. The ZP values did not vary significantly with the changes in the stirring rate. ZP is a surface property which may be altered by variations in the dispersion of the stabilizer and surfactant around the drug. Sufficient stabilizer adsorption is what decides the ZP of an NC formulation. Optimal concentrations of drug, TPGS and SLS, when dispersed by magnetic stirring, an immediate adsorption of stabilizers over the drug particles might have been achieved, and hence, the ZP was not affected by the main effect of the factor, stirring rate (RPM). The interaction effect of TPGS:Eze ratio and stirring rate (RPM) did affect the ZP negatively, though. In summary, the response ZP was determined mainly by the factors, TPGS:Eze ratio and SLS:TPGS ratio.

7.4.1.2.4 Optimization of preparation of ESTNCs

On application of constraints to minimize the PS and PDI and to maximize the ZP by selecting the goals for the input independent variables as 'in range', the predicted optimum levels for the input variables were 1.02 of TPGS:Eze ratio; 0.15 SLS:TPGS ratio and 1489.78 RPM of stirring speed. According to the software, these predicted optimal input levels would generate responses as 372.52 nm PS, 0.039 PDI and 43.65 mV of ZP with a desirability of 0.821. The mean PS, PDI and ZP achieved with the centre point levels of the input variables of the CCD were 353.33 nm, 0.02 and 31.23 mV, respectively. The optimized values suggested by the software with respect to PS and PDI were inferior (considering the constraint 'minimum' for both PS and PDI) compared to the design's own centre point levels of the input variables. The ZP was high though, meeting the requirements of the set constraint, 'maximum'.

A problem was encountered during the ESTNC formulation study, wherein the supposedly direct relation between high ZP values and stability, as per the ZP based

stability of nanoformulations theory, was not evidenced. Literature hypothesizes that the absolute ZP values above 60 mV yield excellent stability, 30 mV indicate good stability, 20 mV result in acceptable short term stability and the values less than 5 mV correspond to fast particle aggregation (valid only in cases of pure electrostatic stabilization or with surfactants of low molecular weight). The hypothesis remains invalid for high molecular weight ionic stabilizers. In general, from the industry point of view, a ZP of 20 mV achieved with a combination of electrostatic and steric stabilization effects is believed to be sufficient for maintaining a stable NC formulation [Srivalli and Mishra, 2014 and 2015a]. The results of the present work did not match with the general hypothesis, higher the ZP values, better the stability.

Observations contradicting the ZP based stability of nanoformulations theory were made during the formulation optimization of ESTNCs. The liquid formulations of the batches formulated as per the CCD generated runs showed very high sedimentation rates when the ZP were high as 47 mV which was undesirable for a stable nanoformulation. However, the ZP value of 47.57 mV was the next highest after 32.21 mV. Unfortunately, based on even the highly efficient rotatable RSM by CCD where the experimental runs were generated with five levels of each of the three factors, the definite understanding of how of much of a ZP value greater than 32.21 mV lead to sedimentation was not derived. Moreover, the batches with high ZP, equal to or above 47.57 mV presented high PS and PDI, as above 526 nm and 0.24, respectively, which were undesirable too. The CCD runs suggested that low PS and PDI were achieved with the observed optimum ZP (≈ 30 mV).

Therefore, in order to simplify the optimization validation procedure, the constraints were applied over again to minimize the PS and PDI and to maximize the ZP by

selecting the goals for the input independent variables as 'equal to' and 'target' in order to match the centre point levels of the input variables as TPGS:Eze ratio = 1; SLS:TPGS ratio = 0.1 and stirring speed (RPM) = 1000. So, with the purpose of avoiding the time consuming, laborious and uneconomical process of varying the constraint goals (based on our observation, the constraint for ZP requires to be changed as 'target ≈ 30 mV') and limits and then performing experiments for confirming the predicted values with experimental values, the ESTNC formulation was optimized based on the repeatability exhibited by the design's centre point levels of the input variables. Since the design facilitated replication of the formulation batch with the center point combination of independent variables, the desirability of the center point combination of independent variables was examined. This time, the predicted responses were close to the mean results of the all the trails performed with centre point levels of the input variables. The desirability was 0.728 with -0.05, -1.5 and 0.2% bias obtained respectively, for the responses, PS, PDI and ZP. Therefore, the centre point levels of the input variables were considered optimum for the confirmatory trials.

7.4.2 Characterization of the optimized ANCs and TNCs prepared as per confirmatory trials

7.4.2.1 Effect of stabilizer type and concentration on the PS, PDI and ZP of NCs

The results signified that the methods employed for the preparation of NCs were capable of producing nanosized Eze (Table 7.42). The nanosizing efficiency was found to be dependent on the type and concentration of stabilizer and the complex interplay of

interactions between drug – stabilizer and stabilizer – media. F3 and F8 showed significantly lower ($p < 0.05$) PS among the ANCs and TNCs, respectively.

Table 7.42. Batches of NCs prepared during confirmatory trials and their PS, PDI, and ZP results (data shown as Mean±SD and n = 3).

NCs - Batch (1% w/v drug)		AA2G %w/v	TPGS %w/v	SLS %w/v	PS	PDI	ZP
ANCs	F1	0.25			1124.4±21.26	0.623±0.27	14.86±1.96
	F2	0.5			944.2±11.17	0.209±0.16	17.57±1.26
	F3	1			624.7±10.26	0.102±0.19	20.54±1.72
PTNCs	F4		0.25		897.8±10.94	0.114±0.11	13.49±1.62
	F5		0.5		744.3±10.12	0.322±0.07	10.29±1.28
	F6		1		572.2±7.24	0.219±0.06	5.61±1.16
ESTNCs	F7		1	0.05	657.8±9.27	0.613±0.05	23.36±1.21
	F8		1	0.1	359.1±5.97	0.008±0.004	30.07±1.54
	F9		1	0.15	511.5±8.16	0.685±0.02	52.37±1.98

Note: In general, a ZP of ±20 mV is considered minimum to ensure stability [Mishra et al., 2009; Pardeike and Müller, 2010]. All the ZP values were obtained with negative sign. Only the magnitude (absolute value) of the ZP values has been reported in this table or discussed in text.

The concentration of stabilizer needs to be optimized because use of insufficient amount of stabilizer fails to provide complete surface coverage of drug molecules which is required to maintain repulsion between particles in nanosuspension and consequently creates stability problems like flocculation or crystal growth [Eerdenburgh et al., 2009; Gao et al., 2008]. Addition of ionic stabilizers causes electric repulsion and addition of non-ionic stabilizers generates steric barrier between suspended particles. Such barriers

are responsible for prevention of particle aggregation and maintenance of PS of nanoformulations [Cerdeira et al., 2012].

The adsorption of stabilizers on to the nanoparticles may be evidenced by altered surface properties and ZP of nanoparticles. In general, a ZP of ±20 mV is considered minimum to ensure stability [Mishra et al., 2009; Pardeike and Müller, 2010]. AA2G, a non-surfactant steric stabilizer and TPGS, a surfactant steric stabilizer, when used solely, provided ZP values around 20 mV and 5 mV, respectively, at concentrations equal to 100% concentration of drug. A good ZP of 30 mV was secured with the stabilizer combination, 1% w/v TPGS and 0.1% w/v SLS.

The effect of 2% and 5% concentrations of AA2G and TPGS on PS was also studied and it was observed that no further reduction in PS may be achieved with higher stabilizer concentrations. The difference in the PS at 2% or 5% concentrations of AA2G/TPGS in comparison to 1% concentration was statistically insignificant ($p > 0.05$). Also, the aim of an NC formulation was to keep the stabilizer concentration as minimum as possible. So, F3 and F8 were considered as optimized formulations and were freeze-dried for further characterization. As per crystal bridge theory, aggregation during freeze drying may occur as the tightly formed crystal bridges may combine during the primary drying phase or as the well dispersed nanoparticles in liquid suspension bind by hydrophobic interactions [Wang et al., 2005]. So, cryoprotectants are added to nanoformulations to counter balance various stresses generated from solidification process and to protect the nanoparticles against aggregation [Ploehn and Russel, 1990; Adamson and Gast, 1997].

Rank-ordering of formulations for dissolution studies and other solid state analyses was based on the PS, PDI and ZP measurements. Accordingly, both, F3 and F8 were

considered as optimized formulations. Figure 7.13 and 7.14 show the PS distribution graphs of F3 and F8, respectively.

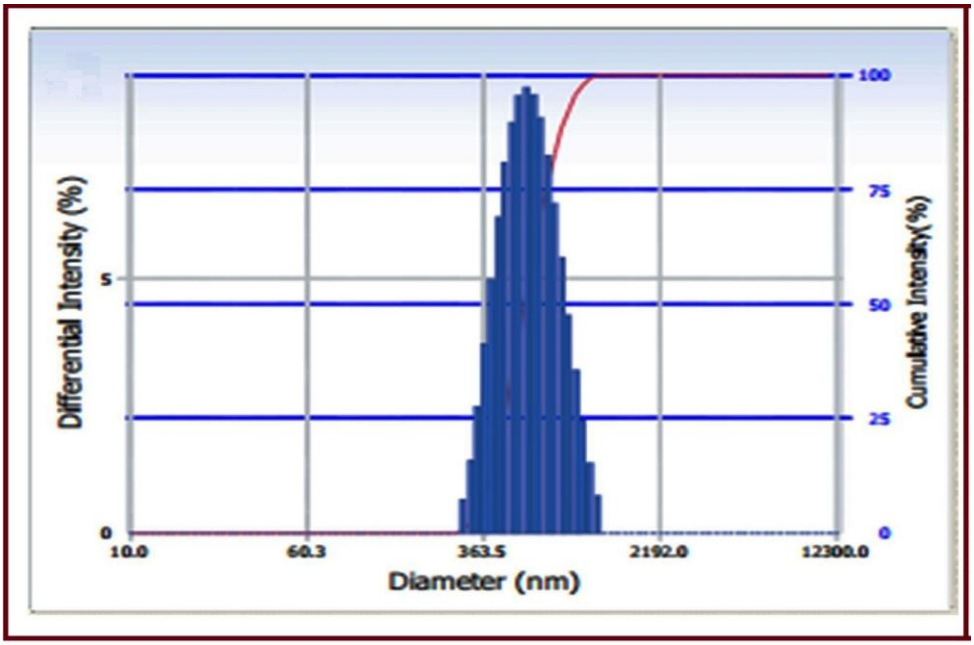

Figure 7.13. Particle size distribution graph of F3.

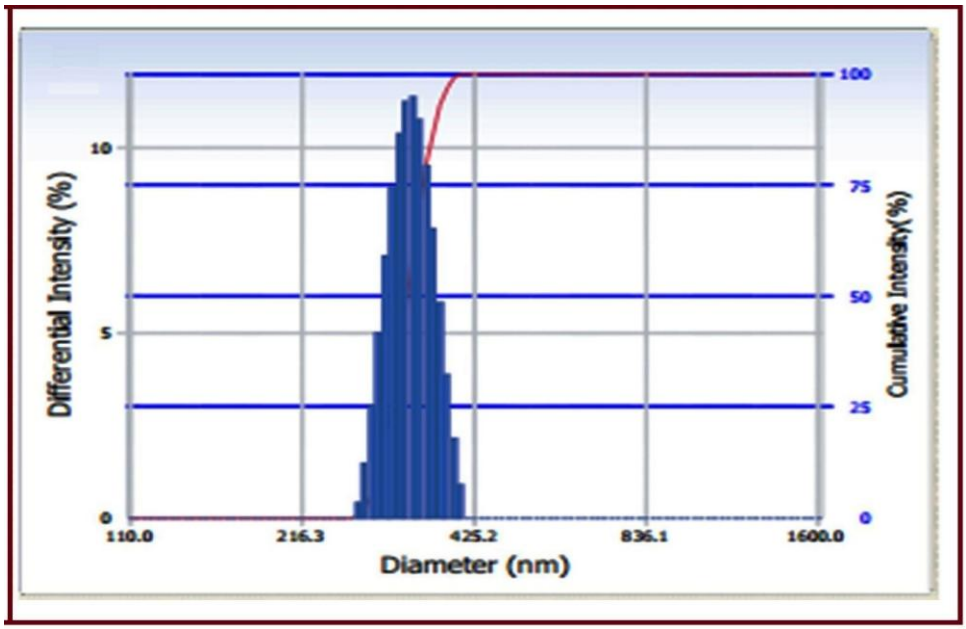

Figure 7.14. Particle size distribution graph of F8.

Mannitol at 1% w/v concentration prevented agglomeration, crystal growth and ensured complete redispersion of freeze-dried NCs. The PS and PDI values recorded after redispersing the lyophilized samples were statistically insignificant ($p > 0.05$) in comparison to the values noted before lyophilization. The PS of lyophilized F3 and F8 upon redispersion were 640.7±4.52 (PDI = 0.174±0.11) and 372.4±5.24 (PDI = 0.128±0.13), respectively.

Figure 7.15 and 7.16 show the ZP-mobility distribution graph of F8 and F3, respectively. In case of ANCs, the magnitude (irrespective of sign) of ZP values improved with the increase in AA2G concentration and since F3 exhibited low PS, PDI and high ZP, it was selected as an optimized formulation.

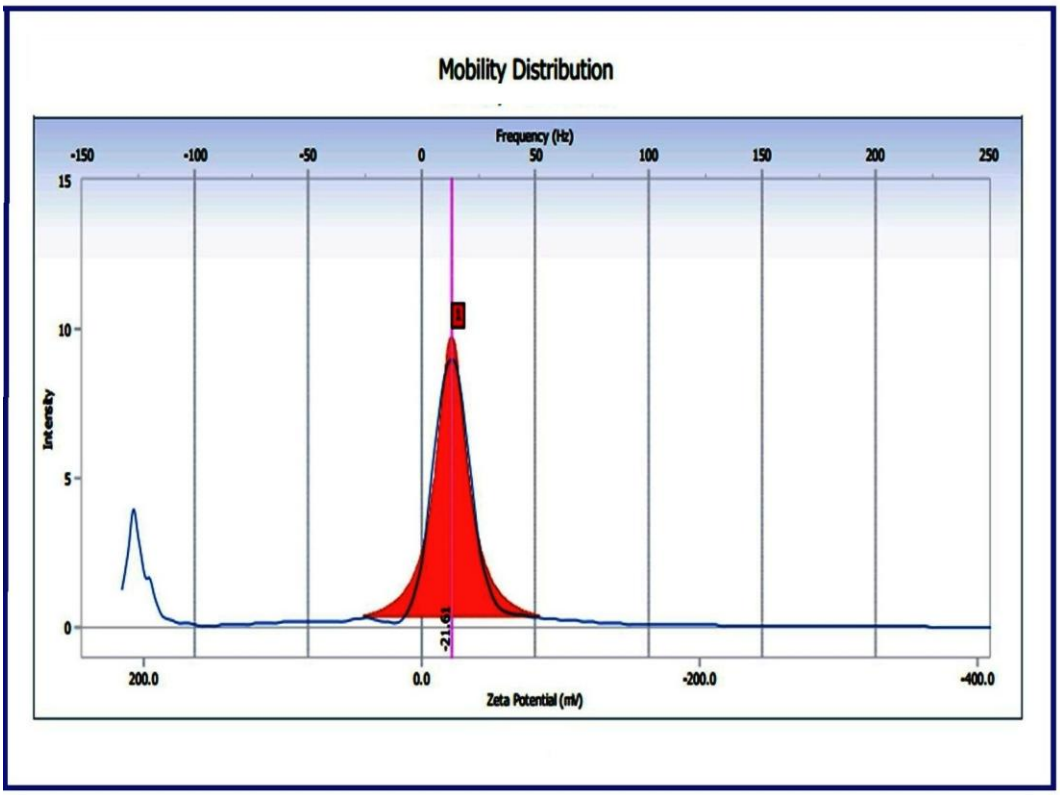

Figure 7.15. Zeta potential – mobility distribution graph of F3.

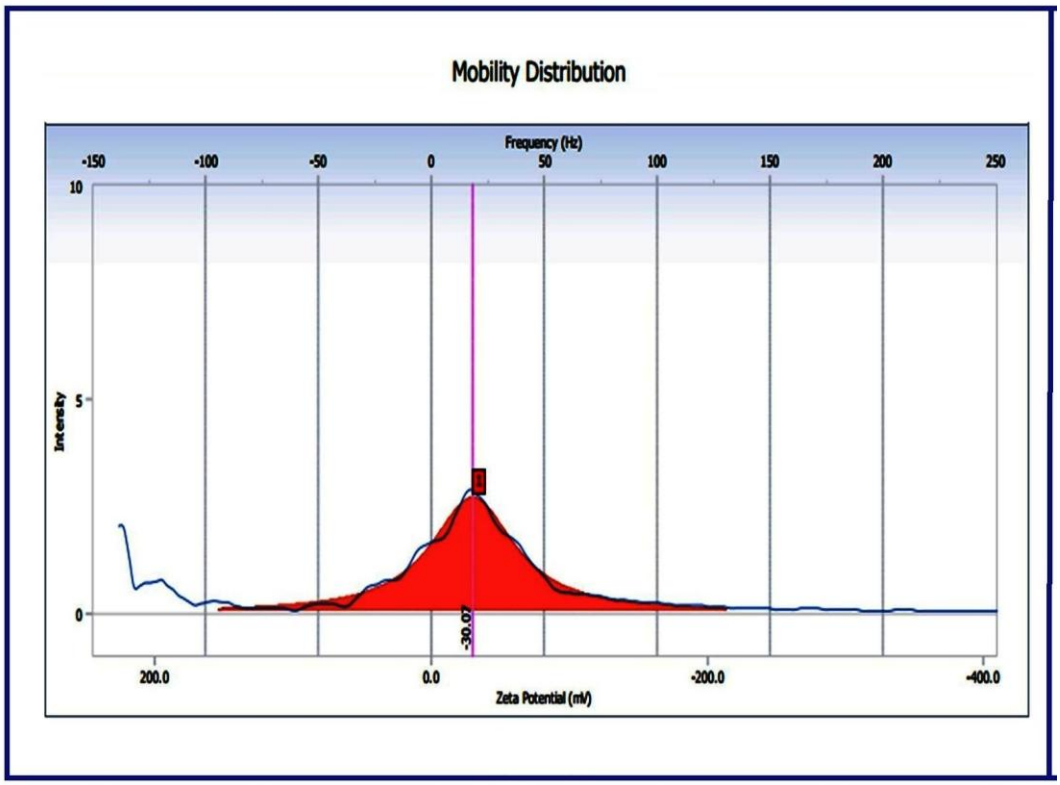

Figure 7.16. Zeta potential – mobility distribution graph of F8.

In contrast to ANCs, the magnitude (irrespective of sign) of ZP values of TNCs dropped with the increase in TPGS concentration. The reduction in ZP with increase in TPGS concentration could not be interpreted as decreased electrostatic repulsion. Instead, it may be perceived as the increase in the distance between the particle surface and the shear plane at which ZP was measured, brought about by the adsorption layer of TPGS. Similar effect of a model electrostatic stabilizer, HPMC was reported in the literature [Georgea and Ghosh, 2013]. The homogenous and effective surface adsorption of TPGS was found to be pronounced at concentration equal to 100% drug concentration in the nanosuspension as evidenced by the smaller PS generated at this concentration. Previous investigations stated that the low viscosity and high surface activity of TPGS

could lead to its superior effectiveness at high concentrations [Eerdenburgh et al., 2009; Ghosh et al., 2011]. At the same time, literature did not recommend the use of further higher concentrations of TPGS which were supposed to be associated with redispersibility problems post lyophilization. The concentration used in the present study could have been efficient in preventing any entanglement of polymer chains during lyophilization as observed by the good redispersibility. The introduction of ionic stabilizer, SLS altered the ZP magnitude in a desirable way [Ghosh et al., 2011]. SLS, as an ionic surfactant stabilizer, increased the ZP potential magnitude (irrespective of sign) of TNCs. Though SLS was studied in the concentration range 0.05 - 0.15% w/v, and an improvement in ZP magnitude (irrespective of sign) was observed with the increase in SLS concentration, the raise in the concentration of SLS was found to accelerate sedimentation problems and result in higher PS and PDI. Based on the reasonably acceptable magnitude of ZP value, F8 was considered as a stable NC formulation and was advanced for future studies. Freeze-dried F3 and F8 were further characterized as described below.

7.4.2.2 Solid state characterization

The FTIR, DSC and PXRD profiles of Eze, AA2G, TPGS, F3 and F8 were presented in Figures, 7.17, 7.18 and 7.19, respectively. The FTIR spectral patterns of the physical mixtures (PMs) were replicates of pure Eze which suggests that the API was compatible with the stabilizers employed in the study. The FTIR spectral patterns of Eze and NCs were also very similar which confirmed that Eze remained chemically stable during the nanonization process.

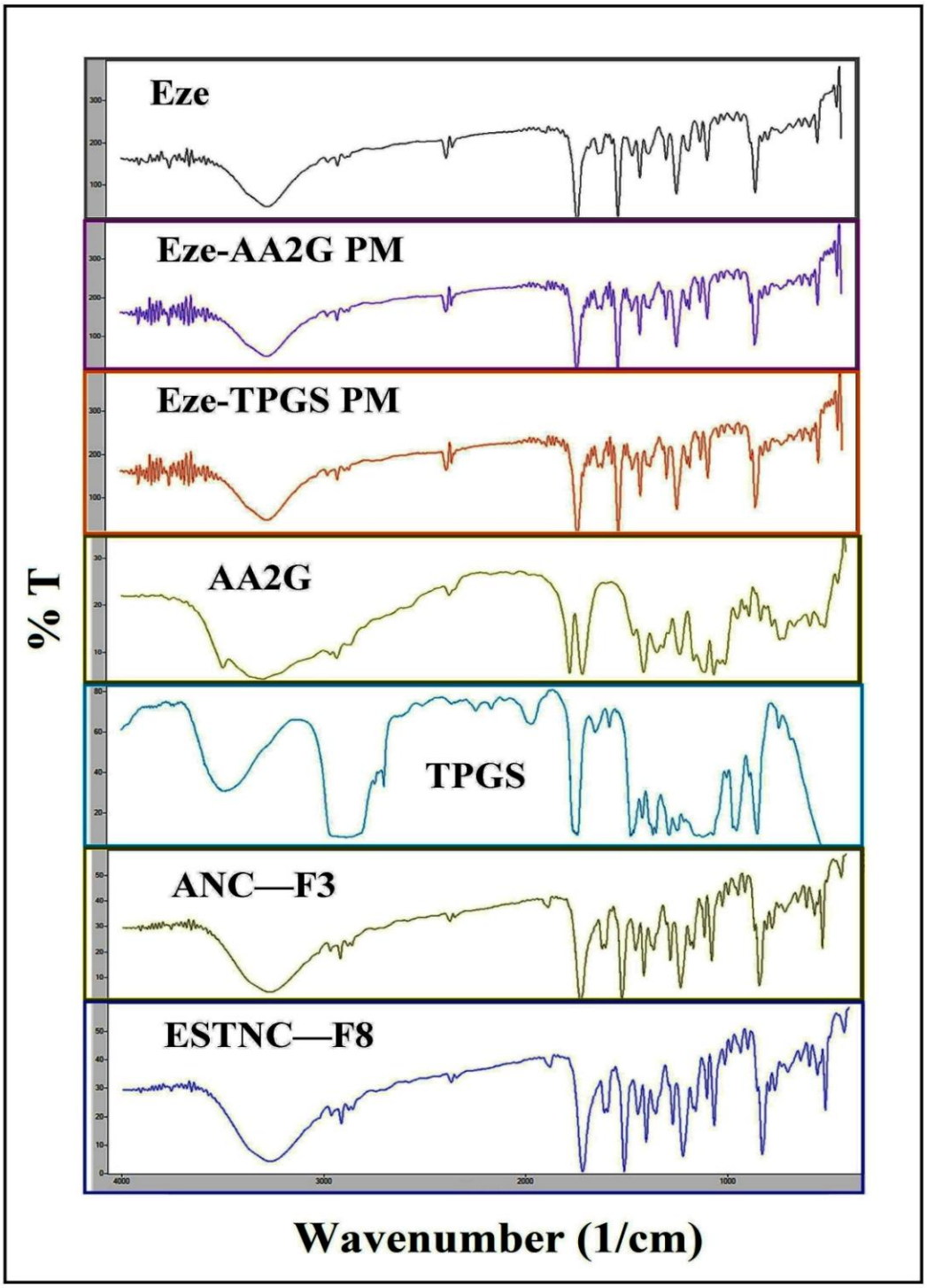

Figure 7.17. FTIR spectra of pure drug, excipients, PMs and NCs.

The retention of physical state crystallinity of the samples was confirmed by DSC analysis. DSC thermogram of Eze showed a sharp peak at 163.56 ˚C. AA2G and TPGS displayed peaks at 170.72 ˚C and 40.43 ˚C, respectively. The DSC thermogram of Eze-AA2G PM retained the peaks corresponding to both the parent components depicting the strong crystalline nature of drug and stabilizer. The thermogram of Eze-TPGS PM showed peak corresponding to Eze alone which relates to dominant crystalline nature of Eze over TPGS. The DSC patterns of both the PMs confirmed that the stabilizers did not alter the crystalline state of the drug which is an essential feature of NCs.

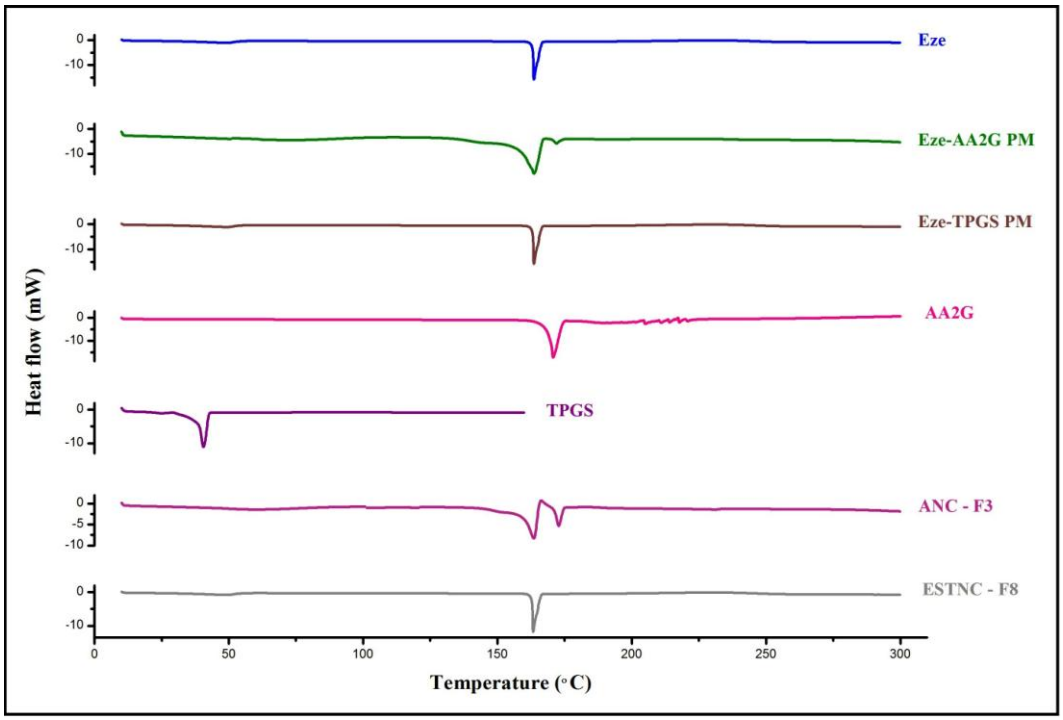

Figure 7.18. DSC thermograms of pure drug, excipients, PMs and NCs.

The DSC curve of F8 was quite identical to the curve of pure drug as depicted by a single sharp endothermic peak. The peak of F8 was observed at 161.8 ˚C. The DSC curve of F3 showed peak of Eze at 162.25 ˚C and peak of AA2G at 168.9 ˚C. TPGS is a

waxy substance, has a simple XRD profile (described below) and the drug could have been completely dispersed in it which resulted in disappearance of melting peak corresponding to TPGS in case of F8. Whereas, AA2G is a strong crystalline substance similar to Eze and therefore, F3, which ensures complete surface coating by AA2G (confirmed by SEM), retained the melting peaks of both the parent compounds. The slight shift in the melting points of NCs toward lower temperature in comparison to the peaks of the corresponding pure parent compounds could be the result of nanonization [Lai et al., 1996].

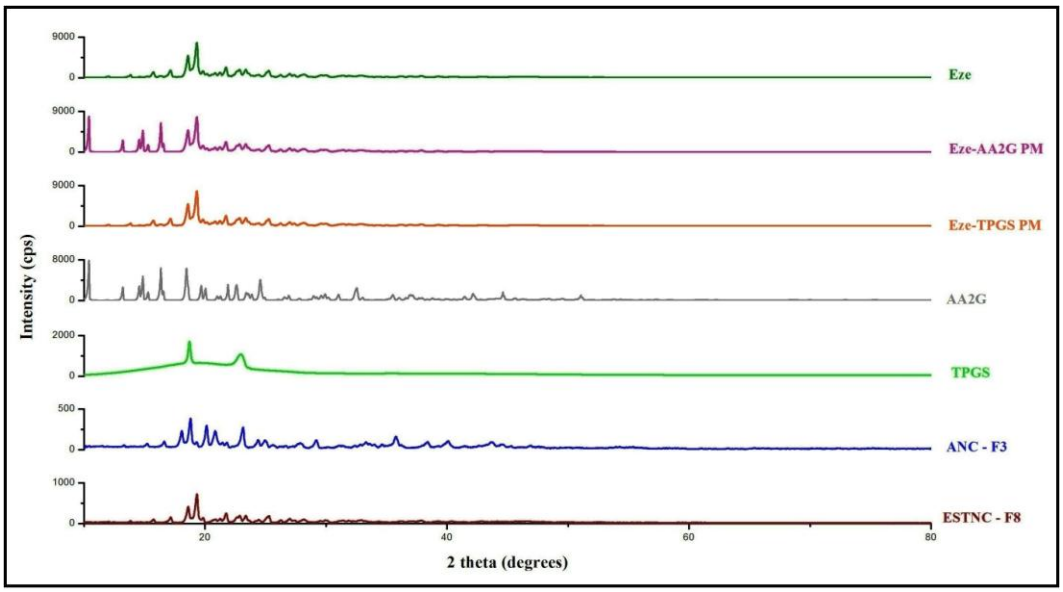

Figure 7.19. X-ray diffractograms of pure drug, excipients, PMs and NCs.

The reduction of particle dimension from micron to nano range significantly increases the surface-volume ratio and the interior "bulk" properties of a drug substance are substantially affected by the consequent surface energy changes. When compared to particles of larger dimension, nanosized particles have surface molecules in higher proportion and the nearest neighbor molecules in lower proportion. Consequently,

nanoparticles are more weakly bound and their thermal motion is less constrained when compared to the molecules in higher crystal bodies [Schmidt et al., 1998]. This alteration brought about by nanonization could be responsible for the lowering of melting point by few degrees centigrade. Similar observations were noted during the PXRD studies where nanoformulations exhibited peak broadening and reduced intensities as compared to pure Eze.

The PXRD peaks intensities of pure Eze and pure AA2G were quite predominant and high while those of TPGS were noted at low intensity range. PXRD pattern of Eze-AA2G PM retained the crystalline peaks and the corresponding intensities pertaining to both the parent components depicting the strong crystalline nature of Eze and AA2G. The PXRD pattern of Eze-TPGS PM showed peak and the corresponding intensities related to Eze alone which confirms the dominant crystalline nature of Eze over TPGS. The PXRD patterns of both the PMs further established that the stabilizers did not alter the crystalline state of the drug which is an essential feature of NCs. PXRD profiles of NCs depicted that Eze retained its crystalline nature following nanonization. Slight broadening of peaks and reduced intensity could be results of the small size of crystals and the complete surface covering offered by AA2G and TPGS. Both F3 and F8 retained their crystalline nature. The profile of F3 was found to be broadened but all the peaks corresponding to the parent Eze were retained with reduced intensity. Such profiles of NCs may be explained by the "particle size broadening" phenomenon that prevails with the PXRD patterns of crystalline materials less than 1 µm [Zhang et al., 2013]. The XRD profile of F8 was a near replicate of Eze, however, with significantly reduced intensity. This could be explained by the simple XRD profile of TPGS which

though was present in F8 in equal percent weight as drug, might not have interfered with the drug peaks.

Crystalline state is the most preferred state on account of its long term physical stability (mobility of drug particles in crystalline phase is minimal when compared to amorphous phase). Both the optimized formulations, F3 and F8 retained their crystalline nature which was also confirmed by the DSC studies. It may be concluded that the crystalline state that could be beneficial to the physicochemical stability was apparently unaltered by the preparation methods under study.

The SEM images of all the samples were presented in Figure 7.20. The AFM photographs presented in Figure 7.21 and 7.22 further established the nanosize and complete dispersion of individual particles.

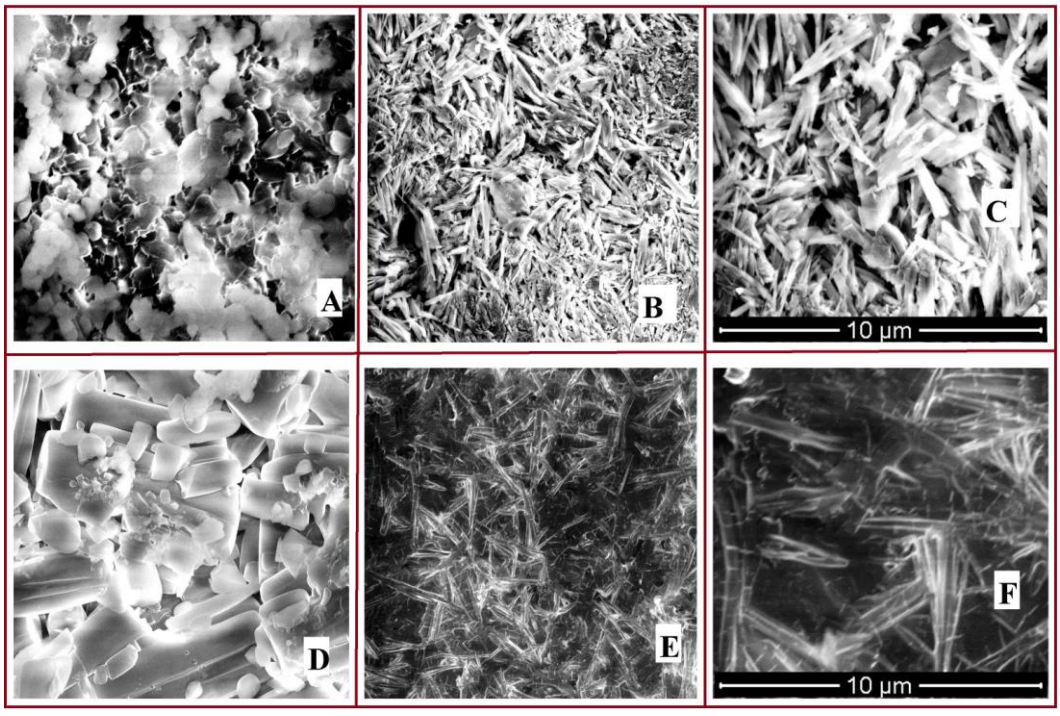

Figure 7.20. SEM images. A: Pure Eze at 2000X. B: F8 at 500X C: F8 at 2000X D: AA2G at 2000X. E: F3 at 500X. F: F3 at 2000X.

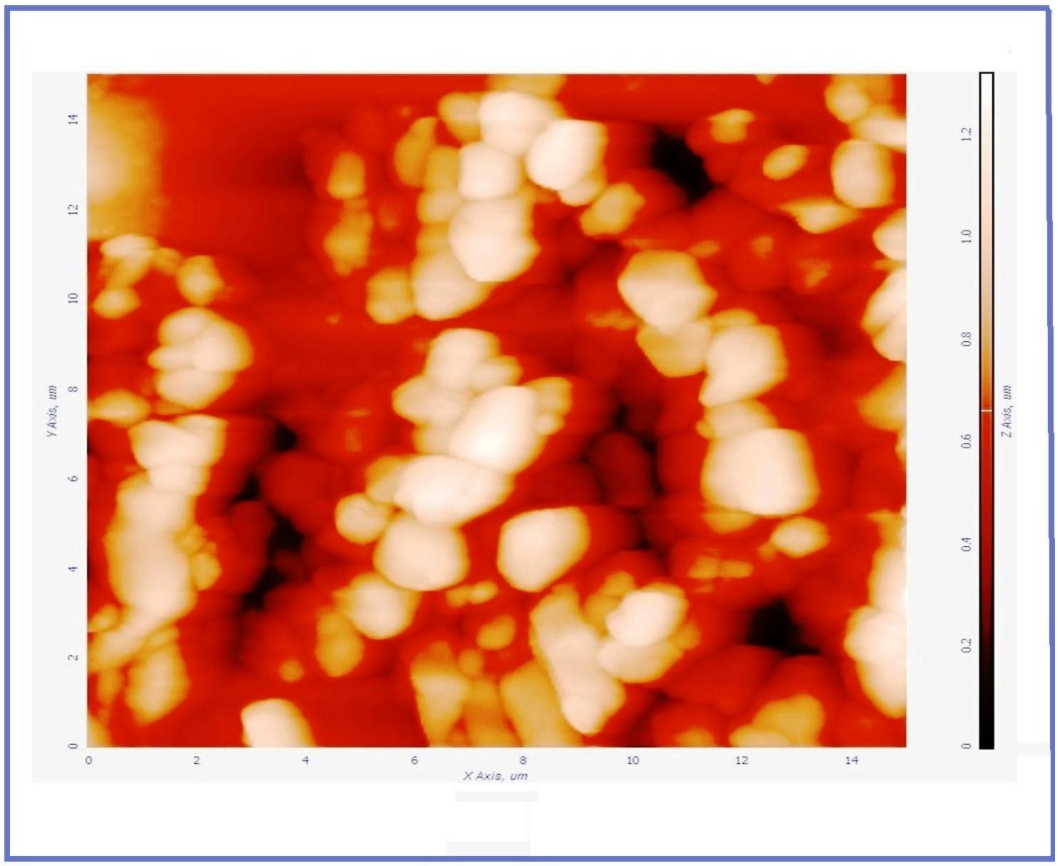

Figure 7.21. AFM picture of plain drug.

PS is one of the most important characterizations of NCs and is generally measured by routine photon correlation spectrophotometer (PCS). PCS is fast, easy to perform and yields accurate results in nano range but this analysis cannot capture larger or micron range particles. SEM also serves the purpose of PS analysis and detects larger particles in nanosuspension. The broad PS distributions in the NC system could be visualized by SEM [Ghosh et al., 2011].

The SEM studies of F3 and F8 indicated that the particles were well below 1 micron range. SEM is further a qualitative method used to visualize the microscopic surface morphology and study the surface structural properties of formulation ingredients and

the finished products. Pure Eze existed as small stone shaped crystals. The images of TPGS could not be drawn because of its waxy consistency. AA2G was observed as long crystalline cylindrical particles. The SEM microphotographs indicated that there was complete disappearance of original morphology of parent ingredients upon nanonization. The stone shaped Eze crystals transformed into cylindrical shaped drug nanoparticles. The surface coating offered by the stabilizers and the process of lyophilization could have contributed to the smoothened surface and altered morphology of drug nanoparticles.

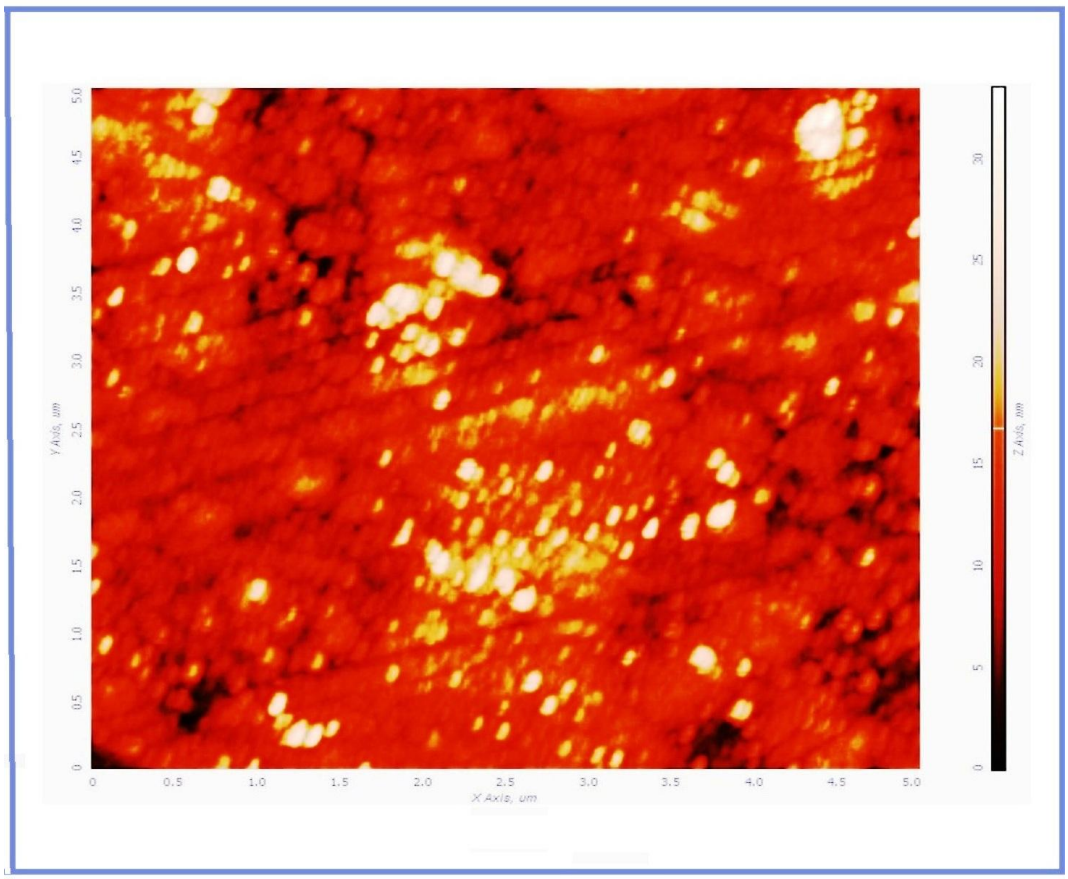

Figure 7.22. AFM picture of F8.

7.4.2.3 Drug content, saturation aqueous solubility and dissolution

Since NCs are not associated with encapsulation problems, all the formulations presented drug content above 97%. The drug content results for F3 and F8 were 99.21±1.15 and 99.78±1.08, respectively. It has been confirmed during preformulation studies that there was no interference of the employed excipients with UV-VIS drug absorption i.e. Eze analysis at 232 nm. Literature also offered supporting publications to the inferences on the non-interference of excipinets with the Eze analysis at 232 nm wavelength. TPGS presents a UV absorption λ_{max} at 284 nm in distilled water and USP acetate buffer [Wang et al., 2009]. AA2G shows a UV absorption λ_{max} at 260 nm in distilled water and USP acetate buffer [http://www.nicnas.gov.au/__data/assets/pdf_file/0016/10393/STD1056FR.pdf; Muto et al., 1990]. The saturation solubility values of pure untreated Eze and the optimized formulations, F3 and F8 were presented in Table 7.43.

Table 7.43. Saturation solubility (n = 3) and dissolution (n = 6) parameters of pure drug, PMs and optimized NCs (data shown as Mean±SD).

System	Saturation aqueous solubility (µg/mL)	DE_{60} (%)	$t_{80\%}$ (min)	$t_{90\%}$ (min)
Eze	1.99±0.62	16.23±2.49	Not achieved	Not achieved
Eze-AA2G PM	Not applicable	16.63±2.08	Not achieved	Not achieved
Eze-TPGS PM	Not applicable	17.28±1.88	Not achieved	Not achieved
ANC – F3	$16.69±0.78^{a***}$	$69.38±1.34^{b***}$	36.73±1.73	41.33±2.58
ESTNC – F8	$24.73±1.24^{@***}$	$83.03±1.27^{\#***}$	$14.29±2.66^{\$***}$	$16.07±2.32^{\$***}$

Symbols and statistical representations = ***$p < 0.001$; a = compared to pure Eze; b = compared to pure Eze, Eze-AA2G PM and Eze-TPGS PM; @ = compared to pure Eze and ANC; # = compared to pure Eze, Eze-AA2G PM, Eze-TPGS PM and ANC; $ = compared to ANC (One way ANOVA followed by Tukey's post hoc test).

The results improved in size-dependent manner. Saturation solubility increased with nanonization. Ostwald Freundlich equation relates smaller PS to higher solubility. According to Noyes Whitney equation also, the saturation solubility of particles improves with the decrease in their particle radius [Müller et al., 2001]. The increase in saturation solubility with nanonization may be also explained by Kelvin's equation which relates the strong curvature of nano sized particles to increased dissolution pressure [Buckton and Beezer, 1992; Hammond et al., 2007; Gao et al., 2007].

Though Eze contains ionisable groups [Figure 2.17 or Figure 6.1], literature suggests that the drug essentially shows a pH independent solubility characteristic across the gastrointestinal pH range. Thus, pH-based strategies to improve the solubility/dissolution characteristics (e.g. salts, addition of pH modifiers) were not a first-line option [Taupitz et al., 2013]. Also, for the same reason, the formulations in this study were optimized by studying their dissolution in just one pH media, the USP acetate buffer medium of pH 4.5, containing 0.45% w/v sodium lauryl sulphate, as suggested by the FDA Dissolution Methods Database guide for Eze.

The dissolution profiles of pure drug, PMs, F3 and F8 were shown in Figure 7.23. The results (Table 7.43) of solubility and dissolution efficiency (DE) were in the order, Eze ≈ Eze-AA2G PM ≈ Eze-TPGS PM < F3 < F8 ($p < 0.05$ for each comparison except between either of the PMs and pure Eze). Pure Eze and PMs could not achieve $t_{80\%}$. The $t_{80\%}$ and $t_{90\%}$ values of F8 were significantly higher compared to F3 ($p < 0.05$).

The enhancement in dissolution rate may be attributed to the smaller size of NCs which provides larger surface area available for dissolution and decreases the diffusion layer thickness [Hintz and Johnson, 1989]. Prandtl equation suggests a reduction in diffusion

distance and increase in dissolution velocity with the increase in particle curvature. As the curvature of a particle in liquid increases (PS decreases), its dissolution pressure increases and this influence of PS on saturation solubility comes into play when PS drops below 1 µm [Mosharraf and Nyström, 1995; Müller and Peters, 1998; Müller et al., 2001].

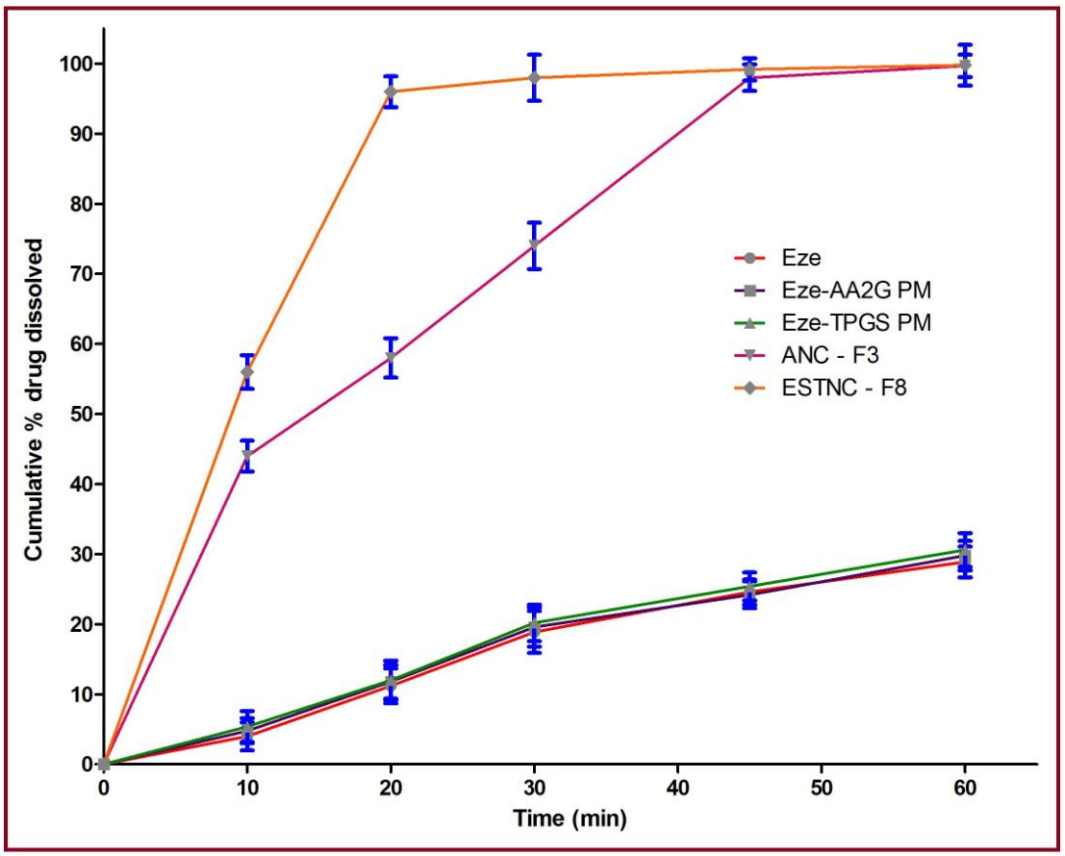

Figure 7.23. Dissolution profiles of pure drug, PMs and optimized NC formulations (vertical bars represent SD, n = 6).

The hydrophilicity of the stabilizers, AA2G and TPGS employed in the study would have not only reduced the PS but also increased the wettability and, therefore, increased the dissolution of drug from their respective formulations. The surfactant mode of

surface wetting offered by TPGS in F8 could have resulted in further enhanced dissolution as compared to pure drug and F3.

7.4.2.4 Mechanism of NC formation

NCs, in the present study, were prepared by bottom up precipitation triggered by solvent-antisolvent addition followed by ultrasonication. The mechanism of formation involves precipitation of Eze in the antisolvent with reduced size and simultaneous surface adsorption of the stabilizer on to the drug crystal surface. The surface coverage offered by stabilizers could have possibly created a layer of hydrodynamic boundary surrounding the nanoparticles inhibiting any further crystal growth and agglomeration [Raghavan et al., 2001; Zimmermann et al., 2009]. Since both, AA2G and TPGS possess hydroxyl groups capable of forming hydrogen bonding with the hydrophobic alkyl and aryl hydrogens of Eze molecule, weak intermolecular hydrophobic and hydrogen bonds are likely to form on account of the surface adsorption process and stabilizer affinity to drug crystal faces. The possibility of similar drug-stabilizer interactions have been reported in literature [Douroumis and Fahr, 2007; Peltonen and Hirvonen, 2010]. TPGS has been known as a unique stabilizer, which by virtue of its hydrophobic interactions with non-polar drug molecules, can bring about not only PS reduction but also improved dissolution [Ghosh et al., 2011].

Ultrasonication, as an energy-addition step, could have reduced the crystal size, controlled the crystal habit and PS distribution, and inhibited the particle agglomeration [Xia et al., 2010; Dhumal et al., 2009; Guo et al., 2005]. The use of high speed homogenization prior to sonication in case of F3 could have intensified the drug dispersion and diffusion of stabilizer onto the drug surface. However, in spite of

application of two energy-addition steps, the PS observed for ANCs was higher compared to TNCs. Accordingly, the saturation solubility and dissolution study results of F3 were inferior to F8. The possible reason could be the surfactant deficient nature of AA2G and consequently, the formulation could not have offered sufficient repulsive barrier and wettability to the interfacial surface of drug nanoparticles. AA2G is a completely hydrophilic molecule and lacks the amphiphilc nature of surfactant. In contrast, TPGS is a non-ionic surfactant that has successfully been in use to prepare stable NCs and to improve the solubility, dissolution and bioavailability of poorly water soluble drugs like nifedipine [Rajebahadur et al., 2006] and paclitaxel [Varma and Panchagnula, 2005]. The concentration of stabilizers was optimized equal to 100% drug concentration in the nanosuspension because use of insufficient amounts of stabilizers failed to reduce PS significantly and provide complete surface coverage of drug molecules which is required to maintain steric or electrostatic repulsion between particles in nanosuspension [Gao et al., 2008].

During NC formation, the precipitation of Eze in antisolvent creates large hydrophobic surface area which is supposed to be covered spontaneously and completely by stabilizer. Any discrepancy in such activity leads to crystal growth and agglomeration. Ultrasonication could have served to counterbalance any time-dependent insufficient adsorption of stabilizer on to the hydrophobic surface of newly formed crystal nuclei. The intensified molecular diffusion caused by ultrasonication could have lead to rapid diffusion of stabilizers to cover the increasing number of newly generated crystal surfaces and aided in the quick attainment of adsorption equilibrium. Though the low energy ultrasonication alone cannot form NCs by comminuting raw drug crystals, it was

efficient enough to break down the agglomerated crystals of nanosuspension [Xia et al., 2010; Varma and Panchagnula, 2005].

7.4.2.5 Stability

The prime aim of stability studies was to assess the storage stability of the optimized NC formulations at 30±2 ˚C/70±5% RH for 6 months. All the freshly freeze dried batches were analyzed in terms of redispersed PS, PDI, ZP, drug content, solubility and dissolution parameters, and the results were noted. For evaluating the stability, samples were drawn from the freshly prepared and stored batches after 6 months and studied for results of all the tests stated above. The protocol for each of the tests was followed as per the afore-mentioned procedures.

The NCs were redispersed and characterized for mean PS, PDI and ZP before and after 6 months stability condition storage. The observed results were tabulated in Table 7.44. The dissolution profiles of stability batches in comparison to fresh batches were shown in Figure 7.24. The statistically insignificant differences in PS, PDI and ZP indicated the highly stable nature of both the NC formulations. The stability studies revealed that both the NCs were stable over the six months study period. Besides, the stability of NCs was further tested in terms of drug content, solubility and dissolution, before and after 6 months. The results suggested that the formulations were stable with statistically insignificant changes in the studied properties.

PS and PDI are the critical factors for nanodrug delivery systems as they influence their stability, drug release properties, pharmacokinetics and absorption. Pharmaceutically superior performance of nanoparticles may be attributed to their high surface area – volume ration. However, nanoformulations tend to aggregate and agglomerate after long

periods of storage resulting in increased PS and compromised performance. The lyophilization approach followed in the preparation procedure proved to be a promising approach in ensuring the formulation stability.

Table 7.44. Stability study data of optimized NC formulations. Data shown as Mean±SD and n = 3 (n = 6 for dissolution data).

Tests		**Properties before stability storage studies**		**30±2 ˚C/70±5% RH storage evaluation after 6 months**	
		ANC – F3 (initial)	**ESTNC – F8 (initial)**	**ANC – F3 (final)**	**ESTNC – F8 (final)**
Description		Fine white powder	Fine white powder	Complies	Complies
PS		640.7±4.52	372.4±5.24	646.2±5.16	376.2±5.48
PDI		0.174±0.11	0.128±0.13	0.178±0.16	0.13±0.14
ZP		-20.52±1.68	-30.02±1.44	-20.54±1.76	-30.04±1.62
Drug content by UV (%)		99.42±1.12	99.88±1.46	99.36±1.24	99.82±1.52
Saturation aqueous solubility (10^{-3} mg/mL)		16.69±0.78	24.73±1.24	16.58±0.92	24.22±1.16
Dissolution by UV	**DE_{120} (%)**	69.38±1.34	83.03±1.27	68.27±1.46	82.22±1.08
	$t_{80\%}$ (min)	36.73±1.73	14.29±2.66	37.11±1.88	14.65±2.72
	$t_{90\%}$ (min)	41.33±2.58	16.07±2.32	41.75±2.68	16.48±2.46

No major changes in the values of PS and PDI were observed after 6 months storage and formulations were found to be stable for the studied period of time. The negligible difference in the results of ZP, drug content, solubility and dissolution tests, before and after 6 months, further confirmed the stability of NCs. Storage of both the NC

formulations, ANC-F3 and ESTNC-F8, at room temperature may be considered acceptable.

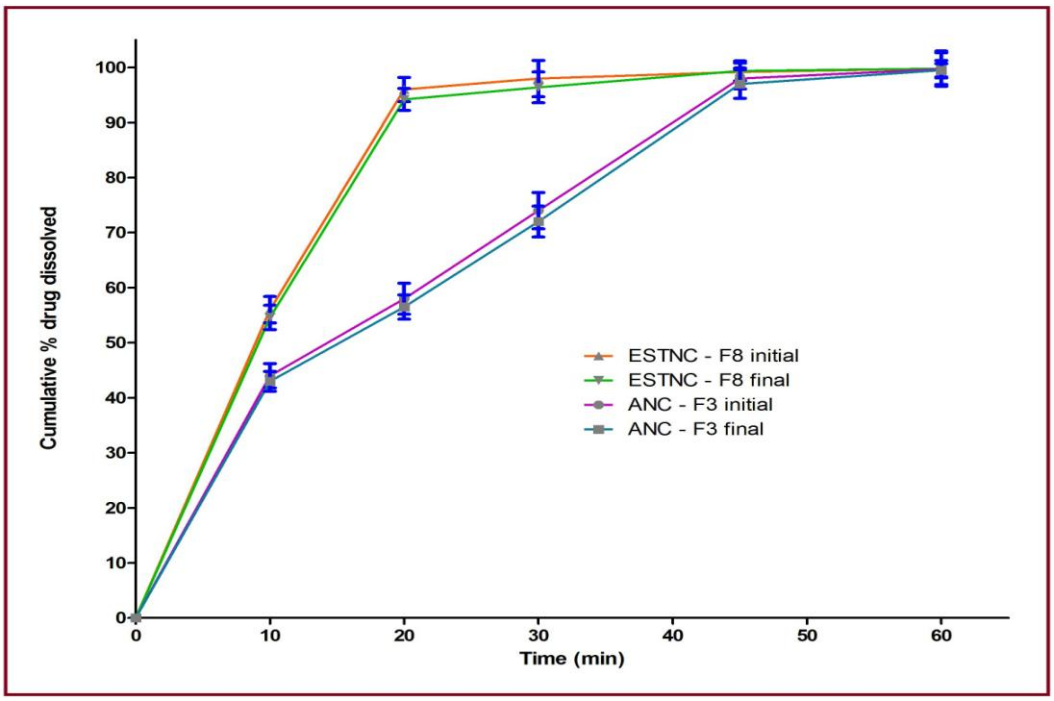

Figure 7.24. Dissolution profiles of stability batches against fresh batches of NCs (vertical bars represent SD, n = 6).

7.4.2.6 *In-vivo* preclinical pharmacokinetic study

7.4.2.6.1 HPLC-UV plasma drug analysis – method development and validation – same as described under the section 5.4.2.8.1.

7.4.2.6.2 Pharmacokinetic parameters

The plasma profiles of total Eze quantified in adult male Albino Wistar rats following single dose oral administration of pure drug suspension, ANC-F3 and ESTNC-F8 were compared. The pharmacokinetic parameters were determined using Kinetica 5.0 pharmacokinetic software (Trial version, PK-PD analysis, Thermofischer) and

Graphpad Prism software (version 5.03, GraphPad Software, USA). The plasma profiles of total Eze quantified in adult male Albino Wistar rats following single dose oral administration of pure drug suspension, ANC F3 and ESTNC F8 were reported in Table 7.45. The peak plasma concentration (C_{max}) and the time to attain C_{max}, T_{max}, were recorded directly from the plasma concentration – time curve. The area under the plasma concentration – time curve was determined by trapezoidal method. It was noticed that the plasma concentration time profile of Eze for NCs showed improved drug absorption than the simple drug suspension.

Table 7.45. Pharmacokinetic parameters derived for pure Eze and optimized NCs (n = 6). Data shown as Mean±SD.

Parameter/Treatment	**Pure drug**	**ANC F3**	**ESTNC F8**
T_{max} (h)	2±0.00	1.5±0.00	1±0.00
C_{max} (ng/mL)	1912±195.92	2841.5±222.54^{a*}	5146.5±535.94$^{@***}$
$AUC_{0\text{-}24h}$ (ng. h/mL)	17848±1306.54	22467±1570.74	46704±1856.13
$AUC_{0\text{-}\infty}$ (ng. h/mL)	18664.43±1324.18	24190.99±1602.68^{a*}	64169.3±1912.32$^{@***}$
$AUMC_{0\text{-}24h}$ (ng. h^2/mL)	163568±3801.65	205701±4402.48	464738±6821.95
$MRT_{0\text{-}24h}$ (h)	9.15±1.02	8.96±2.03	9.94±1.14
% $RB_{(0\text{-}24h)}$	100±0.00	125.87±3.04	261.67±6.3
% $RB_{(0\text{-}\infty)}$	100±0.00	129.6±2.98	343.82±8.08
Symbols and statistical representations = ***p < 0.001 and *p < 0.05; a = compared to pure Eze; @ = compared to pure Eze and ANC-F3 (One way ANOVA followed by Tukey's post hoc test). % RB = % Relative bioavailability with respect to pure drug.			

Pharmacokinetic study was performed to quantify the total plasma Eze concentration (free plasma Eze + plasma EzeG) following single dose oral administration of pure drug

suspension and NCs as 0.25% w/v NaCMC dispersions to male Albino Wister rats. Following oral administration, the absorbed Eze is extensively conjugated to EzeG, a pharmacologically active metabolite. Addition of β-glucuronidase (minimum 100,000 units/mL) to the plasma samples aided in the conversion of EzeG to Eze and the total Eze in plasma was estimated and reported.

The T_{max} was observed in the order, pure drug > ANC-F3 > ESTNC-F8. The T_{max} values of pure drug, ESTNC-F8 and ANC-F3 were noted at 2, 1 and 1.5 h, respectively. ESTNC-F8 and ANC-F3 successfully reduced the T_{max} of pure Eze. ESTNC-F8 particularly reduced the T_{max} of pure drug by half. The parameters, C_{max}, $AUC_{0\text{-}24h}$, $AUMC_{0\text{-}24h}$ and $AUC_{0\text{-}\infty}$ were observed in the order, ESTNC-F8 > ANC-F3 > pure drug. The improvement in the mean C_{max} of Eze was 3 and 1.5 times, as achieved by ESTNC-F8 and ANC-F3, respectively. The C_{max} of ANC-F3 was greater than pure Eze ($p < 0.05$) and the C_{max} of ESTNC-F8 was significantly higher ($p < 0.001$) than both, pure Eze and ANC-F3. Both, the mean $AUC_{0\text{-}24h}$ and mean $AUMC_{0\text{-}24h}$ of Eze were improved by 3 and 1.3 times, respectively, by ESTNC-F8 and ANC-F3. The $AUC_{0\text{-}24h}$ and $AUMC_{0\text{-}24h}$ of ANC-F3 were higher than pure Eze. The $AUC_{0\text{-}24h}$ and $AUMC_{0\text{-}24h}$ of ESTNC-F8 were higher than pure Eze and ANC-F3. The mean $AUC_{0\text{-}\infty}$ value of pure drug was improved by 3.4 and 1.3 times, respectively, by ESTNC-F8 and ANC-F3. The $AUC_{0\text{-}\infty}$ value of ANC-F3 was significantly higher ($p < 0.05$) than pure Eze and that of ESTNC-F8 was significantly higher ($p < 0.001$) than pure Eze as well as ANC-F3. The ESTNC-F8, especially improved the relative bioavailability (RB) of pure drug by 2.6 to 3.4 times, in terms of $AUC_{0\text{-}24h}$ and $AUC_{0\text{-}\infty}$, respectively. The MRT values of pure drug, ESTNC-F8 and ANC-F3 indicated insignificant differences in measured values.

The concentration of Eze, as observed from the study of plasma drug concentration–

time profiles of drug suspension and NC formulations, reached its peak followed by a swift decline and this pattern was reobserved during the 24 h course of study as evidenced by the multiple peaks in the graph. *In-vivo*, Eze gets excreted into the bile after undergoing extensive glucuronidation in the intestine to a phenolic glucuronide. The drug probably gets repeatedly delivered back to its site of absorption, the intestinal tract lumen via enterohepatic recirculation following absorption in the ileum [Bali et al., 2010 and 2011]. This may consecutively enhance the residence time of the drug in the lumen of the intestinal tract and may potentiate its antihyperlipidemic action. The plasma concentration time profiles were shown in Figure 7.25.

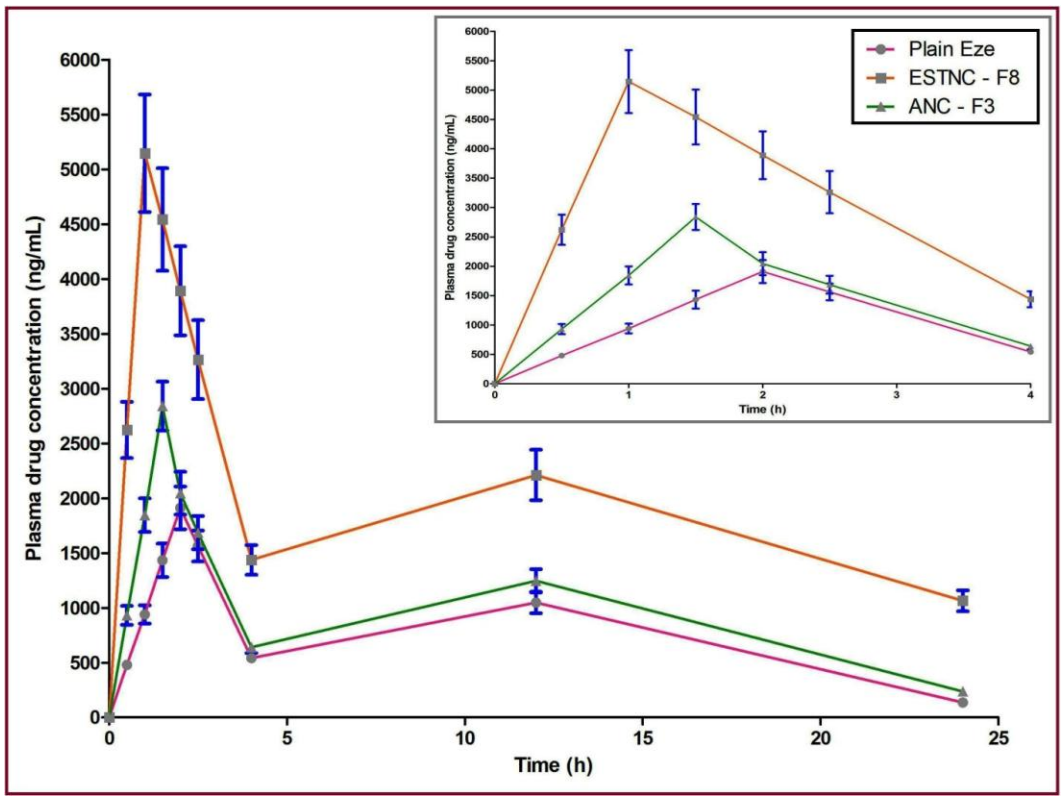

Figure 7.25. Pharmacokinetic profiles of pure drug suspension and optimized NCs (vertical bars represent SD, n = 6). Inset shows the profile up to 4 h.

The nano size particles of the NCs ensured distinctly enormously large surface area for the drug dissolution that lead to fastest drug release and subsequent absorption. Nanonization decreased the number of steps involved in drug dissolution from the dosage form and increased the surface area available for the drug release from the dosage form, both of which contributed towards the observed order of T_{max}. MRT being an intrinsic property of a drug, no change was observed in the intrinsic property of Eze when the drug was formulated into NCs [Bali et al., 2010 and 2011].

The significantly superior bioavailability of ESTNC-F8 in the present study could be most likely due to the enhanced solubility and instant dispersion advantages offered due to the nanosize of the drug. The nanosize accompanied by the stabilizer coating served to disperse the drug particles readily for absorption in the GIT. In addition, Eze being a P-gp substrate drug, in case of ESTNC-F8, the presence of stabilizer TPGS, a surfactant cum potent P-gp inhibitor, unlike AA2G which is a simple hydrophilic excipient, might have resulted in better alteration in the intestinal membrane permeability of Eze due to inhibition of an apocally polarised efflux system.

Since Eze is already available as a once a day formulation in the market, decrease in value of T_{max} observed in case of NCs over pure drug suspension might not serve to change the dosing frequency. However, the enhancement in oral bioavailability of the drug from the NC formulations in comparison to suspension (as evident from the % RB values) might offer a possibility of considerable dose reduction of the drug when administered in the form of an NC formulation, thus affecting the drug dosing regimen beneficially.

7.4.2.7 Antihypercholesterolemic activity

7.4.2.7.1 Principle behind performing the plasma cholesterol determination test for pure Eze and formulations – same as described under the section 5.4.2.9.1.

7.4.2.7.2 Hypocholesterolemic potential of pure drug and optimized formulations

The study was conducted for a total of eight weeks wherein the first four weeks, all the animal groups were fed with 200 mg cholesterol in 2 mL coconut oil as high fat diet for inducing hypercholesterolemia. At the end of fourth week, the plasma cholesterol levels were measured for all the groups and the values were considered as baseline values for the next stage four week study, the actual antihypercholesterolemic activity study. It was noted that all the animals together showed a mean 80-85% elevation in total plasma cholesterol levels at the end of four week hypercholesterolemic induction study, when compared to day one mean value. The percent reduction values in the levels of total plasma cholesterol achieved by various treatment groups were presented in Table 7.46 and Figure 7.26. The antihypercholesterolemic performance of pure Eze was statistically insignificant in comparison to the control group ($p > 0.05$) on all days.

As TPGS is known for its P-gp inhibitory nature, one group was studied treated with Eze-TPGS PM to evaluate the influence of this excipient on the antihypercholesterolemic activity of Eze. The activity of Eze-TPGS PM was statistically insignificant in comparison to the pure Eze ($p > 0.05$) on all days and insignificant compared to control ($p > 0.05$) on days, 7, 14 and 21; on day 28, Eze-TPGS PM reduced the plasma cholesterol levels significantly ($p < 0.05$) compared to control.

Table 7.46. Percent reduction in the total cholesterol levels achieved by pure drug suspension and optimized NCs. Results were expressed as Mean±SD (n = 6).

Treatment/Day	% Decrease in total plasma cholesterol levels			
	Day 7	Day 14	Day 21	Day 28
Control	-4±5.67	-4.8±3.78	-4±5.89	-4±5.75
Eze	1.13±3.21	1.89±5.18	3.02±4.16	3.77±5.84
Eze-TPGS PM	1.89±4.18	3.02±4.96	4.53±3.82	$5.28±5.24^{a*}$
F3	$8.51±4.17^{a**}$	$19.15±7.6^{b***}$	$29.79±5.44^{b***}$	$38.3±6.79^{b***}$
F8	$21.82±8.90^{c***}$	$32.73±8.97^{c***}$	$43.64±7.26^{c***}$	$56.36±8.54^{c***}$

Symbols and statistical representations = ***$p < 0.001$, **$p < 0.01$ and *$p < 0.05$; a = compared to Control; b = compared to Control, Eze and Eze-TPGS PM; c = compared to Control, Eze, Eze-TPGS PM and F3 (Two way ANOVA followed by Bonferroni's post hoc test).

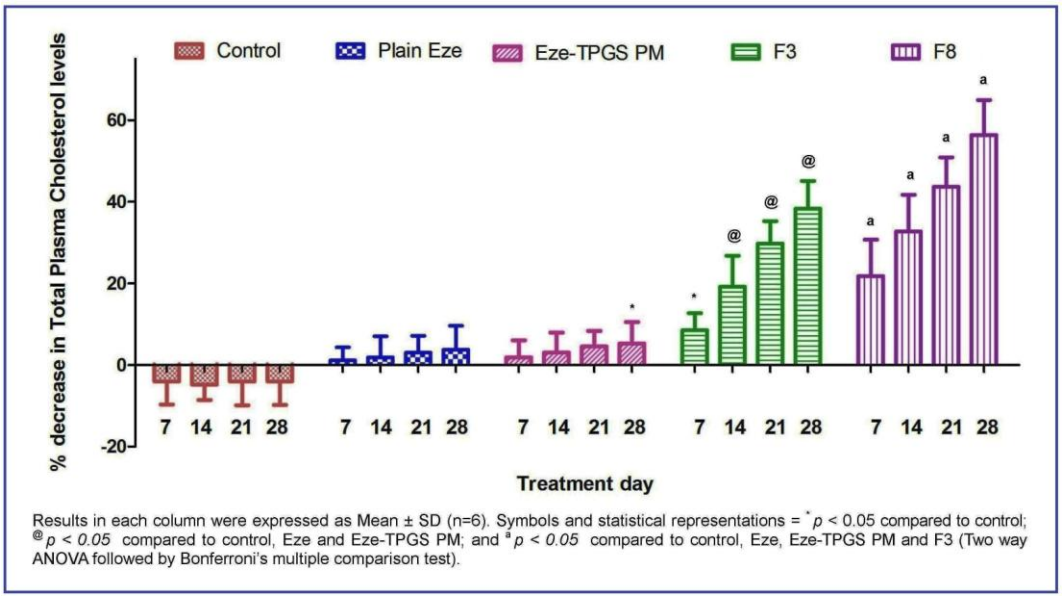

Figure 7.26. Antihypercholesterolemic activity of pure drug suspension, control, and optimized NCs (vertical bars represent SD, n = 6).

The *in-vivo* performance of F3 with respect to the percent reduction in TC was highly significant compared to control or pure Eze or Eze-TPGS PM ($p < 0.001$ except for the

7^{th} day). On day 7, the cholesterol reduction of F3 was higher only compared control ($p < 0.01$). The performance of F8 with respect to the percent reduction in TC was drastically significant compared to control or pure Eze or Eze-TPGS PM ($p < 0.001$ on all days). Besides, the percent reduction levels in TC achieved by F8 were far superior to the levels achieved by F3 ($p < 0.001$) also on all the study days. The superior cholesterol reduction efficiency of F3 and F8 indicated the significant involvement of size factor in the performance. The use of TPGS that has been recognized as one of the most potent P-gp inhibitors could have positively contributed to the better performance of F8 formulation.

Since AA2G has been employed as an NC stabilizer for the first time in our study and since the PS reduction offered by the same was in nanorange, both the NCs were further subjected to plasma lipid profile estimation. The mean percent elevation or decline in plasma lipid levels of all the animals in comparison to day one was noted at the end of four week hypercholesterolemic induction study. The mean elevation levels, calculated for all the animal groups, compared to day one values, were 80-85% for total plasma cholesterol, 75-80% for triglycerides, 200-300% for LDL levels. The mean HDL levels showed a 20-25% decline compared to day one.

NC formulations are unique due to their nano-size and commercialization advantages. In the present part of work, AA2G was employed as an NC stabilizer for the first ever time and TPGS, an established NC stabilizer has been used to nanonize Eze for the first time. Therefore, the effect of both the NCs on the lipid profile of rats was also studied. The effect of both the NCs on the percent changes in the plasma levels of TG, HDL and LDL was also evaluated apart from antihypercholesterolemic activity. Eze has been known to reduce the TC, TG, LDL and increase the HDL in hypercholesterolemic

patients. Eze is the first of its kind hypolipidemic which serves as a cholesterol absorption inhibitor unlike other marketed classes of lipid lowering agents which act by inhibiting the synthesis of cholesterol [Kosoglou et al., 2005]. P-gp efflux interferes with the absorption of Eze as the drug localizes at the small intestinal brush border where it binds to Niemann-Pick C1-Like1 protein, a critical mediator of cholesterol absorption [Garcia-Calvo et al., 2005]. The percent changes in the plasma levels of TG, TC, HDL and LDL for a period of 28 days were shown in Figure 7.27 wherein the statistically differential performance of each treatment group with respect to control was highlighted.

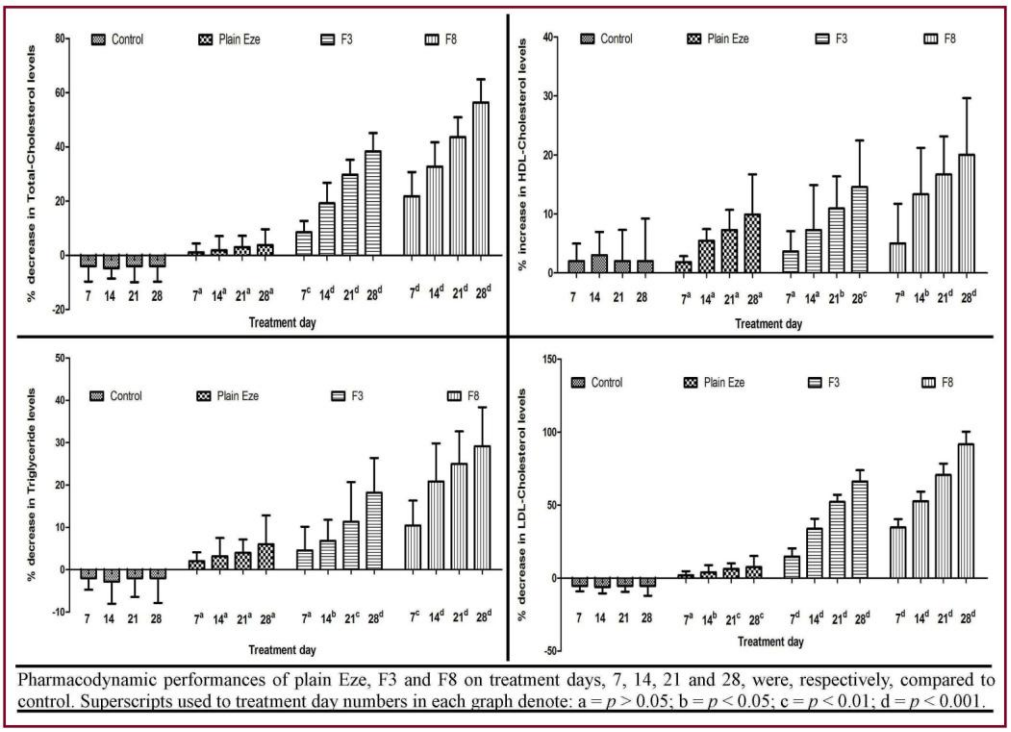

Figure 7.27. Pharmacodynamic performances of pure drug suspension, control, F3 and F8 (vertical bars represent SD, n = 6).

TG, TC and HDL levels were experimentally determined and their values recorded were applied to derive the LDL levels. With respect to the percent reduction in TG levels, except for the 7th day, the performance of F8 was superior to pure Eze ($p < 0.001$) and F3 ($p < 0.05$). The performance of F3 in comparison to pure Eze was significantly superior only on day 28 ($p < 0.01$). The percent increase in HDL of F3 in comparison to pure Eze and that of F8 in comparison to F3 were statistically insignificant ($p > 0.05$) whereas, the performance of F8 in comparison to pure Eze was higher on 21st and 28th days ($p < 0.05$).

The *in-vivo* performances of F3 and F8 with respect to the percent reduction in TC and LDL were drastically significant compared to pure Eze ($p < 0.001$ except for the 7th day TC and LDL reduction of F3) and it could be due to the nanonization and the consequent higher solubility which could have favored faster absorption of drug. Enhanced performance of NCs was also suggested by their superior *in-vitro* dissolution profiles. The bioavailability variations might have been nullified and the drug could have been absorbed completely from these formulations. The percent reduction levels in TC and LDL, achieved by F8 were far superior to the levels achieved by F3 ($p < 0.01$). The use of TPGS that has been recognized as one of the most potent P-gp inhibitors could have positively contributed to the best performance of F8 formulation.

The improved *in-vivo* performance of Eze NCs is in close agreement with the performance of commercially available fenofibrate NCs [Eerdenbrugh et al., 2008b]. Markedly superior hypocholesterolemic performance of NCs has been confirmed by commercialized fenofibrate (FN) NC formulations. TriCor® and Triglide® are oral tablet dosage forms of FN prepared with dried NCs of FN manufactured by top down wet ball milling and high pressure homogenization, respectively. Both the NC formulations of

FN are considered as rational developments as they showed reduced bioavailability variations by eliminating food effects [Eerdenbrugh et al., 2008b]. Current part of investigation identified F8 formulation of Eze to be the best with respect to its *in-vitro* and *in-vivo* performance. The TPGS in F8 could have surmounted P-gp efflux, secured enhanced permeation and reduced the bioavailability variations of Eze. The delivery of drug in solubilized form, increased interfacial area available for intestinal absorption, enhanced wetting due to surfactant effect, improved dissolution velocity and enhanced cellular uptake of Eze caused by inhibition of P-gp efflux, could have cumulatively contributed to the distinct and beneficial pharmacodynamic performance of F8.

7.5 SUMMARY

In the present part of study, Eze NCs were successfully prepared by two different bottom up precipitation methods and optimized by suitable experimental designs. Since AA2G was studied for the first time as an NC stabilizer and sufficient knowledge was unavailable regarding the formulation development, a preliminary screening PBD and an optimizing BBD were applied to arrive at the optimized AA2G NC, F3. TPGS NCs were optimized by applying CCD since the number of factors to be studied was cut down beforehand following the reproducible preliminary trials performed based on literature suggestions. Both, AA2G and TPGS were identified as potential stabilizers in nanonizing Eze by retaining its crystallinity. The concentration of the stabilizers determined the size of the resultant NCs. TPGS in combination with SLS, F8 formulation, may be considered as the most effective stabilizer combination in developing Eze NCs owing to their combined amphiphilic and wetting effect. AA2G, being purely hydrophilic, could reduce the PS of Eze to nanorange but the saturation

solubility and dissolution properties of F3 were inferior to F8. Even the pharmacokinetic and pharmacodynamic performances of F8 were markedly superior to F3 which may be ascribed to the P-gp efflux inhibitory nature of TPGS. The superior plasma concentration-time profile and higher lipid lowering activity of F8 indicated that the inhibition of P-gp efflux transport facilitated higher extent of intestinal absorption and *in-vivo* performance of drug. Based on the results, it may be concluded that the oral delivery of Eze as NCs could be quite beneficial and F8 may be viewed as rational, simple, economic and promising formulation in improving the *in-vitro* and *in-vivo* performance of the drug.

7.6 GRAPHICAL SUMMARY

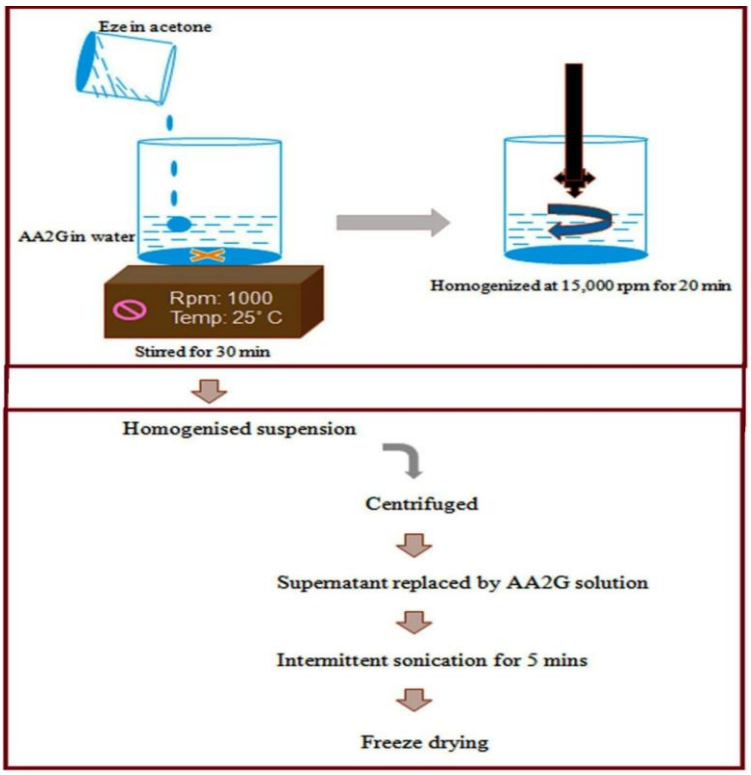

Figure 7.28. Schematic diagram showing formation of ANCs of Eze.

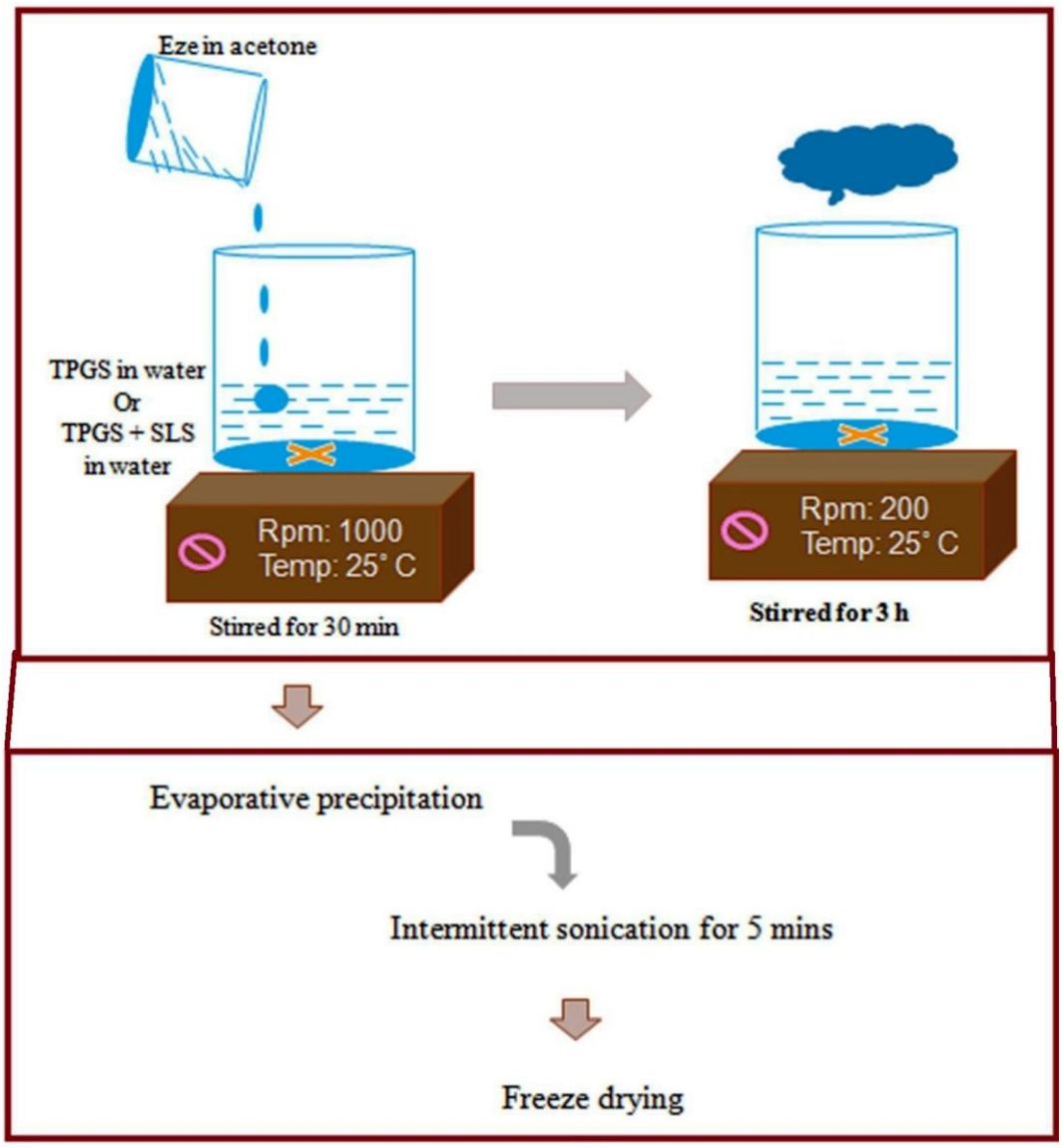

Figure 7.29. Schematic diagram showing formation of TNCs of Eze.

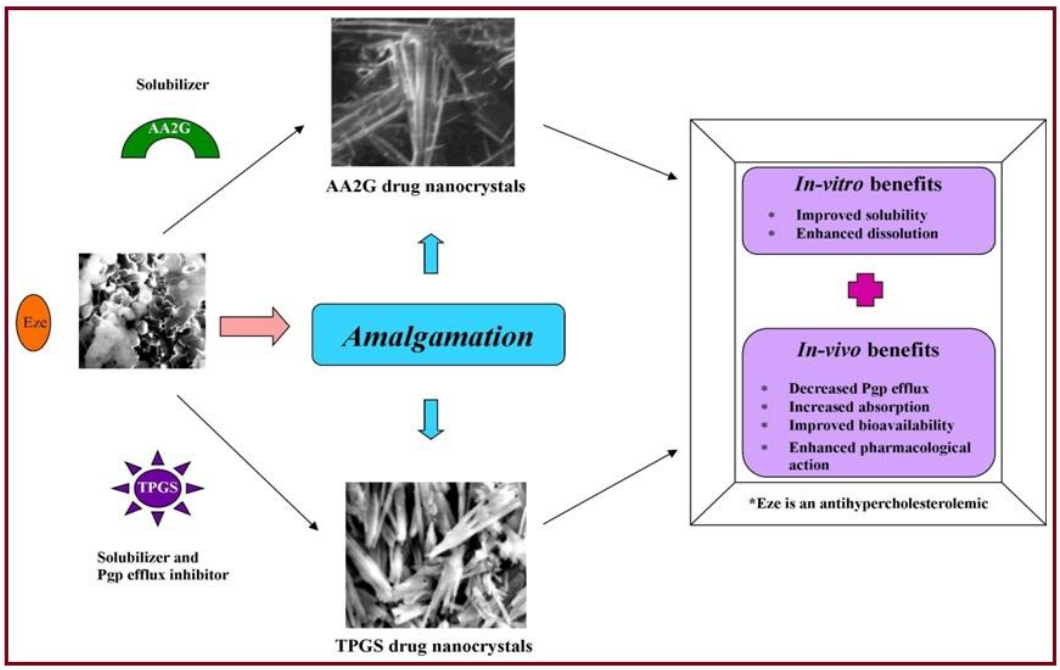

Figure 7.30. Gist of effect of nanocrystallization formulation approach on Eze performance.